

Copyright Undertaking

This thesis is protected by copyright, with all rights reserved.

By reading and using the thesis, the reader understands and agrees to the following terms:

1. The reader will abide by the rules and legal ordinances governing copyright regarding the use of the thesis.
2. The reader will use the thesis for the purpose of research or private study only and not for distribution or further reproduction or any other purpose.
3. The reader agrees to indemnify and hold the University harmless from and against any loss, damage, cost, liability or expenses arising from copyright infringement or unauthorized usage.

IMPORTANT

If you have reasons to believe that any materials in this thesis are deemed not suitable to be distributed in this form, or a copyright owner having difficulty with the material being included in our database, please contact lbsys@polyu.edu.hk providing details. The Library will look into your claim and consider taking remedial action upon receipt of the written requests.

The Hong Kong Polytechnic University

Department of Civil and Structural Engineering

**DEGRADATION OF SYNTHETIC ORGANIC
COMPOUNDS BY SULFATE- AND HYDROXYL
RADICAL-BASED ADVANCED OXIDATION
PROCESSES**



WANG YU RU

A Thesis Submitted in Partial Fulfillment of the Requirements for the
Degree of Doctor of Philosophy

March 2012

CERTIFICATE OF ORIGINALITY

I hereby declare that this thesis is my own work and that, to the best of my knowledge and belief, it reproduces no material previously published or written, nor material that has been accepted for the award of any other degree or diploma, except where due acknowledgement has been made in the text.

_____(Signed)

Wang Yuru _____(Name of Student)

To my parents, brother, sister and the angels in the family,

for their love and support;

To the sorrows that I have suffered;

To so many sleepless nights;

It is not an easy road.

ABSTRACT

Currently, the contamination of water sources by synthetic organic compounds (SOCs) is one of the concerning environmental issues faced throughout the world, leading to a great interest in developing alternative treatment technologies for the removal of SOC in aqueous medium. Among the existing SOC, dyes and herbicides contribute to a large portion of the confirmed toxic organics and thus have to be removed prior to the discharge of the treated water. Against the background, the primary objective of this research work is to explore sulfate- and hydroxyl radical based advanced oxidation processes (AOPs) for the elimination of dyes and herbicides in water and wastewaters.

Firstly, an oxidation process using sulfate radical ($\text{SO}_4^{\bullet-}$) activated by Fe(II)-mediated Oxone[®] process (FO) were evaluated by monitoring the degradation of a Xanthene dye Rhodamine B (RhB) in an aqueous solution. The effects of reactant dosing sequence, Fe(II)/Oxone[®] molar ratio and concentration, solution pH, and inorganic salts on the process performance were investigated. Total RhB removal was obtained within 90 min under an optimal Fe(II)/Oxone[®] molar ratio of 1:1. The RhB degradation was found to be a two-stage kinetics, consisting of a rapid initial decay and a subsequent retarded stage. Additionally, TOC study indicates that stepwise addition of Fe(II) and Oxone[®] can notably improve the process performance by about 20%, and the retention time required can be greatly reduced compared with the conventional one-off dosing method.

On the other hand, it was found that the rapid depletion as well as the slow regeneration of Fe(II) in the above FO process usually terminates the production of $\text{SO}_4^{\bullet-}$ and limits the decay rate. To tackle with the problem, a novel electrochemically enhanced FO

process (i.e. EFO) was proposed. In this oxidation process, once an electric current is applied between the anode (an iron sheet) and the cathode (a graphite bar), a predetermined amount of Oxone[®] is added to the reactor. Ferrous ions generated from the sacrificed Fe anode mediate the generation of $\text{SO}_4^{\cdot-}$ through the decomposition of Oxone[®]. The EFO process was evaluated in terms of a selected herbicide 2,4,5-Trichlorophenoxyacetic acid (2,4,5-T) degradation in aqueous solution. Experimental results demonstrated that low solution pH facilitated the system performance due to the dual effects of weak Fenton's reagent generation and persulfate ion generation, whereas the process was inhibited at basic pH levels through non-radical self-dissociation of Oxone[®] and the formation of $\text{Fe}(\text{OH})_3$. The active radicals involved in the EFO process were identified. The EFO process demonstrates a very high 2,4,5-T degradation efficiency (over 90% decay within 10 min), which justifies the novel EFO as a promising process for herbicide removal in water.

Furthermore, the degradation of 2,4,5-T in aqueous solution by photo-assisted $\text{Fe}(\text{II})/\text{Oxone}^{\text{®}}$ process (FOU) was explored and compared with the FO process. Regarding the involvements of UV, Oxone[®] and/or transition metal, four different processes (i.e., UV alone, Oxone[®]/UV, FO, and FOU) were evaluated in terms of 2,4,5-T decay. For the tests involving the UV irradiation, the effect of various wavelengths of UV light was also investigated. The experimental results indicated that direct photolysis of 2,4,5-T was insignificant (< 19%). The process was improved in the presence of Oxone[®] due to the formation of sulfate and hydroxyl radicals via the photolysis of Oxone[®] with the UV 254 nm irradiation, which exhibits the best performance (> 80%) in comparing with the others (300, 350, 419 nm). In particular, the FO process was dramatically promoted upon the introduction of UV irradiation (i.e. FOU). Subsequently, the role of UV

irradiation was elucidated in-depth by comparing the real-time of [Fe(II)] in the solution during the reaction between the FO process and the FOU process. The effect of initial pH was investigated and optimized to be 3.68. The 2,4,5-T decay by the FOU process under various [Oxone[®]] and [2,4,5-T] was also examined. Besides, the influences of various anions on the decay of 2,4,5-T by the FOU process were examined in detail. The decay pathways for the transformation of 2,4,5-T by UV alone, Oxone[®]/UV, and FOU processes were proposed using LC-ESI/MS analysis. Additionally, the efficiencies of UV alone, Oxone[®]/UV and FOU were further examined in terms of mineralization and Cl⁻ ion accumulation. It was found that the proposed FOU process demonstrates the best removal (100% in 90 min) of the parent and daughter compounds examined with an outstanding mineralization performance (> 83% in 8 h) in comparison with the other two processes investigated in this study.

Finally, an improved process by incorporating the merits of both of EFO and FOU processes was developed, in which the solution treated under EFO system is simultaneously irradiated with UV light (i.e., EFOU). This EFOU process was examined through the degradation of 0.2 mM 2,4,5-TCP under various operating conditions. It was found that the EFOU process yields over 92% of probe removal at a very low applied current (1 mA) in natural pH (4.35) condition. It was demonstrated that an acidic condition is favorable to the process. Furthermore, around 80% of 2,4,5-TCP was decayed at pH of 7.70 in 20 min suggesting that the EFOU process is efficient work even at neutral pH conditions. The mode of current-applying and the strategy of tandem addition of Oxone[®] on the effect of process performance were also investigated. Furthermore, a possible decay pathway of 2,4,5-TCP by EFOU process was proposed based on the identified aromatic intermediates by LC-ESI/MS analysis.

LIST OF PUBLICATIONS

Journal Papers

1. **Wang Y. R.**, Chu W., Degradation of a Xanthene Dye by Fe(II)-mediated Activation of Oxone Process, *Journal of Hazardous Materials*, 186(2-3) (2011), 1455-1461.
2. **Wang Y. R.**, Chu W., Degradation of 2,4,5-Trichlorophenoxyacetic Acid by a Novel Electro-Fe(II)/Oxone Process Using Iron Sheet as the Sacrificial Anode, *Water Research*, 45 (2011), 3883-3889.
3. **Wang Y. R.**, Chu W., Adsorption and Removal of a Xanthene Dye from Aqueous Solution Using Two Solid Wastes as Adsorbents, *Industrial & Engineering Chemistry Research*, 50 (2011), 8734-8741.
4. Chu W., **Wang Y. R.**, H. F. Leung, Synergy of Sulfate and Hydroxyl Radicals in UV/S₂O₈²⁻/H₂O₂ Oxidation of Iodinated X-ray Contrast Medium Iopromide, *Chemical Engineering Journal*, 178 (2011), 154-160.
5. **Wang Y. R.**, Chu W., Photo-assisted Degradation of 2,4,5-Trichlorophenoxyacetic acid by Fe(II)-mediated Activation of Oxone Process: the Role of UV Irradiation, Reaction Mechanism and Mineralization, *Applied Catalysis B: Environmental*, 123-124 (2012), 151-161.
6. **Wang Y. R.**, Chu W., Photo-assisted Degradation of 2,4,5-Trichlorophenol by Electro-Fe(II)/Oxone Process using a Sacrificial Iron Anode: Kinetic Study and Reaction Mechanism, under submission.

Conference Presentation

1. **Wang Y. R.**, Chu W., Degradation of 2,4,5-Trichlorophenoxyacetic Acid by a Novel Electro-Fe(II)/Oxone Process Using Iron Sheet as the Sacrificial Anode, The 16th

International Conference on Advanced Oxidation Technologies for Treatment of Water, Air and Soil (AOTs-16), Town & Country Resort, San Diego, California, USA, 15-18, November, 2010

2. **Wang Y. R.**, Chu W., Yue Shen, Adsorption of Rhodamine B on coal fly ash and kaolin from aqueous solution: feasibility of utilizing coal fly ash and kaolin as adsorbents, Water & Industry 2011, IWA Specialist Conference, Valladolid, Spain, 1-4, May 2011.
3. Chu W., **Wang Y. R.**, H. F. Leung, Photodegradation of iodinated X-ray contrast medium iopromide using combined oxidants of $\text{S}_2\text{O}_8^{2-}$ and H_2O_2 promoted by UV irradiation, The 3rd International Postgraduate Conference on Infrastructure and Environment, 11-12 July, 2011, Hong Kong.

ACKNOWLEDGEMENTS

First and foremost, I wish to express my heart-felt gratitude to my supervisor, Prof. Wei Chu, for providing me the opportunity to pursue my PhD study and for his generous support, endless encouragement and invaluable guidance throughout the research project. I would also like to express my thanks to the technicians in the Water and Wastewater Laboratory, especially Mr. Wai-Shung Lam for his tremendous help and technical support. I also wish to extend my thanks to my Master's supervisor, Prof. Qing-zhong Bai for his support.

Thanks are due to all the members of my examination committee of my PhD thesis, including Prof. Dionysios. D. Dionysiou, Prof. Irene M.C. LO, and Prof. C. S. Poon, for their time spent on examining the thesis and their constructive comments/advice which are of great value both for improving my PhD thesis and for my future research.

Special thanks go to my colleagues/friends, Dr. Yong-Fang Rao, Ms. Mei-Juan Chen, and Dr. Wei Song etc for their valuable advice, persistent encouragements, and friendships which helped me get through those difficulties.

Thanks are due to The Research Committee of Hong Kong Polytechnic University for the financial support.

Last but not least, I am deeply grateful to my beloved parents and family. My nephews and niece are the angles of the family who bring happiness to my life. At the same time, I wish to express my appreciation to my uncle, aunt, and their lovely daughter in Xi-ning for their concerns and moral support.

TABLE OF CONTENTS

CERTIFICATE OF ORIGINALITY	I
ABSTRACT	III
LIST OF PUBLICATIONS	VI
ACKNOWLEDGEMENTS.....	VIII
TABLE OF CONTENTS	IX
LIST OF FIGURES	XIV
LIST OF TABLES AND SCHEMES.....	XX
LIST OF ABBREVIATIONS	XXI
CHAPTER 1 Introduction	1
1.1 Background	1
1.2 Aims and Objectives	4
1.3 Organization of the Thesis	5
CHAPTER 2 Literature Review	8
2.1 Probe Contaminants	8
2.1.1 Rhodamine B.....	8
<i>2.1.1.1 Background</i>	<i>8</i>
<i>2.1.1.2 Toxicological effects</i>	<i>9</i>
<i>2.1.1.3 Previous degradation studies of RhB</i>	<i>9</i>
2.1.2 2,4,5-Trichlorophenoxyacetic acid.....	10
2.1.2.1 Background	10
2.1.2.2 Toxicological effects	11
2.1.2.3 Previous degradation studies of 2,4,5-T	12
2.1.3 2,4,5-Trichlorophenol.....	13
2.1.3.1 Background	13

2.1.3.2 Toxicological effects	14
2.1.3.3 Previous degradation studies of 2,4,5-TCP	15
2.2 Advanced Oxidation Processes	15
2.2.1 Fenton's reagent-based AOPs	16
2.2.1.1 Classical Fenton process	16
2.2.1.2 Electro-Fenton process	19
2.2.1.3 Photo-Fenton and photo-Fenton-like processes	21
2.2.2 Sulfate radical-based AOPs	24
2.2.2.1 Sulfate radical generation via the activation of $S_2O_8^{2-}$	27
2.2.2.2 Sulfate radical generation via the activation of Oxone [®]	29
CHAPTER 3 Materials and Methodology	33
3.1 Introduction	33
3.2 Materials and Methods	33
3.2.1 Chemicals and reagents	33
3.2.2 Experimental procedures	35
3.2.2.1 Degradation of RhB by FO process	36
3.2.2.2 Degradation of 2,4,5-T by EFO system	36
3.2.2.3 Degradation of 2,4,5-T by FOU process	37
3.2.2.4 Degradation of 2,4,5-TCP by EFOU process	38
3.2.3 Analytical procedures	40
3.2.3.1 Analysis by HPLC	40
3.2.3.2 Analysis by LC-ESI/MS	43
3.2.3.3 TOC and solution pH measurement	44
3.2.3.4 Determination of Fe(II)	45
3.2.3.5 Chloride ion measurement	45

CHAPTER 4 Degradation of RhB by Fe(II)-Mediated Activation of Oxone[®]

Process	46
4.1 Introduction	46
4.2 Results and Discussion.....	48
4.2.1 Dosing sequence of reactants	48
4.2.2 Effect of Fe(II): Oxone [®] ratio on RhB degradation	50
4.2.3 Effect of pH level on RhB degradation.....	54
4.2.4 Effect of various inorganic salts.....	57
4.2.5 Mineralization of RhB	62
4.3 Summary	64

CHAPTER 5 Degradation of 2,4,5-T by Electro-Fe(II)/Oxone[®] Process using Iron

Sheet as the Sacrificial Anode	65
5.1 Introduction	65
5.2 Results and Discussion.....	67
5.2.1 Comparative study of different processes	67
5.2.2 Effect of applied current.....	69
5.2.3 Effect of electrolyte concentration	72
5.2.4 Effect of 2,4,5-T and oxidant dosage	73
5.2.5 Effect of initial pH	76
5.2.6 Radical quenching study	79
5.3 Summary	80

CHAPTER 6 Degradation of 2,4,5-T by Fe(II)/Oxone[®] Process with UV

Irradiation.....	82
6.1 Introduction	82
6.2 Results and Discussion.....	85

6.2.1 Comparison of direct photolysis and Oxone [®] /UV	85
6.2.2 Fe(II)-activated Oxone [®] under irradiation at various wavelengths.....	87
6.2.3 Effect of [Fe(II)] and the role of UV irradiation	89
6.2.4 Effect of initial solution pH.....	94
6.2.5 Effect of [Oxone [®]] and the primary intermediate	97
6.2.6 Variation of 2,4,5-T concentration	100
6.2.7 The influence of various anions and the variation of solution pH	102
6.2.8 Identification of intermediates and decay pathways	107
6.2.8.1 UV alone process	109
6.2.8.2 Oxone [®] /UV process	113
6.2.8.3 FOU process	116
6.2.9 TOC removal and time-course of Cl ⁻ ions.	119
6.3 Summary	120
CHAPTER 7 Degradation of 2,4,5-TCP by Electro-Fe(II)/Oxone[®] Process with UV Irradiation.....	123
7.1 Introduction	123
7.2 Results and Discussion.....	125
7.2.1 Comparison of Oxone [®] alone, UV alone, FOU, EFO, and EFOU	125
7.2.2 Effect of applied current.....	128
7.2.3 Effect of initial solution pH.....	130
7.2.4 Mode of current-applying	132
7.2.5 Tandem addition of Oxone [®]	133
7.2.6 Proposed mechanism of 2,4,5-TCP decay	135
7.3 Summary	137
CHAPTER 8 Conclusions and Recommendations	139

8.1 Conclusions	139
8.1.1 The degradation of RhB by FO process	139
8.1.2 The degradation of 2,4,5-T by EFO process	140
8.1.3 The degradation of 2,4,5-T by FOU process	141
8.1.4 The degradation of 2,4,5-TCP by EFOU process	143
8.2 Recommendations for Future Works.....	144
REFERENCES.....	146
APPENDIX I: Chemistry of Oxone®	I-1

LIST OF FIGURES

Figure 2-1:	Reaction pathways of the photo-Fenton or photo-Fenton-like process.	24
Figure 2-2:	Absorbance spectrum of 2.5 mM Oxone [®] in aqueous solution.	30
Figure 3-1:	Sketch of electrolytic cell.	37
Figure 3-2:	Sketch of the photoreactor Luzchem CCP-4V.	38
Figure 3-3:	Sketch of electrolytic cell with UV irradiation.	40
Figure 3-4:	The HPLC system used for the quantification of selected probes.	41
Figure 3-5:	Absorbance spectrum of 0.01 mM RhB in aqueous solution.	42
Figure 3-6:	Absorbance spectrum of 0.02 mM 2,4,5-T in aqueous solution.	42
Figure 3-7:	Absorbance spectrum of 0.05 mM 2,4,5-TCP aqueous solution.	43
Figure 3-8:	The LC-ESI/MS system employed for the aromatic intermediate analysis.	44
Figure 4-1:	Effect of reactants adding order on RhB degradation. Experimental conditions were 0.02 mM [RhB] ₀ , 0.20 mM [Fe(II)] ₀ , and 0.10 mM [Oxone [®]] ₀ without pH adjustment.	49
Figure 4-2:	Effect of different ratios of RFO on dye degradation. Conditions were 0.02 mM [RhB] ₀ , 0.10 mM [Oxone [®]] ₀ for (a) & 0.02 mM [RhB] ₀ , 0.20 mM [Oxone [®]] ₀ for (b).	53
Figure 4-3:	Degradation performance as a function of Fe(II)/Oxone [®] molar ratio	54
Figure 4-4:	Effect of initial solution pH after adding Oxone [®] . Experimental conditions were set at 0.02 mM [RhB] ₀ with RFO molar ratio of 1:10:10.	55
Figure 4-5:	Degradation performance as a function of initial solution pH after	56

adding Oxone[®]. Experimental conditions were set at 0.02 mM [RhB]₀ with RFO molar ratio of 1:10:10.

Figure 4-6: The pH variation before and after Oxone[®] addition. Experimental conditions were set at 0.02 mM [RhB]₀ with RFO molar ratio of 1:10:10.

Figure 4-7: Effect of inorganic salts: NaCl, NaNO₃, Na₂SO₄. Experimental conditions were set at 0.02 mM [RhB]₀ with RFO molar ratio of 1:10:10 without pH adjustment.

Figure 4-8: Effect of ionic strength: Na₂SO₄. Experimental conditions were set at 0.02 mM [RhB]₀ with RFO molar ratio of 1:10:10 without pH adjustment. Na₂SO₄ was added in different amount.

Figure 4-9: Effect of ionic strength: NaCl. Experimental conditions were set at 0.02 mM [RhB]₀ with RFO molar ratio of 1:10:10 without pH adjustment. NaCl was added in different amount.

Figure 4-10: Effect of Cl⁻ on the RhB degradation. Experimental conditions were 0.02 mM [RhB]₀, 0.20 mM [Oxone[®]]₀ without catalyst and pH adjustment.

Figure 4-11: TOC removal as a function of reaction time. Experimental conditions: [RhB]₀ = 0.10 mM, without pH adjustment. (a) RFO = 1:10:10, (b) RFO = 1:50:50, (c) RFO = 1:50:50, stepwise addition of Fe(II) and Oxone[®], (d) RFO = 1:10:50, stepwise addition of Oxone[®].

Figure 5-1: 2,4,5-T degradation under various reaction conditions. Experimental conditions: [2,4,5-T]₀ = 0.10 mM, [Na₂SO₄]₀ = 0.05 M as supporting electrolyte, no pH adjustment.

Figure 5-2: Effect of applied current on 2,4,5-T decay by EFO. The inset shows

the kinetic constants of herbicide decay at various applied currents. Experimental conditions: $[2,4,5\text{-T}]_0 = 0.10 \text{ mM}$, $[\text{Oxone}^{\text{®}}]_0 = 0.25 \text{ mM}$, $[\text{Na}_2\text{SO}_4] = 0.05 \text{ M}$ as supporting electrolyte, $I = 10 \text{ mA}$, no pH adjustment.

Figure 5-3: Iron ion accumulation in the solution. (Anode: Fe; Cathode: Graphite; $0.05 \text{ M Na}_2\text{SO}_4$ as electrolyte; $I = 10 \text{ mA}$). 72

Figure 5-4: Effect of $[\text{Na}_2\text{SO}_4]$ on herbicide decay by EFO. The inset shows the decay rate constants as a function of $[\text{Na}_2\text{SO}_4]$. Experimental conditions: $[2,4,5\text{-T}]_0 = 0.10 \text{ mM}$, $[\text{Oxone}^{\text{®}}]_0 = 0.25 \text{ mM}$, $I = 10 \text{ mA}$, no pH adjustment. 73

Figure 5-5: Degradation of various initial $[2,4,5\text{-T}]$ by EFO. The inset shows the decay rate constants as a function of $[2,4,5\text{-T}]$. Experimental conditions were $[\text{Oxone}^{\text{®}}]_0 = 0.25 \text{ mM}$, $[\text{Na}_2\text{SO}_4] = 0.05 \text{ M}$ as supporting electrolyte, $I = 10 \text{ mA}$, no pH adjustment. 74

Figure 5-6: Decay of 2,4,5-T with different $[\text{Oxone}^{\text{®}}]$ by EFO. Experimental conditions: $[2,4,5\text{-T}]_0 = 0.10 \text{ mM}$, $[\text{Na}_2\text{SO}_4] = 0.05 \text{ M}$, $I = 10 \text{ mA}$, no pH adjustment. 75

Figure 5-7: Effect of initial solution pH on the decay of 2,4,5-T. The inset shows the decay rate constants as a function of solution pH. Experimental conditions were $[2,4,5\text{-T}]_0 = 0.10 \text{ mM}$, $[\text{Oxone}^{\text{®}}]_0 = 0.25 \text{ mM}$, $[\text{Na}_2\text{SO}_4] = 0.05 \text{ M}$, $I = 10 \text{ mA}$. 78

Figure 5-8: Degradation of herbicide by Electro-Fe(II) system in $\text{pH} = 1.5$ solution without the presence of $\text{Oxone}^{\text{®}}$. Experimental conditions were $[2,4,5\text{-T}]_0 = 0.10 \text{ mM}$; $[\text{Na}_2\text{SO}_4] = 0.05 \text{ M}$ as supporting electrolyte; $I = 10 \text{ mA}$. 79

- Figure 5-9: Effect of different radical quenching agents on herbicide 80
degradation by EFO. Experimental conditions: $[2,4,5\text{-T}]_0 = 0.10$
mM, $[\text{Oxone}^{\text{®}}]_0 = 0.25$ mM, $[\text{Na}_2\text{SO}_4] = 0.05$ M, $I = 10$ mA, no pH
adjustment.
- Figure 6-1: Comparison of 2,4,5-T degradation by UV alone and Oxone[®]/UV. 87
Two UV lamps were employed, $[2,4,5\text{-T}]_0 = 0.1$ mM, $[\text{Oxone}^{\text{®}}]_0 =$
0.25 mM.
- Figure 6-2: 2,4,5-T photo-decay by FOU process under different wavelengths. 88
Two UV lamps were employed, $[2,4,5\text{-T}]_0 = 0.1$ mM, $[\text{Oxone}^{\text{®}}]_0 =$
0.25 mM, $[\text{Fe(II)}]_0 = 0.25$ mM.
- Figure 6-3: (a) Effect of Fe(II) dosage on the degradation of 2,4,5-T by FO 90
process; (b) Change of the remaining $[\text{Fe(II)}]$ over reaction time.
 $[2,4,5\text{-T}]_0 = 0.1$ mM, $[\text{Oxone}^{\text{®}}]_0 = 0.25$ mM.
- Figure 6-4: (a) Effect of Fe(II) dosage on the photodegradation of 2,4,5-T by 91
FOU process; (b) Change in the remaining $[\text{Fe(II)}]$ over reaction
time. Two 254 nm UV lamps were employed, $[2,4,5\text{-T}]_0 = 0.1$ mM,
 $[\text{Oxone}^{\text{®}}]_0 = 0.25$ mM.
- Figure 6-5: (a) Effect of initial solution pH on the photodegradation of 2,4,5-T 96
by FOU process; (b) pseudo first-order rate constant as a function of
initial pH. Two 254 nm UV lamps were employed, $[2,4,5\text{-T}]_0 = 0.1$
mM, $[\text{Oxone}^{\text{®}}]_0 = 0.25$ mM, $[\text{Fe(II)}]_0 = 0.10$ mM.
- Figure 6-6: (a) Photo-decay of 2,4,5-T at different Oxone[®] concentrations by 99
FOU process. (b) Evolution of 2,4,5-TCP upon photodegradation of
2,4,5-T by FOU process at different $[\text{Oxone}^{\text{®}}]$ Two 254 nm UV
lamps were employed, $[2,4,5\text{-T}]_0 = 0.10$ mM, $[\text{Fe}^{2+}]_0 = 0.10$ mM.
- Figure 6-7: (a) Photo-decay of 2,4,5-T at different initial concentrations by 101

FOU process. (b) Evolution of 2,4,5-TCP at different [2,4,5-T] by FOU process. Experimental conditions: $[\text{Oxone}^{\text{®}}]_0 = 0.25 \text{ mM}$, $[\text{Fe(II)}]_0 = 0.10 \text{ mM}$, two 254 nm UV lamps were employed.

Figure 6-8: The influence of various anions on the photodegradation of 2,4,5-T 103 by the FOU process. Two 254 nm UV lamps were employed, $[2,4,5\text{-T}]_0 = 0.1 \text{ mM}$, $[\text{Fe}^{2+}]_0 = 0.10 \text{ mM}$, $[\text{Oxone}^{\text{®}}]_0 = 0.25 \text{ mM}$, $[\text{anions}] = 0.01\text{M}$.

Figure 6-9: Trends of pH variation with the addition of different anions during 103 the treatment of 2,4,5-T by the FOU process. Two 254 nm UV lamps were employed, $[2,4,5\text{-T}]_0 = 0.1 \text{ mM}$, $[\text{Fe}^{2+}]_0 = 0.10 \text{ mM}$, $[\text{Oxone}^{\text{®}}]_0 = 0.25 \text{ mM}$, $[\text{anions}] = 0.01\text{M}$.

Figure 6-10: The evolution profiles of 2,4,5-T and aromatic intermediates during 110 the photolysis of 0.5 mM 2,4,5-T under the irradiation of two UV 254 nm lamps.

Figure 6-11: The evolution profiles of 2,4,5-T and aromatic intermediates for the 114 photo-decay of 2,4,5-T by the Oxone[®]/UV process. Two 254 nm UV lamps were employed, $[2,4,5\text{-T}]_0 = 0.5 \text{ mM}$, $[\text{Oxone}^{\text{®}}]_0 = 2.5 \text{ mM}$.

Figure 6-12: The evolution profiles of 2,4,5-T and aromatic intermediates for the 117 photo-decay of 2,4,5-T by the FOU process. Two 254 nm UV lamps were employed, $[2,4,5\text{-T}] = 0.5 \text{ mM}$, $[\text{Fe}^{2+}] = 0.50 \text{ mM}$, $[\text{Oxone}^{\text{®}}] = 2.5 \text{ mM}$.

Figure 6-13: Time-course of the concentration of TOC, Cl^- for the degradation of 120 2,4,5-T by UV alone, Oxone[®]/UV and FOU processes.

Figure 7-1: Degradation of 0.2 mM 2,4,5-TCP by various processes. $[\text{Oxone}^{\text{®}}]_0$ 127 = 0.5 mM; for FOU, the addition of Fe(II) is 0.2 mM; for EFO and

EFOU, $I = 1 \text{ mA}$; $\text{pH} = 4.35$; $50 \text{ mM Na}_2\text{SO}_4$ were used as electrolyte; two UV 254 nm lamps were employed.

Figure 7-2: Degradation of 0.2 mM 2,4,5-TCP by EFOU process. $[\text{Oxone}^{\text{®}}]_0 = 127$
 0.50 mM , $50 \text{ mM Na}_2\text{SO}_4$ were used as electrolyte, $I = 1 \text{ mA}$, $\text{pH} =$
 4.35 , two UV 254 nm lamps were employed. After 10 min reaction,
a second dosage of $0.50 \text{ mM Oxone}^{\text{®}}$ was added into the system.

Figure 7-3: Degradation of 0.2 mM 2,4,5-TCP by EFOU process under various 128
applied currents. $[\text{Oxone}^{\text{®}}]_0 = 0.50 \text{ mM}$, $50 \text{ mM Na}_2\text{SO}_4$ were used
as electrolyte, $\text{pH} = 4.35$, two UV 254 nm lamps were employed.

Figure 7-4: Figure 7-4: The release of Fe(II) into the Electro-Fe(II)/UV system 129
under various applied currents. $50 \text{ mM Na}_2\text{SO}_4$ were used as
electrolyte, two UV 254 nm lamps were employed

Figure 7-5: Degradation of 0.2 mM 2,4,5-TCP by EFOU process under various 131
initial solution pH levels. $[\text{Oxone}^{\text{®}}]_0 = 0.50 \text{ mM}$, $50 \text{ mM Na}_2\text{SO}_4$
were used as electrolyte, $I = 1 \text{ mA}$, two UV 254 nm lamps were
employed.

Figure 7-6: Degradation of 0.2 mM 2,4,5-TCP by EFOU process under various 133
current-applying modes. $[\text{Oxone}^{\text{®}}]_0 = 0.50 \text{ mM}$, $\text{pH} = 4.35$, 50 mM
 Na_2SO_4 were used as electrolyte, $I = 1 \text{ mA}$, two 254 nm UV lamps
were employed.

Figure 7-7: Degradation of 0.2 mM 2,4,5-TCP by EFOU process under tandem 135
addition of $\text{Oxone}^{\text{®}}$. $50 \text{ mM Na}_2\text{SO}_4$ were used as electrolyte, $I = 1$
 mA , two 254 nm UV lamps were employed.

LIST OF TABLES AND SCHEMES

Table 2-1:	Summary of physiochemical characteristics of RhB.	8
Table 2-2:	Summary of physiochemical characteristics of 2,4,5-T.	11
Table 2-3:	Summary of physiochemical characteristics of 2,4,5-TCP.	14
Table 2-4:	Redox potentials of selected radicals.	25
Table 2-5:	Standard reduction potentials of some most commonly reported oxidants.	26
Table 3-1:	List of chemicals and solvents used in this study.	34
Table 5-1:	The electrical energy required to degrade 0.1 mM 2,4,5-T at various applied current by EFO.	71
Table 6-1:	Summary of identified aromatic intermediates determined by LC/ESI-MS upon degradation of 2,4,5-T.	108
Scheme 6-1:	Proposed decay pathways of 2,4,5-T by UV alone (dotted line), Oxone [®] /UV (solid line with single arrow) and FOU (solid line with double arrow) processes.	118
Scheme 7-1:	Proposed reaction pathway of the degradation of 2,4,5-TCP by the EFOU process.	136

LIST OF ABBREVIATIONS

Abbreviation	Full name
AOPs	Advanced oxidation processes
CPs	Chlorophenols
EF	Electro-Fenton
EFO	Electro-Fe(II)/ Oxone [®]
EFOU	Electro-Fe(II)/Oxone [®] with UV irradiation
FO	Fe(II)/Oxone [®] or Fe(II)-mediated Oxone [®] process
FOU	Fe(II)/Oxone [®] /UV or Fe(II)-mediated Oxone [®] process with UV irradiation
HDA	Hydroxyl-dichlorophenoxyacetic acid
HPLC	High performance liquid chromatography
MW	Molecular weight
RFO	RhB:Fe(II):Oxone [®]
RhB	Rhodamine B
SHE	Standard hydrogen electrode
SOCs	Synthetic organic compounds
SR-AOPs	Sulfate radical based-advanced oxidation processes
2,4-D	2,4-Dichlorophenoxyacetic acid
2,4-DCP	2,4-dichlorophenol
2,4,5-T	2,4,5-Trichlorophenoxyacetic acid
2,4,5-TCP	2,4,5-Trichlorophenol
IS	Ionic strength
TOC	Total organic carbon

CHAPTER 1

Introduction

1.1 Background

“The house is new, the money is enough, but the water is foul, and life is short.”

——A popular saying in China’s developed eastern region (Schmidt, 2002).

Water shortage is already a major global concern of the twenty-first century. It is estimated that more than half of the world’s population will be affected by water shortages by the year of 2032 (Vass, 2002). China is one of the countries with a severe water shortage problem with more than 400 out of the 667 cities in China facing water shortage (Jiang et al., 2010). The annual per capita renewable freshwater availability in China is less than 2200 m³ (only one fourth of the world’s average) (Cheng and Hu, 2011) and it will go down to around the water stress threshold of 1700 m³ suggested by Falkenmark and Widstrand (1992) by the year of 2030 due to population growth, accelerated urbanization and rapid industrialization (Cheng et al., 2009). Unfortunately, water shortages in China are further deteriorated by water pollution. It is reported that nearly half of China’s 1.3 billion people drink water contaminated with chemicals and biological wastes (Schmidt, 2002). Against this background, actions should be taken to reduce water pollution, thereby protecting water sources.

There is an overwhelming increase in the production and utilization of synthetic organic compounds (SOCs) to meet the ever-increasing requirements of human beings since the

1930s. Although many of them have played an important role in the development of modern society, one major concern is the environment and human health risks posed by the application of SOC_s as most of them are persistent to biodegradation, highly toxic and may even cause carcinogenic and mutagenic effects on living organisms (Eleren and Alkan, 2009). Currently, the contamination of water sources by SOC_s is one of the concerning environmental issues faced throughout the world. SOC_s are reported to be common contaminants in both plant wastewater and drinking water (Moeser et al., 2002). Among the existing SOC_s, dyes and herbicides contribute to a large portion of the confirmed toxic organics and have gained much environmental concern in the past few decades, thus leading to a significant interest in developing alternative treatment technologies for the removal of dyes and herbicides in aqueous medium.

Dyes are widely used in industries, such as textiles, plastics, paper, dyeing, leather, jute, food and cosmetic, etc. It is estimated that around 10^6 tons of different commercial dyes are produced annually world-wide and about 5% - 10% of the dyestuffs are lost in the industrial effluents (Figueroa et al., 2009, Sanroman et al., 2005) with a concentration varying from the range of 10 to 10, 000 mgL⁻¹. Therefore, effluents from these industries contain various synthetic dyes. In China, large amounts of dye wastewater are directly discharged into natural water sources without treatment, particularly in rural area of China. The annual discharge of dye-containing wastewater in China is reported to be over 1.6×10^9 m³ (Liu et al., 1999). The complex aromatic structures and stable properties make most of the dyes resistant to biological degradation and photodegradation (Ai et al., 2007, Mittal and Venkobachar, 1996), which indicates that conventional wastewater treatment technologies are normally ineffective for these compounds (Migliorini et al., 2011). In addition, color interferes with the penetration of

sunlight into waters, retards photosynthesis, inhibits the growth of aquatic biota and interferes with gas solubility in water bodies (Couto, 2009). Besides, dyes are also aesthetically undesirable due to their visibility even at rather low concentration (Kusic et al., 2011). Moreover, many of dyes can cause health problems such as allergic dermatitis, skin irritation (Donia et al., 2009) and some of them are even toxic, carcinogenic and mutagenic (Panda et al., 2009). Therefore, dyes in wastewater have now been considered as environmental pollutants and there is an urgent need for the decoloration and elimination of dyes from industrial effluent before being discharged into water bodies.

Synthetic organic herbicides, one of the subclasses of pesticides, are employed to kill unwanted plants or control the growth of nuisance weeds and extensively used in agriculture to minimize economic losses. Herbicides usually have sufficient water solubility and thus can be easily washed away to the surface water bodies via runoff or leaching into the ground water. Generally, herbicides may enter into aquatic ecosystems by two routes: intentionally through the use of registered aquatic herbicides or unintentionally as non-point source pollution (Freeman and Rayburn, 2006). China is a leading agricultural country and agriculture in China feeds around 22% of the global population (Piao et al., 2010), which makes the use of herbicides ranking first worldwide. Presently, around a half million tons of herbicides are annually consumed in China and 70% - 80% of them are directly released into the environment. The long-term abuse of herbicides has resulted in rising contaminations of surface water and ground water systems. Thus, herbicides are among those of the most frequently detected organic pollutants in natural waters and are a major concern for water quality. They are generally found in the range of nano- to micro-grams per liter in surface and ground

waters. Besides, the rapid population increase and the corresponding increase in agricultural product demand in china are expected to substantially increase the use of herbicides, thereby unambiguously deteriorating the herbicide pollution situation in the near future. These pollutants are particularly hazardous, as they are chemically developed to be toxic and usually persistent, and recalcitrant, leading to the ineffective elimination of these substances by traditional wastewater treatment processes. As a result, the past decades have witnessed increasing research interest in the investigation of reliable wastewater treatment technologies, aiming to explore a feasible and economical wastewater treatment method which can be applied to effectively degrade herbicides from the waste waters.

1.2 Aims and Objectives

In this study, sulfate- and hydroxyl radical-based advanced oxidation processes (AOPs) such as Fe(II)/Oxone[®], Electro-Fe(II)/Oxone[®] process, Fe(II)/Oxone[®]/UV and Electro-Fe(II)/Oxone[®]/UV process for the destruction of SOC_s in aqueous solution are studied to evaluate their potential to degrade three selected kinds of SOC_s. Since the information concerning the removal of SOC_s by Electro-Fe(II)/Oxone[®] process with or without UV irradiation is very limited as revealed in the literature review presented in Chapter 2, to the best of our knowledge, the present study is the first attempt to explore the possibility of sulfate radical generation by electrochemical enhanced advanced oxidation processes (AOPs) to degrade SOC_s. Therefore, the major objective of this study is to examine the use of different treatment processes with respect to their potential for the removal of SOC_s present in wastewater before discharging to the public. The specific research tasks of the present thesis are as following:

- 1) To investigate the feasibility of degrading three selected kinds of SOC_s (i.e. RhB, 2,4,5-T and 2,4,5-TCP) by different types of wastewater treatment processes such as Fe(II)/Oxone[®] process, Electro-Fe(II)/Oxone[®], Fe(II)/Oxone[®] assisted with UV irradiation, and UV-assisted Electro-Fe(II)/Oxone[®] throughout this study.
- 2) To identify the crucial factors governing the degradation performance of these processes such as variations of initial pH level, pollutant concentration, oxidant dosage, ferrous dosage, inorganic salt, applied current, electrolyte concentration, light intensity and wavelength. To optimize process performance through proper design of operating conditions.
- 3) To explore and compare the reaction mechanisms and decay pathways of a selected SOC_s (i.e. 2,4,5-T) by the treatment of UV alone, Oxone[®]/UV and FOU processes through examining the evolution of aromatic intermediates by LC/MS-ESI analysis.
- 4) To elucidate the role of UV irradiation by investigating the degradation of 2,4,5-T by FO and FOU processes assisted with monitoring and comparing the evolution of Fe(II) in these two system.
- 5) To evaluate the efficiency of ultimate pollutant removal by investigating the mineralization efficiency of selected process.

1.3 Organization of the Thesis

This thesis is composed of eight chapters. The present chapter first provides the background information and the objectives of the thesis. Finally, this chapter

summarizes the thesis organization.

A comprehensive literature review of issues related to this study is given in Chapter 2, where background information referring to RhB, 2,4,5-T and 2,4,5-TCP is provided and AOPs are described in detail. Particularly, the theories of Fenton's reagent-based AOPs and sulfate radical-based AOPs are discussed in-depth, respectively.

In Chapter 3, the detailed descriptions of materials and methodology employed in this study are reported.

The work presented in Chapter 4 reports the experimental results in terms of RhB degradation by Fe(II)-mediated activation of Oxone[®] process. The effect of various parameters including Fe(II)/Oxone[®] ratio, initial pH values of the solution and various inorganic salts on the performance of Fe(II)/Oxone[®] process is investigated. In addition, the mineralization of RhB under various conditions is also monitored.

Chapter 5 addresses the investigation on the decay of 2,4,5-T by Electro-Fe(II)/Oxone[®] process through examining the effect of several important parameters including applied current, electrolyte concentration, initial solution pH, 2,4,5-T and oxidant dosage. Besides, radical quenching study is conducted to identify the main radicals dominating in the reaction.

In Chapter 6, degradation of 2,4,5-T by FOU process is explored. Effects of various UV wavelengths, Fe(II) concentration, initial solution pH, Oxone[®] dosage and various anions on the process performance are examined. Especially, the role of UV irradiation

in FOU process is elucidated in-depth. Furthermore, main aromatic intermediates of 2,4,5-T decay by UV alone, Oxone[®]/UV, and FOU processes are identified by LC-ESI/MS analysis, and corresponding decay mechanisms and pathways are proposed accordingly in this chapter.

Based on the processes reported in Chapters 5 and 6, Chapter 7 is focused on the development of combining the EFO and FOU together to form a more efficient process, in which the 2,4,5-TCP aqueous solution treated under Electro-Fe(II)/Oxone[®] is simultaneously exposed to UV irradiation (i.e., EFOU). This EFOU process is examined through the degradation of 2,4,5-TCP under various operating conditions. Especially, the mode of current-applying and tandem addition of Oxone[®] on the effect of process performance are also explored. Furthermore, the reaction mechanism and decay pathways of 2,4,5-TCP in this system is proposed according to the aromatic intermediates observed by LC-ESI/MS analysis incorporating with cited literature.

Chapter 8 illustrates conclusions of the thesis. Besides, some recommendations are also presented, where the remaining questions and possible following up investigations related to this study are discussed.

CHAPTER 2

Literature Review

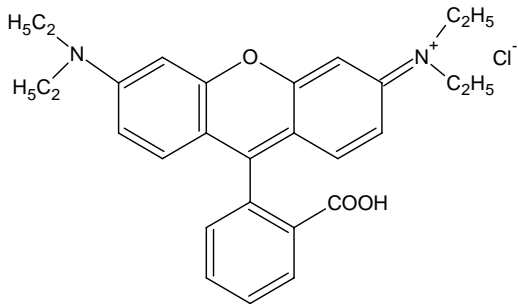
2.1 Probe Contaminants

2.1.1 Rhodamine B

2.1.1.1 Background

Rhodamine B (RhB) is an important representative of xanthene-based dyes. It is extensively used as a colorant in various textile-processing industries and food stuffs, including dyeing silk, wool, jute, leather, cotton and so on, as a tracer to determine the rate and direction of flow and transport within water. Additionally, it is also a well-known water tracer fluorescent and has a variety of applications in modern photochemistry. Besides, it is also employed as a dye laser material and sensitizer because of its good stability (Asilturk et al., 2006). Its physiochemical characteristics are tabulated in Table 2-1.

Table 2-1: Summary of physiochemical characteristics of RhB.

parameter	Value/Information
Chemical structure	
Suggested name	Rhodamine B

	<i>Cont'd Table 2-1</i>
Molecular formula	C ₂₈ H ₃₁ N ₂ O ₃ Cl
Formula weight	479.01
C.I. number	45170
C.I. name	Basic violet 10
Ionization	Basic
Appearance	green crystals or reddish-violet powder
Solubility in water	0.78%
Solubility in ethanol	1.47%
pK _a	6.41

2.1.1.2 Toxicological effects

The LD₅₀ for RhB in oral mouse is 887 mg/kg. Human exposure to RhB may cause harmful health effects. RhB is harmful if swallowed by human beings and animals, and can cause irritation in contact with skin, eyes and respiratory tract (Rochat et al., 1978). The carcinogenicity, reproductive and developmental toxicity, neurotoxicity and chronic toxicity towards humans and animals have been experimentally proven (Mirsalis et al., 1989). In California, USA, it is required that products containing RhB must contain a warning on their labels.

2.1.1.3 Previous degradation studies of RhB

RhB is a common organic pollutant. It is a very stable non-volatile water-soluble dye. RhB has a comparatively high resistance to photo and oxidation degradation and high stability to light, temperature and detergent. Apart from the toxicological effects and relative persistence of RhB, color due to the discharge of RhB-containing wastewater is

another major environment concern. Based on the above concerns, the treatment of effluents containing such compound is of great importance to avoid any hazardous and harmful effects towards environment and human health.

Conventional physico-chemical processes including chemical coagulation, membrane filtration, and adsorption (Anandkumar and Mandal, 2011) have demonstrated effective removal of RhB from wastewaters, however, these processes are generally non-destructive and suffer from certain limitations (Blackburn, 2004). Thus, there have been a number of research works focusing on developing efficient treatment techniques for the decoloration and/or degradation of RhB. Amongst, growing interest is now focused on the removal of RhB from effluent using AOPs, such as UV/H₂O₂ (AlHamedi et al., 2009), Ozone-based AOP (Bai et al., 2011), photocatalytic process (Merka et al., 2011), and Fenton-like process (Hou et al., 2011). Nevertheless, it is worth mentioning that no information is available regarding the degradation of RhB by using Fe(II) activated decomposition of Oxone[®] process based on a review of the scientific literature.

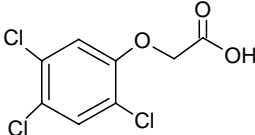
2.1.2 2,4,5-Trichlorophenoxyacetic acid

2.1.2.1 Background

2,4,5-Trichlorophenoxyacetic acid (2,4,5-T), an organochlorine compound, was developed in the late 1940s and belongs to the chlorophenoxy acetic acid herbicides. It has been used worldwide on a large scale in agriculture to selectively control the growth of broad-leaved weeds on cereal crops, grasslands and lawns and also used in post-emergence applications until being phased out, starting in the late 1970s due to toxicity concerns. Its use in aquatic weed control was also reported (Bukowska, 2004).

Apart from agricultural uses, 2,4,5-T was also a major ingredient in Agent Orange, a herbicide blend used by the U.S. military in Vietnam between January 1965 and April 1970 as a defoliant. Its physiochemical characteristics were summarized in Table 2-2.

Table 2-2: Summary of physiochemical characteristics of 2,4,5-T

parameter	Value/Information
Chemical structure	
IUPAC name	(2,4,5-Trichlorophenoxy)acetic acid
Molecular formula	C ₈ H ₅ Cl ₃ O ₃
Formula weight	255.48
Appearance	Off-white to yellow crystalline solid
Solubility in water	278 ppm at 25°C
Melting point	154 - 158°C
pK _a	2.88
Biodegradation	> 205 days for ring cleavage in soil suspension

2.1.2.2 Toxicological effects

2,4,5-T is considered to be of moderate toxicity by the World Health Organization. It has potential toxicity towards human beings and animals. It has been stated that the oral dose required to produce symptoms in man is probably 3-4 g, while the LD₅₀ for 2,4,5-T in mice and in rats is 389 mg/kg and 500 mg/kg, respectively. Human exposure to 2,4,5-T has been associated with numerous clinical manifestations, such as nervous system and brain damage. Disturbances in cell division and inhibition of embryo development on sea urchin eggs have been observed after being exposed to 2,4,5-T

(Graillet and Girard, 1994). Besides, it is considered to be toxic by ingestion and inhalation and may be harmful to skin by contact. Additionally, it may also act as a human carcinogen and may cause reproductive damage. In USA, 2,4,5-T is classified as neurotoxin and thus has been banned from use by EPA since 1985.

2.1.2.3 Previous degradation studies of 2,4,5-T

2,4,5-T was once extensively used worldwide for agricultural and non-agricultural purposes last century. Although its use was terminated in many developed countries, it is still widely used in practice nowadays in most developing countries to control weeds and enhance crops yield. Due to its relatively high solubility in water, it can be readily washed away to the surface water bodies or reach water-bearing aquifers below ground from application onto crop fields. On the other hand, it is considered to be less readily biodegradable than the analogous herbicide 2,4-D (Chaudhary et al., 2009) and persists for long periods of time in the environment. The half-life for the degradation of 2,4,5-T is estimated to be 12-59 days (1996). As a result, 2,4,5-T can be detectable in both of surface water and groundwater not only during the application of the herbicide, but also after a long period of use due to its comparative resistance to biodegradation. Thus, as a potential contaminant of ground and surface waters, there is pressing need to destroy such compound in aqueous medium for the protection of waters and environment.

Currently, various processes including adsorption (Gomezjimenez et al., 1987), biological degradation (Daubaras et al., 1996, de Lipthay et al., 2007) and AOPs have been investigated and developed to degrade 2,4,5-T for the environmental concern. Among these emerging treatment technologies, it has been well established that AOPs are one of the most promising alternatives and therefore are gaining significant

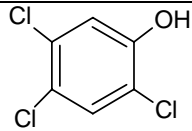
importance in water treatment applications (Chan and Chu, 2009) nowadays. A variety of AOPs have been explored for the degradation of 2,4,5-T from contaminated water, such as Electro-Fenton process (Brillas et al., 2004), Photoelectro-Fenton process (Boye et al., 2003), photolytic-electrolytic system (Chaudhary et al., 2009) and UV/TiO₂ (Hemant et al., 2007). Nevertheless, up to date, the role of highly powerful sulfate- and hydroxyl radicals generated by the Electro-Fe(II)/Oxone[®] process or Fe(II)/Oxone[®] assisted with UV irradiation has seldom been discussed, according to a review of literature on the issue recently conducted by the author of this thesis.

2.1.3 2,4,5-Trichlorophenol

2.1.3.1 Background

2,4,5-trichlorophenol (2,4,5-TCP) is an important representative of chlorinated organic compounds and has been widely used as disinfectant, fungicide, wood preserver and plant growth regulator over the past few decades. For example, it is used as a fungicide to destroy or inhibit the growing of fungi by the paper and pulp mills. Besides, 2,4,5-TCP has also been used in the production of a variety of biocides. It is used in the manufacture of the herbicide 2,4,5-T and of the bactericide, hexachlorophene (Hay, 1978). Especially, it is also formed as the primary intermediate upon the decay of 2,4,5-T by the treatment of AOPs (Boye et al., 2003, Brillas et al., 2004) and also microbial activities (Daubaras et al., 1995). 2,4,5-TCP is also found in the pulp bleaching wastewater. Although its use as a biocide has been banned in many countries, the application of 2,4,5-TCP as a fungicide in wood and leather impregnation can be still found. Its physiochemical characteristics were summarized in Table 2-3.

Table 2-3: Summary of physiochemical characteristics of 2,4,5-TCP.

parameter	Value/Information
Chemical structure	
IUPAC name	1-hydroxy-2,4,5-trichlorobenzene
CAS name	2,4,5-Trichlorophenol
Molecular formula	C ₆ H ₃ Cl ₃ O
Formula weight	197.46
Appearance	White crystalline powder
Solubility in water	1200 ppm at 20°C
Melting point	68°C
pK _a	7.4
Log K _{OW}	3.72
Residence time in soil	> 72 days for complete disappearance

2.1.3.2 Toxicological effects

2,4,5-TCP is considered to have significant toxicological effects and potential carcinogenicity. It is well known that the toxicity, persistence and bioaccumulative potential of chlorophenols increase with the degree of chlorination (Annachhatre and Gheewala, 1996). Sharma et al. (1997) reported that the trend of increasing toxicity of phenols with increasing chlorination is evident and 2,4,5-TCP has the highest toxicity among the four tested phenols (i.e., 2,4,5-TCP, 2,4-dichlorophenol, 4-chlorophenol, and phenol). 2,4,5-TCP has been included in the “persistent, bioaccumulative, and toxic chemical list” by the United States Environmental Protection Agency (U.S. EPA),

representing a serious threat to human health and natural ecosystems.

2.1.3.3 Previous degradation studies of 2,4,5-TCP

2,4,5-TCP is resistant to biodegradation in aerobic and anaerobic system (Matus et al., 1996), thereby tending to bioaccumulate in the environment. 2,4,5-TCP is considered to be more resistant to biodegradation than other trichlorophenols (Marsolek et al., 2007). As a result, it is listed as one of the priority pollutants by U.S. EPA (Sitting, 1981). The broad application of 2,4,5-TCP during the past few decades has lead to its widespread distribution in the natural environment. Low levels of 2,4,5-TCP were found in drinking water in several places in the world (Zaghouane-Boudiaf and Boutahala, 2011). 2,4,5-TCP has also been detected in the leachates from municipal landfills (Pouloupoulos et al., 2007). The wide presence of 2,4,5-TCP in the aquatic environment poses a pollution concern because of its high toxicity and stability. Removal of this pollutant from aquatic environments is therefore a major task of wastewater treatment. In recent years, 2,4,5-TCP has been subjected to various treatment methods, including adsorption (Zaghouane-Boudiaf and Boutahala, 2011), biodegradation (Joshi and Gold, 1993, Marsolek et al., 2007), the combination of biological and photocatalytic treatment (Li et al., 2011, Suryaman and Hasegawa, 2010), and so on. However, the need for the disposal of adsorbed sorbent is an apparent limitation of the adsorption method; the microbiological treatment shows a limited ability to remove 2,4,5-TCP (Matus et al., 1996), which only occurs at low concentration due to inhibition (Li et al., 2011) and usually requires a longer treatment time. In the present study, an attempts will be made to find a more appropriate way to degrade 2,4,5-TCP.

2.2 Advanced Oxidation Processes

AOPs, which are considered to be one of the most effective wastewater treatment methods, are generally defined as the processes involving the generation and use of powerful oxidizing radical intermediates, especially hydroxyl radicals ($\cdot\text{OH}$) and sulfate radicals ($\text{SO}_4^{\cdot-}$), leading to the elimination of target contaminants. These processes include the utilization of sole or combined high oxidation potential oxidants such as ozone, hydrogen peroxide, persulfate and peroxymonosulfate, usually coupled with one or several of the following enhancement tools: irradiation (e.g., UV, solar and visible light), specific catalysts (e.g., TiO_2 and WO_3), sonolysis, electrical energy, thermal activation, microwave, and so on. In general, the list of AOPs that have been considered for wastewater treatment is long and increasing as new processes are developed (Mantzavinos et al., 2009). Processes such as $\text{O}_3/\text{H}_2\text{O}_2$, $\text{O}_3/\text{H}_2\text{O}_2/\text{TiO}_2$, $\text{Fe}^{2+}/\text{H}_2\text{O}_2$, $\text{Fe}^{2+}/\text{H}_2\text{O}_2/\text{UV}$, $\text{H}_2\text{O}_2/\text{UV}$, $\text{S}_2\text{O}_8^{2-}/\text{Ag}^+$, Oxone[®]/Co(II) and $\text{UV}/\text{S}_2\text{O}_8^{2-}$ are the most widely investigated AOPs, where highly reactive species (e.g., HO^{\cdot} and/or $\text{SO}_4^{\cdot-}$) are generated to attack and destroy refractory contaminants present in water and wastewater. The above-mentioned various possible ways for HO^{\cdot} and/or $\text{SO}_4^{\cdot-}$ generation enhance AOPs as a versatile technology, promising a better compliance with specific treatment requirements. In this section, background information concerning the development of sulfate radical-based AOPs and the generation of sulfate and hydroxyl radicals by processes such as Fe(II)/Oxone[®], Fe(II)/Oxone[®]/UV, and Electro-Fe(II)/Oxone[®] process with or without UV irradiation are summarized as follows.

2.2.1 Fenton's reagent-based AOPs

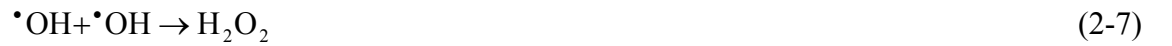
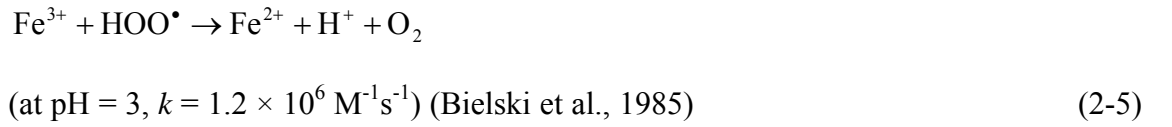
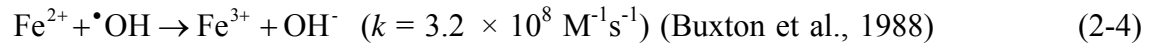
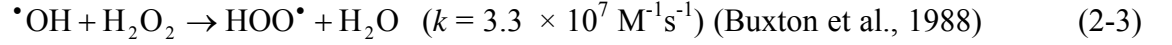
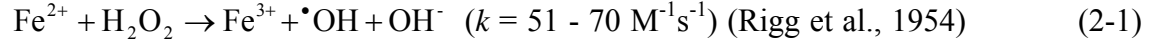
2.2.1.1 Classical Fenton process

Fenton process is one of these typical AOPs and is known for more than a century, dating back to 1894 when H.J.H. Fenton first reported that hydrogen peroxide (H_2O_2)

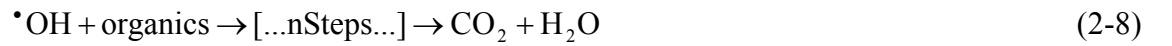
could be activated by ferrous ions for the oxidation of tartaric acid (Fenton, 1894). Nevertheless, the application of Fenton process was introduced to destroy toxic organics in the late 1960s. Usually, the combination of hydrogen peroxide and ferrous salt typically referred to as “Fenton’s reagent” is employed in a classical Fenton process, during which H_2O_2 is rapidly catalyzed in the presence of ferrous ions to generate very reactive oxidizing hydroxyl radicals in accordance with the classical Fenton’s reaction (i.e., Eq. 2-1). $\cdot\text{OH}$ reacts with organics by three mechanisms: electron transfer, hydrogen abstraction, and hydrogen addition. Hydroxyl radicals with the characteristics of a high oxidation potential (1.8 - 2.7 V, depending on the solution pH), fast reaction kinetics with the reaction rates of the order of $10^9 \text{ M}^{-1}\text{s}^{-1}$ (Neyens and Baeyens, 2003) and relative lack of selectivity are capable of completely degrading most toxic organics into harmless compounds such as carbon dioxide, water and simple organic acids. As a result, Fenton process has been demonstrated to be very effective in treating different types of wastewater, including removal of herbicides from agriculture effluents (Chan and Chu, 2003, Kaichouh et al., 2004), treatment of dye-containing wastewater (Ashraf et al., 2006), and removal of COD and color from landfill leachate (Deng and Englehardt, 2006, Lopez et al., 2004), and so on.

The dose of hydrogen peroxide, the ferrous ion concentration and the solution pH, especially the latter, are the determining parameters that significantly influence the performance of Fenton process. It is well established that Fenton’ reagent is a highly pH-dependent process. The optimal pH of Fenton’s reagent has been observed to be in the range of 2-4 according to previous researchers (Fu et al., 2010, He and Wei, 2010, Zazo et al., 2007, Zimbron and Reardon, 2009). Generally, the classical Fenton process

in the dark and in the absence of organic compounds involves the sequence of reactions summarized as follows (Eq. 2-1 to 2-7):



The attack of hydroxyl radicals towards the organic compounds can be simplified as indicated in Eq. 2-8



It can be concluded that Fenton process is attractive due to the fact that ferrous salt is widely available, non-toxic and relative cheap and that the end product of H_2O_2 is environmentally benign. Besides, it is easy to operate and maintain as compared to other AOPs. However, it has to overcome some limitations in the practical application, such as the requirement of low pH environment, extensive consumption of chemicals and inconvenient transportation of hydrogen peroxide. Large amounts of ferric/ferrous hydroxide sludge formation at the end of the reaction which needs further treatment and disposal as solid waste is also one of the drawbacks (Jeong and Yoon, 2005). Besides, it can be noted that the rate constant of Eq. 2-1 is between 51 and 70 $\text{M}^{-1}\text{s}^{-1}$, while the rate

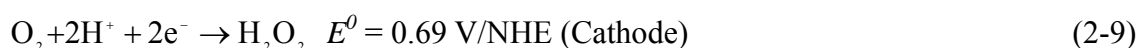
constant of Eq. 2-2 is only $0.01 - 0.02 \text{ M}^{-1}\text{s}^{-1}$. Consequently, the slow regeneration of the ferrous ion catalyst becomes another major weakness of Fenton process. Additionally, careful catalyst and oxidant ratio should be provided because both of ferrous ions and hydrogen peroxide can work as hydroxyl radical scavenger when their amount is overdosed as shown in Eqs. 2-3 and 2-4, which are justified by previous researches (Kassinis et al., 2009, Masomboon et al., 2009).

Driven by the need of overcoming these shortcomings of conventional Fenton's reagent, various modified Fenton or Fenton-like processes have been investigated in the past two decades, such as Fenton-like process using zero valence iron or iron (III) oxide instead of ferrous ions (Cao et al., 2009, Hwang et al., 2010), Electro-Fenton (Anotai et al., 2006, Liu et al., 2007, Sires et al., 2007, Ventura et al., 2002, Yuan et al., 2006), photo-Fenton (Feng et al., 2006, Perez-Estrada et al., 2005), microwave-enhanced Fenton (Li et al., 2010, Yang et al., 2009), and so on.. The modified Fenton processes related to this study will be described as follows.

2.2.1.2 Electro-Fenton process

Among the various modified Fenton technologies currently available, the application of indirect oxidation of electrochemical method in Fenton process called Electro-Fenton (EF) has attracted considerable attention due to its outstanding performance in eliminating toxic organics from aqueous media. The generally accepted EF mechanism involves the in situ electro-generation of hydrogen peroxide and ferrous ions electrochemically, either separately or concurrently. Namely, three kinds of EF processes have been explored: (a) the on-site electrochemical generation of H_2O_2 coupled with the addition of a small quantity of ferrous ions as catalyst, (b) the

simultaneous electro-generation of H_2O_2 and Fe(II) , and (c) ferrous ions were electro-generated from a sacrificial iron anode, while hydrogen peroxide was externally added. Theoretically, H_2O_2 can be electro-generated via the two-electron reduction of dissolved oxygen at the cathode, while ferrous ions can be electrically generated on a sacrificial anode through iron oxidation and regenerated on the cathode through the equations as follows:



Once an electrical current is applied, the EF will be formed and the powerful oxidizing hydroxyl radicals are generated upon the reaction of H_2O_2 with ferrous ions through Eq. 2-1. The other side reaction, which simultaneously occurs at the cathode, is the reduction of ferric ions shown as follows:



In classical Fenton process, the rapid depletion and slow regeneration of ferrous ions throughout the reaction is one of the main drawbacks. However, it is not a limitation during the EF process mainly because that the catalytic reaction is propagated by Fe(II) regeneration at the cathode as shown in Eq. 2-11. This immediate regeneration of Fe(II) guarantees the continuous production of $\cdot\text{OH}$ and also allows a better control of hydroxyl radical production. Moreover, the EF process avoids the need of transporting large quantity of chemicals and thus lowers the application cost.

Currently extensive research studies regarding the EF process have been focused on the electro-generation of hydrogen peroxide. Under this situation, the performance of EF process mainly depends on the cathode materials used in the study. As a result, various

cathode electrodes have been developed to enhance the EF process efficiency. Cozmen et al. employed a carbon felt as the cathode to elucidate the mechanism and kinetics of bisphenol A conversion under EF conditions and determined the efficiency of the electrochemically induced Fenton process (Gozmen et al., 2003). Pimentel et al. also presented that 100% of TOC from phenol aqueous solution was removed by using added soluble ferrous ions as catalyst and carbon felt as working electrode (Pimentel et al., 2008). In another study, corrosion-resistant platinum of 99.9% purity electrode was utilized to examine the decomposition of nitrotoluenes (Chen and Liang, 2008). Other materials, including boron doped diamond, carbon sponge (Ozcan et al., 2009), graphite rod (Liu et al., 2007) and self-made electrodes (Li et al., 2009a), and so on, have been extensively explored as the cathodes for the production of H_2O_2 during EF process.

Nevertheless, it is worth mentioning that the in situ generation of Fe(II) using iron as sacrificial anode has been reported in only a few studies for a very limited number of cases (Li et al., 2007).

2.2.1.3 Photo-Fenton and photo-Fenton-like processes

Another alternative to the Fenton's reagent is the photo-Fenton process. It is well known that the generation of hydroxyl radicals as well as its production rate of Fenton process could be enhanced in the presence of an irradiation source (UV-Visible irradiation or solar irradiation), thus increasing the performance of the process, which is the so-called photo-Fenton process. The irradiation employed in the process involves the utilization of UVA ($\lambda = 315\text{-}400\text{ nm}$), UVB ($\lambda = 285\text{-}315\text{ nm}$), and UVC ($\lambda < 285\text{ nm}$) as energy source. The positive effect of irradiation on the performance efficiency is primarily attributed to the photo-reduction of ferric ions to ferrous ions, which can generate additional hydroxyl radicals and is also an essential step that promises the further

reaction of hydrogen peroxide with photo-generated ferrous ion catalyst. The photo-reduction of ferric ions follows Eq. 2-12 as below:



It can be noted that the above reaction leads to the continuous generation of Fe(II), enhances the catalytic cycle of Fe(III)/Fe(II), thereby minimizing the required catalyst concentration. It was determined that Fe(III) exists approximately as half of ferric ions and half of $\text{Fe}(\text{OH})^{2+}$ in the optimum pH range (acidic conditions) of photo-Fenton process. Additionally, $\text{Fe}(\text{OH})^{2+}$ has absorption bands between 290 and 400 nm (Gogate and Pandit, 2003). Considering that UV light only accounts for a small portion (~ 5%) of the sun spectrum in comparison to the visible region (~ 45%) (Rao and Chu, 2009), the absorption characteristic of $\text{Fe}(\text{OH})^{2+}$ makes the use of near-UV and even solar energy as a light source feasible, resulting in a more energy efficient treatment process for commercial applications. Besides, the direct photolysis of H_2O_2 also contributes to the production of hydroxyl radicals according to Eq. 2-13, although $\cdot\text{OH}$ formation by this process is very slow.



In general, the production of $\cdot\text{OH}$ is enhanced in the photo-Fenton process due to three simultaneous reactions including Fenton process, photolysis of ferric ions to ferrous ions and direct photolysis of hydrogen peroxide ($\text{H}_2\text{O}_2/\text{UV}$). Consequently, the photo-Fenton process has gained increasing attention as a very promising water treatment method for the degradation of recalcitrant organic pollutants, including dyes (Chacon et al., 2006, Garcia-Montano et al., 2006), herbicides (Farre et al., 2006), landfill leachate (Primo et al., 2008), etc.

Recently, ferric ions or iron-based organometallic complexes and hydrogen peroxide coupled with UV irradiation was found to be a more attractive process than the classical Fenton process and exhibited an equivalent toxic organic removal efficiency compared with the photo-Fenton ($\text{Fe(II)/H}_2\text{O}_2/\text{UV}$), which was identified as photo-Fenton-like process. Alaton and Gurses (2004) reported that UV-A light assisted Fenton-like ($\text{Fe}^{3+}/\text{H}_2\text{O}_2/\text{UV-A}$) process presented a much better COD and TOC removal of procaine penicillin G formulation effluent in comparison with the process without irradiation. Kwan's study demonstrated that the transformation of 2,4-Dichlorophenoxy acetic acid was significantly improved when a higher light sensitive organometallic complex (ferrous oxalate) instead of ferrous ions was employed in the photo-Fenton-like process (Kwan et al., 2007), and the experimental results concluded that the $\text{Fe}^{2+}/\text{oxalate}/\text{H}_2\text{O}_2/\text{UV}$ system presented the most effective and efficient treatment among the several investigated processes including UV only, oxalate/UV, $\text{H}_2\text{O}_2/\text{UV}$, oxalate/ $\text{H}_2\text{O}_2/\text{UV}$, $\text{Fe}^{2+}/\text{H}_2\text{O}_2/\text{UV}$ and $\text{Fe}^{2+}/\text{oxalate}/\text{H}_2\text{O}_2/\text{UV}$.

Overall, the reaction pathways for the photo-Fenton or photo-Fenton-like process with the primary photolysis of the dissolved Fe(III) complexes to ferrous ions can be mechanically illustrated in Figure 2-1 (Gogate and Pandit, 2003).

From the above mechanism of the photo-Fenton or photo-Fenton-like process, it can be concluded that these processes have the advantages of accelerating the catalytic reaction of Fe(III) to Fe(II) , thus lowering the amount of the required Fe(II) dosages and preventing the production of iron complexes sludge, and providing additional $\cdot\text{OH}$. However, there is still room to improve. Strict acidic limitation of operating pH is still a critical factor affecting the performance of the photo-Fenton based processes.

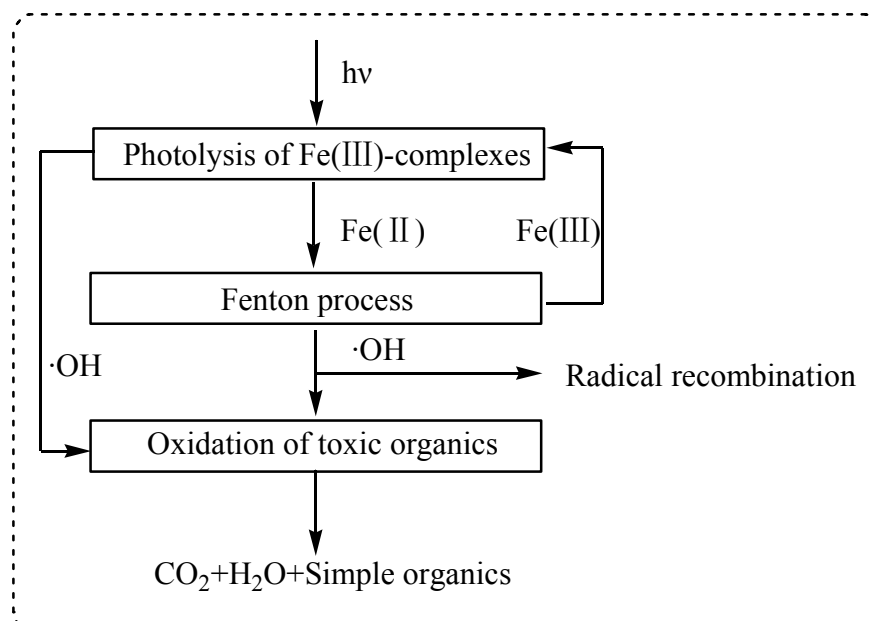
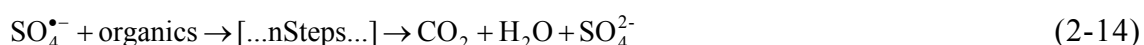


Figure 2-1: Reaction pathways of the photo-Fenton or photo-Fenton-like process.

2.2.2 Sulfate radical-based AOPs

To overcome the limitations of Fenton's reagent-based AOPs, there has been significant research in an alternative method for the degradation of various organic contaminants. One important type of these technologies involves the utilization of persulfate ($\text{S}_2\text{O}_8^{2-}$) or peroxymonosulfate (Oxone®) as oxidant for the generation of highly powerful sulfate radicals that can oxidize most organics in wastewater in a broad pH range ($1 \leq \text{pH} \leq 10.5$) (Anipsitakis and Dionysiou, 2004b), which are the well-known sulfate radical-based AOPs. The interaction of $\text{SO}_4^{\bullet-}$ toward organic compounds can be depicted in Eq. 2-14.



Sulfate radicals are considered to demonstrate higher standard reduction potential (2.5 – 3.1 V) than hydroxyl radicals at neutral pH (Chan and Chu, 2009) and more selective

for oxidation than hydroxyl radicals at acidic pH. In fact, $\text{SO}_4^{\bullet-}$ is among the strongest oxidants known, much stronger than oxidants commonly used in industry, such as permanganate and hypochlorous acid. The comparison of redox potential of some radicals is summarized in Table 2-4 and the standard reduction potentials of some most commonly reported oxidants are given in Table 2-5. Anipasitakis and Dionysiou (2004a) have reported that sulfate radicals are more efficient oxidants than hydroxyl radicals at least for the transformation of 2,4-dichlorophenol (2,4-DCP), atrazine, and naphthalene under certain conditions.

Table 2-4: Redox potentials of selected radicals.

Selected radicals	Redox potentials
$\text{SO}_4^{\bullet-} + e^- \rightarrow \text{SO}_4^{2-}$	2.5-3.1 V
$\cdot\text{OH} + e^- \rightarrow \text{OH}^-$	1.8 V
$\cdot\text{OH} + e^- + \text{H}^+ \rightarrow \text{H}_2\text{O}$	2.7 V or 2.38 V
$\text{HO}_2^{\bullet} + 3\text{H}^+ + 3e^- \rightarrow 2\text{H}_2\text{O}$	1.65
$\text{HO}_2^{\bullet} + \text{H}^+ + e^- \rightarrow \text{H}_2\text{O}_2$	1.44
$\text{SO}_5^{\bullet-} + e^- \rightarrow \text{SO}_5^{2-}$	1.1 V

(Reference from:(Anipsitakis and Dionysiou, 2003, Brillas et al., 2009))

Similarly to $\cdot\text{OH}$, $\text{SO}_4^{\bullet-}$ react with organic compounds mainly by the mechanisms of electron transfer, hydrogen abstraction or hydrogen addition (Neta et al., 1977). Nevertheless, the half life of sulfate radicals is longer than that of hydroxyl radicals due to that $\text{SO}_4^{\bullet-}$ is more selective for electron transfer reactions while $\cdot\text{OH}$ can participate in a variety of reactions with equal preference (Rastogi et al., 2009). Thus, sulfate radical acts as a more efficient oxidant than hydroxyl radical because of its better selectivity for

oxidation. As a result, sulfate radical-based-AOPs are currently gaining significant scientific interest in wastewater treatment applications.

Table 2-5: Standard reduction potentials of some most commonly reported oxidants.

Oxidant	E^0/V vs SHE
Fluorine (F ₂)	3.05
Ferrate ion ([FeO ₄] ²⁻)	2.20
Atomic oxygen (O)	2.42
Ozone (O ₃)	2.075
Persulfate ion (S ₂ O ₈ ²⁻)	2.05
Peroxymonosulfate (HSO ₅ ⁻)	1.82
Hydrogen peroxide (H ₂ O ₂)	1.763
Potassium permanganate (KMnO ₄)	1.67
Chlorine dioxide (ClO ₂)	1.50
Hypochlorous acid (HClO)	1.49
Dichromate ion (Cr ₂ O ₇ ²⁻)	1.36
Chlorine (Cl ₂)	1.358
Manganese dioxide (MnO ₂)	1.23
Oxygen (O ₂)	1.229
Bromine (Br ₂)	1.065

SHE- standard hydrogen electrode

(Reference from: (Brillas et al., 2009, Lin and Yeh, 1993))

One way for enhancing the development of activation of persulfate or Oxone[®] for the generation of SO₄^{•-} is based on the mechanism of Fenton process that the powerful oxidizing radicals were generated by the combination of a transition metal with

common oxidant. Thus, numerous transition metals as well as oxidants were explored as the possible conjunction of the highly oxidizing radical generation in the past few years. Theoretically, extensive metal cations in their lower oxidization state can be employed as metal catalysts for powerful oxidizing radical generation. According to Anipsitakis and Dionysiou' study, among the nine investigated transition metals (Fe^{2+} , Fe^{3+} , Ag^+ , Ce^{3+} , Co^{2+} , Mn^{2+} , Ni^{2+} , Ru^{3+} , V^{3+}) and three oxidants (H_2O_2 , peroxymonosulfate, persulfate), Fe(II) and Fe(III) were the most efficient transition metals toward catalyzing H_2O_2 as expected, Co(II) and Ru(III) demonstrated the best results toward the activation of peroxymonosulfate for sulfate radicals generation, while for the activation of persulfate, Ag(I) showed the best catalytical result (Anipsitakis and Dionysiou, 2004a). More recently, numerous studies showed that sulfate radicals generated by the combination of persulfate or peroxymonosulfate with transition metals (e.g., Fe^{2+} , Ag^+ and Co^{2+}) have presented great promise in the degradation of organic contaminants in wastewater. Other methods to activate the decomposition of persulfate ($\text{S}_2\text{O}_8^{2-}$) or Oxone[®] include the utilization of photolytic activation or thermal activation. These activation processes lead to the formation of one type of radical, $\text{SO}_4^{\bullet-}$, or a mixture of $\text{SO}_4^{\bullet-}$ and $^{\bullet}\text{OH}$ depending on the oxidant employed. The generation of highly reactive species by the decomposition of persulfate or Oxone[®] activated via different methods will be discussed in the following sections.

2.2.2.1 Sulfate radical generation via the activation of $\text{S}_2\text{O}_8^{2-}$

Persulfate ion ($\text{S}_2\text{O}_8^{2-}$) is a thermodynamically strong, two-electron oxidant ($E^0 = 2.05$ V) which has been widely used in the petroleum industry for the treatment of hydraulic fluids or as a reaction initiator. Reduction of $\text{S}_2\text{O}_8^{2-}$ leads to the production of two sulfate anions in accordance with Eq. 2-15:



Presently, $\text{S}_2\text{O}_8^{2-}$ has drawn increasing attention as an alternative oxidant for treating toxic organics in wastewater (Li et al., 2009b, Waldemer et al., 2007) and contaminated soil (Killian et al., 2007). The use of $\text{S}_2\text{O}_8^{2-}$ bears several significant advantages, including being highly aqueous soluble, cost-efficient, readily available, relatively stable at room temperature, and capable of producing environmental benign inert SO_4^{2-} as the end product (Lau et al., 2007). Nevertheless, if without appropriately activation, $\text{S}_2\text{O}_8^{2-}$ slowly reacts with many organics at ambient temperate. Thermal, photolytic or transition metal activated decomposition of persulfate ions for the generation of $\text{SO}_4^{\bullet-}$ has been proposed as the possible alternative of enhancing the process and has been widely studied (Johnson et al., 2008, Liang and Su, 2009). The thermal or photolytic decomposition of persulfate can be described as below:



While the activation of $\text{S}_2\text{O}_8^{2-}$ in the presence of a transition metal (e.g., Ag^+ and Fe^{2+}) can be expressed as follows:



Among these suggested persulfate decomposition accelerating method, transition metal activation is considered to be the most viable method for field applications (Rastogi et al., 2009). The activation properties and mechanisms of $\text{S}_2\text{O}_8^{2-}$ by Ag^+ and Fe^{2+} were reported in previous studies (Cao et al., 2008, Dulman et al., 2004, Oh et al., 2009). Anipsitakis and Dionysiou (2004a) illustrated that the coupling of $\text{S}_2\text{O}_8^{2-}$ with Ag^+ demonstrated very high reactivity toward transforming 2,4-DCP at acidic conditions. A study reported by Liang et al. showed that the degradation of Trichloroethylene was

significantly accelerated by the persulfate-water process when appropriate amounts of ferrous ions were applied (Liang et al., 2008). According to these above-mentioned previous studies, the overall reactions between $S_2O_8^{2-}$ and these transition metals can be described by the following equations:



Similarly to Fenton process, when excess catalyst ions are present, they will adversely affect the efficiency of the process through equations as follows:



2.2.2.2 Sulfate radical generation via the activation of Oxone[®]

Oxone[®] ($2KHSO_5 \cdot KHSO_4 \cdot K_2SO_4$), a triple salt solid compound manufactured by DuPont, is the source providing active ingredient peroxymonosulfate ion (HSO_5^-) which is a more efficient oxidant than hydrogen peroxide (Kennedy and Stock, 1960) as can be seen from Table 2-5 and is reported to intervene in degradation processes in a more efficient way than does persulfate (Pandurengan and Maruthamuthu, 1981). Oxone[®] is a versatile oxidant for the transformation of a wide range of organic compounds. Besides, Oxone[®] is an acidic oxidant and thus the addition of Oxone[®] into the aqueous solution provokes pH dropping, which can be controlled by optimizing experimental parameters without costly pH adjustment since wastewaters usually contain various buffer salts (Chen et al., 2007). Similar to $S_2O_8^{2-}$, if without activation, Oxone[®] shows relatively slow consumption rate itself due to its stability at room temperature. The absorbance spectrum of 2.5 mM Oxone[®] in aqueous solution is illustrated in Figure 2-2.

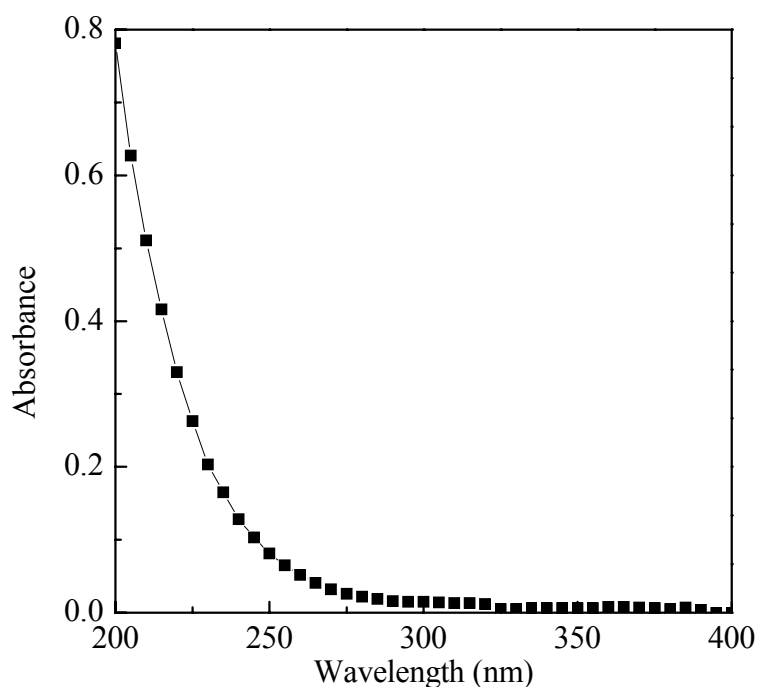


Figure 2-2: Absorbance spectrum of 2.5 mM Oxone[®] in aqueous solution.

It has been well established that many transition metal ions (e.g., Co^{2+} , Ag^+) can activate the decomposition of Oxone[®] via a one-electron transfer reaction, which is analogous to the Fenton' reagent. For the activation of Oxone[®] by transition metal ions, Co^{2+} was reported to be the most efficient transition metal (Anipsitakis and Dionysiou, 2004a) to produce $\text{SO}_4^{\bullet-}$ (see Eq. 2-22). The combination of Oxone[®] with Co^{2+} has demonstrated promising results for the degradation of certain organic waste waters. Anipsitakis and Dionysiou (2003) reported that the degradation efficiencies of 2,4-DCP, atrazine and naphthalene by cobalt/Oxone[®] process were much higher than by Fenton process. Sun et al. (2009) also demonstrated that the combination of Oxone[®] with Co^{2+} illustrated higher degradation performance of COD, SS and color for landfill leachate treatment and showed more advantages compared to Fenton process.



Nevertheless, cobalt (II) has been shown to be toxic and slightly carcinogenic upon inhalation in mice and might result in environmental problem when discharged along

with the effluent. It is therefore worth extending more transition metals as environmentally friendly catalysts for the activation of Oxone[®].

Among the numerous investigated transition metal ions, Fe²⁺, which is abundance in soil and sediment and has the property of environmentally friendly nature; and commonly exists in printing and dyeing industrial effluent, becomes the focus of interest for the activation of Oxone[®] in the past few years (see Eq. 2-23). Rastogi et al. (2009) reported that Fe(II) mediated activation of peroxymonosulfate was very effective in degrading Polychlorinated biphenyls in a sediment-slurry system with around 80% TOC removal being achieved. Besides, they identified that sulfate radicals is the dominating reactive species in Fe(II)/HSO₅⁻ system via indirect radical identification studies using ethanol and *tert*-butyl alcohol as quenching agents. Nevertheless, only a very limited amount of research is available regarding to the conjunction of Fe(II) and Oxone[®] for the degradation of synthetic organic compounds existing in wastewaters.



Besides the transition metal activation method, heat and UV light can also activate the decomposition of Oxone[®] to generate reactive radicals. Moreover, unlike the symmetrical structure of S₂O₈²⁻ and H₂O₂, HSO₅⁻ is an unsymmetrical peroxide, which is considered to be more easily activated than S₂O₈²⁻ and H₂O₂ (Anipsitakis and Dionysiou, 2004b, Anipsitakis et al., 2006). HSO₅⁻ can undergo homolytic cleavage leading to the formation of one sulfate radical and one hydroxyl radical under the activation of heat or UV light, which was reported by previous researchers by the following reaction as described in Eq. 2-24 (Hayon et al., 1972a, Yang et al., 2010). Therefore, it can be noted that the decomposition of Oxone[®] activated by heat or UV light irradiation possesses the potential of both S₂O₈²⁻ and H₂O₂. Guan et al. (2011)

confirmed the formation of $\text{SO}_4^{\bullet-}$ and $\cdot\text{OH}$ in the UV/HSO_5^- system and found that the rate of HSO_5^- photolysis into $\text{SO}_4^{\bullet-}$ and $\cdot\text{OH}$ increased with the value of pH at the range of 8-10.



Although the activation of Oxone[®] by either transition metal ions or UV light irradiation has been extensively explored, the decomposition of Oxone[®] involving both of these two activation methods is very limited. Several existing studies are focused on the utilization of cobalt-based transition metal activated decomposition of HSO_5^- assisted with UV irradiation (Anipsitakis and Dionysiou, 2004b, Bandala et al., 2009, Chen et al., 2007). Chen et al. (2007) revealed that UV and visible light can accelerate the decolorization and mineralization process of Acid Orange 7 (AO7) in the Co/HSO_5^- system due to the mechanisms of direct decomposition of HSO_5^- by UV irradiation and photosensitization of AO7 molecules under irradiation of visible light, respectively. Bandala et al. reported that cobalt/ HSO_5^- /UV system demonstrated the highest initial reaction rate compared with the other processes tested (i.e., Fenton, photo-Fenton, cobalt/ HSO_5^-). Based on these very limited existing studies, it can be noted that the performance of cobalt/ HSO_5^- system could be significantly enhanced upon the introduction of UV irradiation. Generally, the combination of two or more Oxone[®] activation methods, especially applying UV irradiation to the system, leads to an enhanced generation of highly reactive radicals, thereby eventually resulting in higher oxidation rates. Thus, it would be interesting to explore the use of Oxone[®] activated by the combination of transition metal ions and photolysis or even some new activation methods as an alternative wastewater treatment method, which can overcome the drawbacks existing in each individual process, improve the performance and provide a significant savings.

CHAPTER 3

Materials and Methodology

3.1 Introduction

In this chapter, the methodology regarding to the whole study is described, where the detailed descriptions of experimental setup and reactors for the wastewater treatment processes are given. Some important chemicals and reagents employed in this study are listed. The sampling and analytical methods of probe compounds can also be obtained in this chapter. In addition, some other instruments used to determine the solution parameters (e.g. TOC, pH and ferrous ions) are also provided.

3.2 Materials and Methods

3.2.1 Chemicals and reagents

All chemicals are of analytic reagent grade and all solvents are of HPLC grade and used as received without further purification. All the chemical and solvents used in this study were summarized in Table 3-1. The stock solutions were prepared in deionized and distilled water with a resistivity of 18.2 M Ω from a Bamstead NANOpure water treatment system (Thermo Fisher Scientific Inc., USA). Acetonitrile was degassed before being used in high performance liquid chromatography (HPLC). Nitric acid and/or sodium hydroxide were used to adjust the initial pH of the solutions. Excess methanol was employed to quench the reaction, unless otherwise stated.

Table 3-1: List of chemicals and solvents used in this study

Chemicals	MW, g mol ⁻¹	Formula	Purchased from
<u>Target Compounds</u>			
Rhodamine B (90%)	479.01	C ₂₈ H ₃₁ N ₂ O ₃ Cl	Sigma Aldrich Inc.
2,4,5-T (97%)	255.48	C ₈ H ₅ Cl ₃ O ₃	Sigma Aldrich Inc.
2,4,5-TCP (95.0%)	197.45	C ₆ H ₃ Cl ₃ O	Wako Pure Chemical Industries, Ltd.
<u>Oxidants and catalyst</u>			
Oxone [®] (95%)	614.76	2KHSO ₅ ·KHSO ₄ ·K ₂ SO ₄	Sigma Aldrich Inc. (DuPont product)
Ferrous Sulfate Heptahydrat (99.0%)	278.05	FeSO ₄ ·7H ₂ O	Sigma Aldrich Inc.
<u>Intermediates</u>			
2,4-dichlorophenoxyacetic acid (99%)	221.04	C ₈ H ₆ Cl ₂ O ₃	Riedel-de Haen
2,4-dichlorophenol (neat)			Supelco
2,5-dichlorohydroquinone (98%)	179.00	Cl ₂ C ₆ H ₂ (OH) ₂	Sigma Aldrich Inc.
4,6-dichlororesorinol	179.00	Cl ₂ C ₆ H ₂ (OH) ₂	Tokyo Chemical Industries
<u>Solvents</u>			
Acetonitrile (HPLC grade)	41.05	C ₂ H ₃ N	Tedia
Methanol (HPLC grade)	32.04	CH ₄ O	Tedia
tert-butanol (99.5%)	74.12	C ₄ H ₉ OH	Sigma Aldrich Inc.

Cont'd Table 3-1

Acetic acid (99.8%)	88.11	CH ₃ COOH	Lab-scan
<u>Others</u>			
Sodium carbonate (99.7%)	105.99	NaCO ₃	BDH, England
Sodium bicarbonate (99.9%)	84.01	NaHCO ₃	BDH, England
Sodium dihydrogen phosphate	119.98	NaH ₂ PO ₄	BDH, England
Sodium oxalate	134.00	Na ₂ C ₂ O ₄	BDH, England
Sodium acetate anhydrous (99%)	82.03	CH ₃ COONa	BDH, England
Sodium Chloride (99.5%)	58.44	NaCl	Sigma Aldrich Inc.
Sodium nitrate (99.5%)	84.99	NaNO ₃	Sigma Aldrich Inc.
Sodium Sulfate (99%)	142.04	Na ₂ SO ₄	Sigma Aldrich Inc.
Sulfuric acid	98.08	H ₂ SO ₄	Tedia
Nitric acid	63.01	HNO ₃	Tedia
Sodium hydroxide (96%)	40.00	NaOH	Uni-Chem
Sodium azide	65.00	NaN ₃	Sigma Aldrich Inc.
1,10-phenanthroline hydrate	198.22	C ₁₂ H ₈ N ₂ ·H ₂ O	International Laboratory

3.2.2 Experimental procedures

All the experiments were homogeneous and performed in an air-conditioned laboratory at 23±2°C. The tests were duplicated and average values were used in presenting the results. The Fe(II) and Oxone[®] solutions were freshly prepared before each experiment to minimize variations in concentration caused by precipitation, oxidation of ferrous solution and self-decomposition of oxidant. In addition, Fe(II) solution was prepared in

degassed H₂SO₄ solution at pH 3 to prevent Fe(II) from precipitation and/or oxidation.

3.2.2.1 Degradation of RhB by FO process

The degradation experiments were performed in 50 mL batch reactors. RhB stock solution (1.0 mM) was prepared in deionized distilled water and specific aliquots of the solution were added into the reactors to achieve a predetermined initial concentration. The reactions were initiated by pipetting appropriate amounts of Fe(II) and Oxone[®] into the reactor to achieve the predefined molar ratios of RhB:Fe(II):Oxone[®] (RFO). The initial volume of the reaction solution was fixed at 50 mL. The pH values were adjusted with 0.10 M nitric acid and/or 0.10 M sodium hydroxide whenever required. At predetermined time intervals, the sample aliquots were withdrawn from the reactor and mixed immediately with specific amount of methanol to quench the reaction. The solution was then analyzed by HPLC to quantify the remaining dye. For TOC measurement, sodium sulfite, an inorganic salt, was chosen as the quencher to minimize the carbon interference resulting from the background.

3.2.2.2 Degradation of 2,4,5-T by EFO system

Stock solution of 0.5 mM 2,4,5-T was prepared and appropriate amounts of 2,4,5-T stock solution was used to obtain the desired initial concentration. The EFO experiments were conducted under constant current electrolysis conditions in a 50 mL undivided single-compartment glass cell (see Figure 3-1) by using steel (Fe) sheet as sacrificial anode to continuously release ferrous ions and a graphite bar as cathode. An Agilent E3641A DC potentiationstat-galvanostat power supply was employed to provide the constant current. Experiments were carried out in 50 mL 0.10 mM 2,4,5-T aqueous solution containing 0.05 M Na₂SO₄ as background electrolyte without adjusting pH

unless otherwise stated. The reaction will be initiated by adding appropriate amounts of Oxone[®] into the reactor once a specified constant electrical current is applied between the anode and cathode. Reaction medium was continuously agitated by a magnetic stirrer to ensure the homogeneity of the solution throughout the reaction. Predetermined amounts of aliquots (0.5 mL) were withdrawn from the system at certain time intervals and mixed with the same amounts of methanol to quench the reaction and the samples were then filtered with 0.45 μm PTFE filters from Whatman before their analysis.

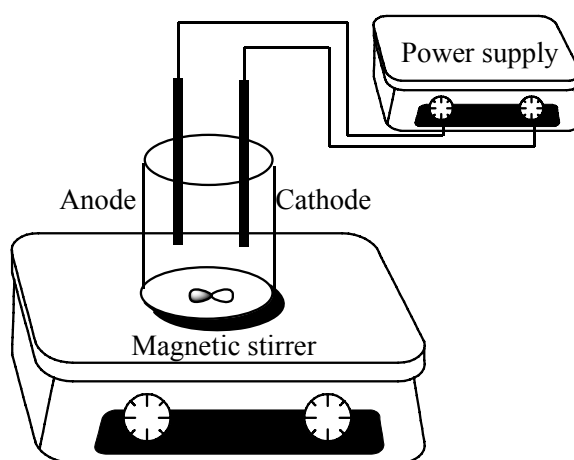


Figure 3-1: Sketch of electrolytic cell.

3.2.2.3 Degradation of 2,4,5-T by FOU process

For FOU photocatalytic reactions, the degradation of 0.1 mM 2,4,5-T was performed in a 50 mL quartz beaker, which was placed in the center of a computer-controlled CCP-4V photochemical reactor (see Figure 3-2) purchased from Luzchem Research Inc. A cooling fan was installed in the photochemical reactor to control the temperature. The light sources were two phosphor-coated low-pressure mercury lamps symmetrically placed in the reactor, emitting 253.7 nm monochromatic UV at a light intensity of 1.5×10^{-6} Einstein $\text{L}^{-1} \text{s}^{-1}$, unless otherwise stated. For the wavelength effect tests, four different lamps at 254, 300, 350 and 419 nm were investigated. According to the

manufacturer's data, each of the latter three types of UV lamp generates a light intensity of around 10^{-6} Einstein $L^{-1} s^{-1}$. The required amount of ferrous ions was added to the aqueous solution containing the probe contaminant and mixed by a magnetic stirrer to maintain a complete homogeneity of the solution throughout the reaction. The reaction was then initiated by adding an appropriate amount of Oxone[®] to the mixture and simultaneously switching on the UV lamps. If the lamps are cool, they need to be warmed up for 10 min in advance to ensure a stable light source. The initial volume of the reaction solution was fixed at 50 mL. At pre-determined time intervals, exactly 0.5 mL of the illuminated sample was withdrawn from the photoreactor and quenched with the same volume of methanol. Thereafter, the samples were filtered through 0.45 μm PTFE filters (Whatman) before analyzed by HPLC. The FO tests were conducted in the same quartz beaker and the same procedures were followed without using irradiation. In terms of TOC measurement, sodium azide instead of methanol was used as the quenching agent to minimize any interference. It should be noted that the addition of 0.25 mM Oxone[®] resulted in a solution pH of ~ 3.68 if no pH adjustment, and this pH level was used throughout this study, unless stated otherwise.

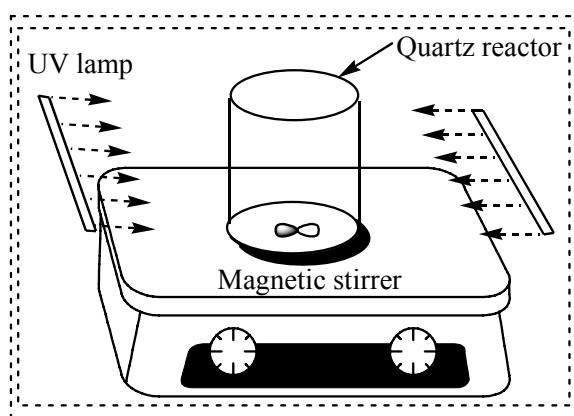


Figure 3-2: Sketch of the photoreactor Luzchem CCP-4V.

3.2.2.4 Degradation of 2,4,5-TCP by EFOU process

The reactions were carried out in a 50 mL undivided single-compartment quartz beaker placed in the center of a computer-controlled CCP-4V photochemical reactor (from Luzchem Research Inc), where a cooling fan was equipped to maintain constant temperature. Two phosphor-coated low-pressure mercury lamps emitting monochromatic light at 253.7 nm with light intensity of 1.5×10^{-6} Einstein $\text{L}^{-1} \text{s}^{-1}$ for each lamp were symmetrically arranged within the photoreactor as the irradiation source. The UV lamps were warmed up for at least 10 min prior to reaction to obtain constant output. Oxone[®] solutions were freshly prepared before each experiment to minimize variations in concentration caused by self-decomposition of the oxidant. An Agilent E3641A DC potentiationstat-galvanostat power supply was employed to provide the constant current by using commercial iron (Fe) sheet with total surface area of $\sim 10 \text{ cm}^2$ as the sacrificial anode and a graphite bar as the cathode. The sketch of electrolytic cell with UV irradiation is depicted in Figure 3-3. The probe (0.20 mM 2,4,5-TCP) and electrolyte (0.05 M Na_2SO_4) were used without pH adjustment, unless otherwise stated. The reaction is initiated by adding an appropriate amount of Oxone[®] into the reactor and simultaneously switching on the UV lamps once a specified constant electrical current is applied between the anode and cathode. The initial volume of the reaction solution was fixed at 50 mL. The solution was continuously agitated by a magnetic stirrer to ensure homogeneity throughout the reaction. Exact amount of an aliquot (0.5 mL) was withdrawn from the solution at predetermined time intervals and mixed with the same amount of methanol to quench the reaction, and the samples were then filtered with 0.45 μm PTFE filters (Whatman) before the LC analysis.

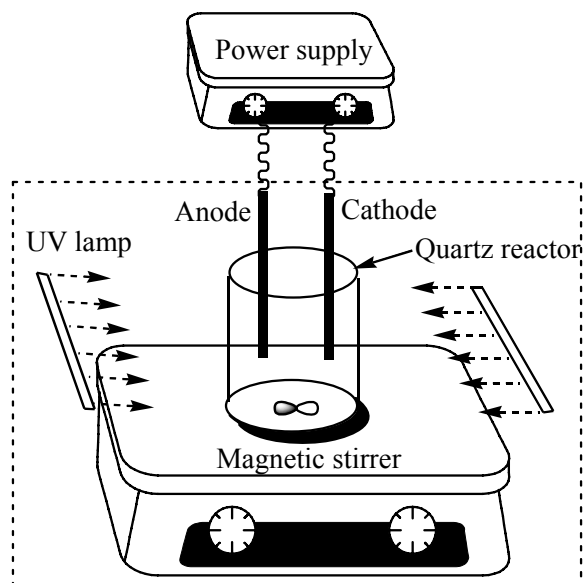


Figure 3-3: Sketch of electrolytic cell with UV irradiation.

3.2.3 Analytical procedures

3.2.3.1 Analysis by HPLC

The HPLC as shown in Figure 3-4 is consisted of a Waters 515 HPLC pump, a Waters 2489 UV/Visible Detector and a Water 717 plus Autosampler. The chromatographic separations were performed on a Pinnacle DB C18 reversed phase column (250 mm \times 4.6 mm with i.d. of 5 μ m) from RESTEK. (1) For the quantification of RhB, the mobile phase was composed of 60% acetonitrile and 40% water (V/V). The flow rate was 1 mLmin⁻¹ and injection volumes were 10 μ L. Retention time for RhB was 6.0 min at the above conditions. The UV/Visible Detector was set at 553 nm, which was the maximum absorbance wavelength of RhB solution and determined by scanning the spectra of the tested samples from 200 nm to 900 nm using a spectrophotometer Spectronic (R) GenesysTM with a 1 cm path length spectrometric quartz cell, as shown in Figure 3-5. For comparison, the decolorization of RhB was also determined by monitoring decrease in absorbance at the maximum wavelength (553 nm) using UV-Vis spectrophotometer. (2) For the analysis of 2,4,5-T, a mixture of acetonitrile, water and phosphoric acid in

the ratio of 50:50:0.05 (V/V/V) was selected as the mobile phase with a flow rate of 1.2 mL/min and an injection volume of 10 μ L. The UV/Visible detector was set at 289 nm, which is the maximum absorbance wavelength of 2,4,5-T as shown in Figure 3-6. Retention time for 2,4,5-T was around 8.0 min at the above conditions. A five-point calibration curve was established by injecting an appropriate amount of standard solutions at various concentrations for each analysis. (3) For the quantification of 2,4,5-TCP, The mobile phase was a mixture of acetonitrile and water in the ratio of 50:50 (V/V). The flow rate was set at 1.5 mL \cdot min⁻¹ and the injection volume was 10 μ L. The UV/Visible detector wavelength was set at 289 nm, which is the maximum absorbance wavelength of 2,4,5-TCP (see Figure 3-7) determined by scanning its spectra from 200 to 900 nm using the spectrophotometer Spectronic (R) GenesysTM. Retention time for 2,4,5-TCP was around 7.0 min at the above conditions.

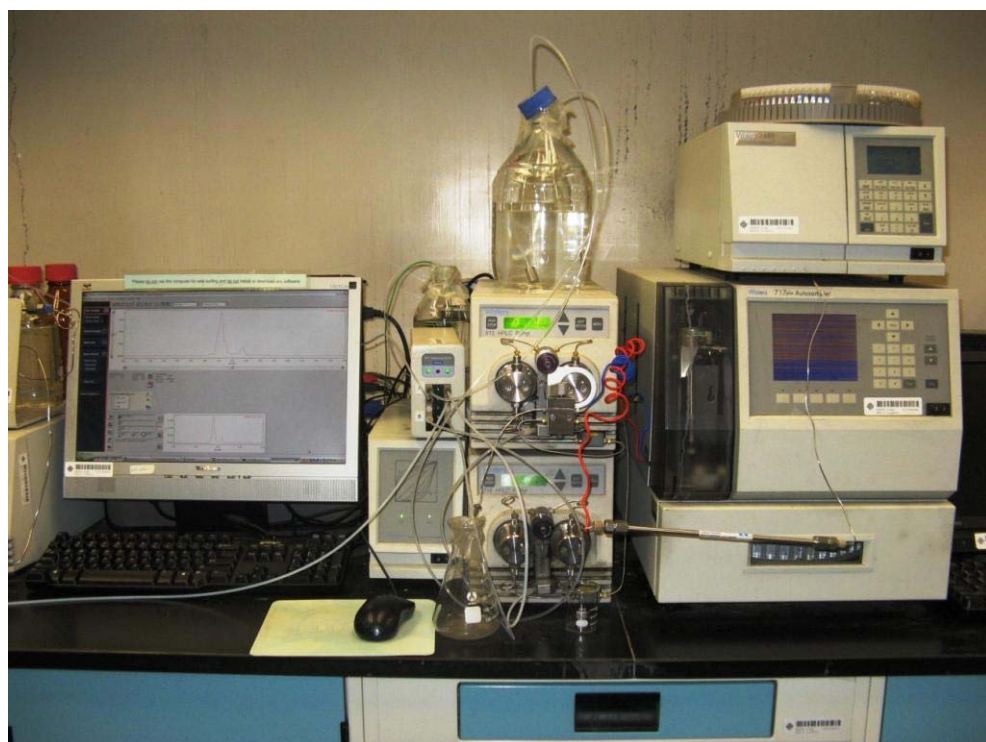


Figure 3-4: The HPLC system used for the quantification of selected probes.

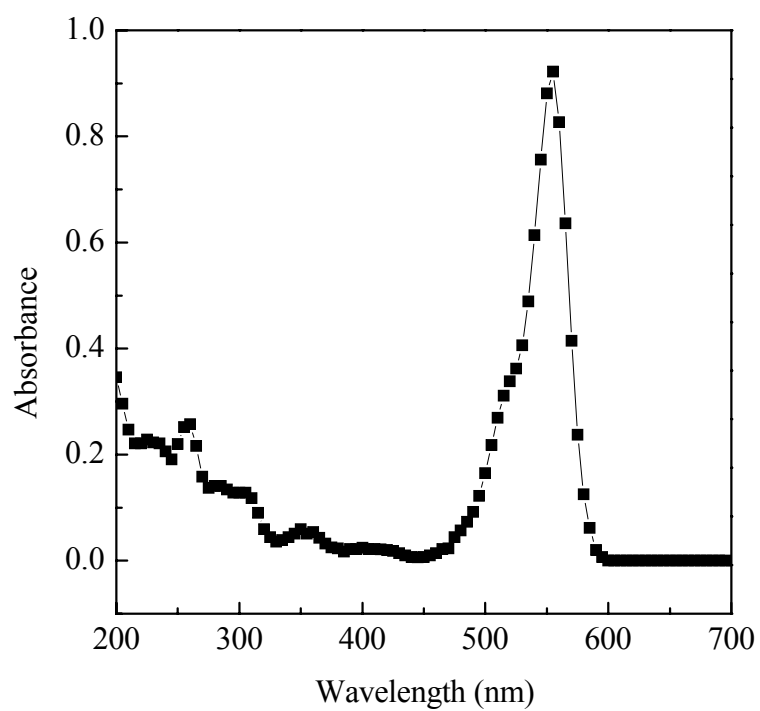


Figure 3-5: Absorbance spectrum of 0.01 mM RhB in aqueous solution.

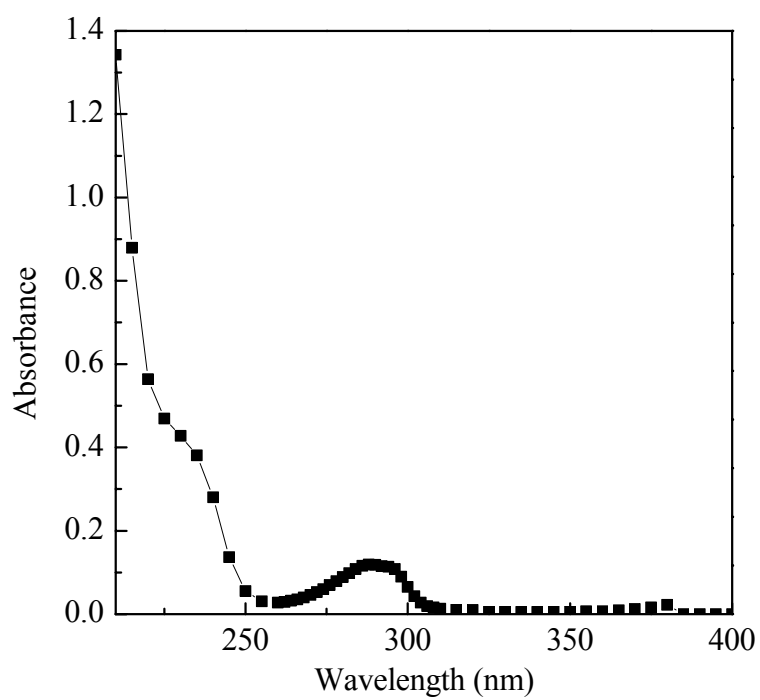


Figure 3-6: Absorbance spectrum of 0.02 mM 2,4,5-T in aqueous solution.

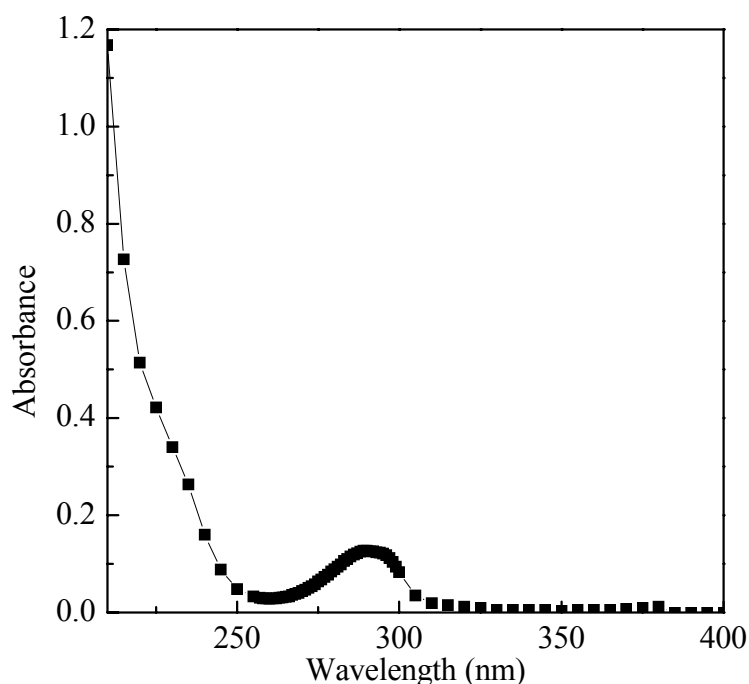


Figure 3-7: Absorbance spectrum of 0.05 mM 2,4,5-TCP aqueous solution.

3.2.3.2 Analysis by LC-ESI/MS

The identification of intermediates upon the decay of 2,4,5-T was conducted by a Finnigan SpectraSYSTEM® LC cooperated with a Thermo Quest Finnigan LCQ Duo mass spectrometer system which was equipped with an electrospray ionization interface operating at a negative mode with capillary temperature of 225 °C (LC-ESI/MS, $[M-H]^-$ ions). Figure 3-8 shows the photo of the LC-ESI/MS system employed in this study. The eluent at flow rate of $1.0 \text{ mL} \cdot \text{min}^{-1}$ was delivered by a gradient system from a Thermo P4000, coupled to a Thermo AS3000 autosampler with a 20 mL injection loop, partitioned by a C18 reversed phase column ($250 \text{ mm} \times 4.6 \text{ mm}$ with i.d. of $5 \text{ } \mu\text{m}$, Restek), and detected by a Spectra System UV6000LP photodiode array UV detector scanning from 200-700 nm. The mobile phase was a mixture of 0.05% acetic acid (A) and 100% acetonitrile (B) at a flow rate of $1.0 \text{ mL} \cdot \text{min}^{-1}$. The mobile phase was carried out with a gradient mode according to the following: 1) 100% of A was kept during the

first 2 min; 2) from 2 to 47 min, B was linearly increased from 0 to 60%, while A was steadily decreased to 40%, where held for 5 min; 3) from 52 to 55 min, the mobile phase turned to the initial composition until the end of the run. The data were collected in the range of m/z 50-400.

If the intermediate compounds can not commercially be purchased, they were quantified by comparing their ion intensities with that of the probe compound. This approximation is acceptable based on the fact that the UV absorbance may be ascribed to the resonance structure of the ring, which is basically identical (Adams and Randtke, 1992).



Figure 3-8: The LC-ESI/MS system employed for the aromatic intermediate analysis.

3.2.3.3 TOC and solution pH measurement

TOC was measured by a Shimadzu TOC-5000A analyzer equipped with an ASI-5000A autosampler to identify the mineralization of the organic contaminants. The solution pH level was determined by a CD510 digital pH meter.

3.2.3.4 Determination of Fe(II)

The quantification of Fe(II) (in both ionic and complex forms) was colorimetrically monitored by spectrophotometric method at 510 nm after adding 1,10-phenanthroline to form the reddish Fe(II)-phenanthroline complexes. The detection limit of this method for Fe(II) was 1.8×10^{-4} mM (Tamura et al., 1974).

3.2.3.5 Chloride ion measurement

The concentration of chloride ions released during the degradation of 2,4,5-T was followed by ion chromatography (Dionex Series 4500i) equipped with a Dionex IonPac® AS14 anion column (4 mm × 250 mm), a Dionex CD25 conductivity detector and a Dionex AS 40 automated sampler. A mixture of 1 mM NaHCO₃ and 3.5 mM Na₂CO₃ with a flow rate of 1 mL·min⁻¹ was used as the mobile phase.

CHAPTER 4

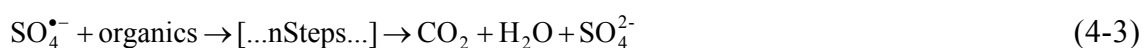
Degradation of RhB by Fe(II)-Mediated Activation of Oxone[®] Process

4.1 Introduction

It is estimated that around 10^6 tons of commercially different dyes are produced annually world-wide and about 5% - 10% of the dyestuffs are lost in the industrial effluents (Sanroman et al., 2005) with a concentration varying from the range of 10 to 10, 000 mgL^{-1} (Figueroa et al., 2009). The complex structures and stable properties make most of the dyes resistant to biological degradation and photodegradation (Ai et al., 2007, Mittal and Venkobachar, 1996) and some of them are even toxic, carcinogenic and mutagenic (Panda et al., 2009). Besides, color caused by dye contaminants interferes with penetration of sunlight into waters, retards photosynthesis, inhibits the growth of aquatic biota and interferes with gas solubility in water bodies (Couto, 2009). As a result, various treatment techniques have been investigated and developed to decolorize and/or degrade dye contaminants (Forgacs et al., 2004), including electro-oxidation (Dogan and Turkdemir, 2005), AOPs (Papic et al., 2006), adsorption (Gad and El-Sayed, 2009, Kadirvelu et al., 2005), biological degradation and filtration processes (Pazdzior et al., 2009), and so on.

AOPs are considered to be one of the most effective methods due to the generation of highly reactive radicals. AOPs involve the utilization of sole or combined high oxidation potential oxidants such as ozone, hydrogen peroxide, persulfate, ferrate(VI),

sometimes coupled with one or several of the following enhancement tools: irradiation (e.g., UV, solar and visible light), specific catalysts, ultrasonic, thermal activation and microwave. Fenton's process by coupling H₂O₂ with a transition metal (Fe²⁺) is a rapid and inexpensive process (Zazo et al., 2005). However, the requirement of low pH environment is the major limitation (Anipsitakis and Dionysiou, 2003). On the basis of the Fenton's process, sulfate radicals generated by the combination of oxidants (persulfate or peroxymonosulfate) with transition metals (Fe²⁺, Ag⁺, Co²⁺) demonstrate higher standard reduction potential at neutral pH (Anipsitakis and Dionysiou, 2003, Chan and Chu, 2009). Anipasitakis and Dionysiou (2004a) have reported that sulfate radicals are more efficient than hydroxyl radicals at least for the transformation of 2,4-dichlorophenol, atrazine, and naphthalene under certain conditions. The SO₄^{•-} generation mechanism and its interaction with organic compounds were reported by previous studies (Anipsitakis and Dionysiou, 2004a, Bandala et al., 2007, Chan and Chu, 2009, Rastogi et al., 2009):



where the end product SO₄²⁻ is practically inert and is considered environmentally benign. Therefore, persulfate and peroxymonosulfate, as an oxidant alternative for the degradation of organic contaminants, have received considerable attention recently.

Oxone[®] (2KHSO₅·KHSO₄·K₂SO₄), a triple salt compound, is the source providing peroxymonosulfate (HSO₅⁻) which is reported to be a more efficient oxidant than hydrogen peroxide or persulfate (Richard and Albert, 1960). Therefore, Oxone[®] was chosen as the oxidant source in this study. To activate the relatively stable Oxone[®] in the

generation of $\text{SO}_4^{\bullet-}$, Anipsitakis et al (2004) demonstrated that Co^{2+} is an efficient transition metal to trigger the process at neutral pH. Nevertheless, cobalt (II) has been shown to be toxic and slightly carcinogenic upon inhalation in mice and might result in environmental concern when discharged along with the effluent. Thus, Fe^{2+} which shows considerable activation of Oxone[®] and commonly exists in printing and dyeing industrial effluent was selected as the transition metal in this work.

Rhodamine B (RhB), a water-soluble xanthene dye and famous for its good stability as dye laser materials (Asilturk et al., 2006), is widely used in dyestuff industries and modern photochemistry, and most important it is a suspected carcinogen (Jain et al., 2007, Mirsalis et al., 1989). Therefore, the degradation of RhB by sulfate radicals generated based on the Fe(II)-Mediated Oxone[®] process was explored in this study.

In this chapter, the performance of Fe(II)/Oxone[®] process was evaluated. Effects of some critical parameters, including transition metal and oxidant concentration, solution pH, and different electrolytes on the dye degradation efficiency were investigated. Moreover, the mineralization behavior of RhB in the Fe(II)/Oxone[®] process was also evaluated by monitoring the TOC decrease under the selected experimental conditions.

4.2 Results and Discussion

4.2.1 Dosing sequence of reactants

Initially, control experiments were conducted to determine the RhB removal solely by ferrous sulfate or Oxone[®]. As the ratio of Fe(II)/RhB is 10, the [RhB] remained the same throughout the whole process (90 min), under the same condition, 5% of [RhB] decay was observed at a ratio of Oxone[®]/RhB of 5. Accordingly, it can be concluded

that the dye degradation by sole ferrous or Oxone[®] is negligible as shown in Figure 4-1.

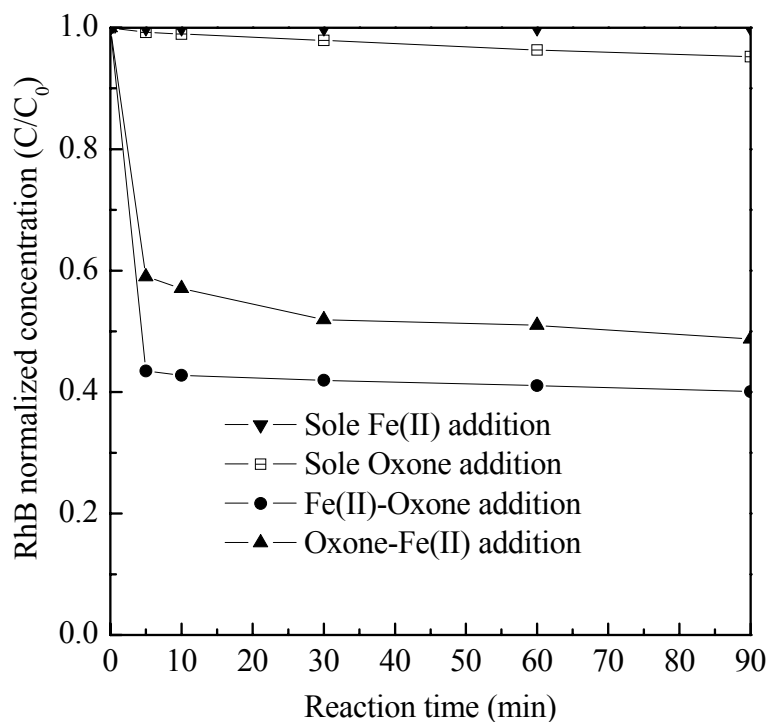


Figure 4-1: Effect of reactants adding order on RhB degradation. Experimental conditions were 0.02 mM [RhB]₀, 0.20 mM [Fe(II)]₀, and 0.10 mM [Oxone[®]]₀ without pH adjustment.

There are two critical reagents involved in the Fe(II)/Oxone[®] system, experiments were therefore performed to verify the effect of reactant dosing sequence on the dye degradation. Two tests were conducted, one was by adding ferrous sulfate (as a source of Fe(II) catalyst) into RhB solution and followed by adding Oxone[®] to initiate the reaction, and the other was by adding Oxone[®] first then ferrous sulfate. It is interesting to note that Fe(II)-Oxone[®] addition demonstrates a better and faster dye degradation performance, even when the two dosages were separated by 30s apart, as shown in Figure 4-1. The overall RhB removal was 60% and 50% for Fe(II)-Oxone[®] and Oxone[®]-Fe(II) addition, respectively; indicating that the Fe(II)-Oxone[®] addition showed a higher oxidation capacity. This might be attributed to two reasons: although the non

catalyst-mediated decomposition of Oxone[®] is slow, there was still a portion of Oxone[®] directly react with the dye when the oxidant (Oxone[®]) was added first (as justified in the Figure 4-1, the 5% removal). In addition, the RhB used in this experiment was a commercial dye coming with about 10% of impurity, the added Oxone[®] (in the form of HSO_5^-) may also react with these impurities. They both resulted in a lower generation of sulfate radicals in the later Fe(II)/Oxone[®] process upon the addition of Fe(II). In the case of Fe(II)-Oxone[®] addition, once the oxidant was dosed into the reactor, large amounts of $\text{SO}_4^{\bullet-}$ were instantaneously generated in the presence of the previous added catalyst (Fe(II)). Because sulfate radicals are more selective for oxidation via electron transfer than that of hydroxyl radicals, it can be speculated that the higher degradation efficiency was likely due to the preferred selective oxidation reaction between sulfate radical and RhB. Fe(II)-Oxone[®] addition sequence was therefore adopted in the remaining study.

4.2.2 Effect of Fe(II): Oxone[®] ratio on RhB degradation

In the Fe(II)/Oxone[®] system, Fe(II) was used as a catalyst for the activation of Oxone[®] to generate the radicals. Thus, the generation of $\text{SO}_4^{\bullet-}$ can be affected by the molar ratio and/or the concentration of Fe(II) and Oxone[®]. Optimum Fe(II)/Oxone[®] molar ratio was identified by varying Fe(II)/Oxone[®] ratios ranging from 1:10 to 10:1 with constant [Oxone[®]] at 0.10 mM and 0.20 mM. Control experiments were carried out with Oxone[®] alone in the absence of Fe(II).

Dye degradation at different Fe(II)/Oxone[®] molar ratios was depicted in Figure 4-2. It can be noted that dye degradation by Oxone[®] alone was ineffective. From Figure 4-2, two different types of reaction were identified. When the $\text{Fe(II)/Oxone}^{\text{®}} \leq 1$, the RhB

showed a rapid degradation in the first 5 min and then followed by a much slower decay, i.e., a two-stage reaction consisting of a rapid degradation stage and a subsequent retarded slow reaction. Additionally, the rate constants of both stages increased as Fe(II)/Oxone[®] ratio increased until 1:1 was reached. The removal efficiency increased from 23.7% to 63.3% for Figure 4-2a and from 31.6% to 100% for Figure 4-2b with [Oxone[®]] at 0.10 and 0.20 mM, respectively.

However, as the ratio Fe(II)/Oxone[®] > 1, the [RhB] in the solution dropped sharply within the first few minutes and then the curves leveled off, suggesting the reaction was completed right after the reaction was started. This observation is very useful for real application, especially if the space available for a large reactor is limited.

To optimize the process, the decay curves were further analyzed as shown in Figure 4-3, where the dye decay at a specific reaction time is apparently a function of the Fe(II)/Oxone[®] ratio. In general, the closer the ratio to 1, the better the degradation efficiency of the system. Moreover, the higher the Oxone[®] concentration, the faster the decay rate as well as the higher the performance for the fixed catalyst and oxidant molar ratio. In this study, 100% dye degradation was observed within 90 minutes when the ratio of Fe(II)/Oxone[®] was 1 and the Oxone[®] was fixed at 0.20 mM.

In the Fe(II)-mediated Oxone[®] process, sulfate radical was generated through the decomposition of Oxone[®] catalyzed by the Fe(II) via Eq. 4-2. Compared with Fenton's reaction which has a reaction rate constant around $k = 53\text{--}76 \text{ M}^{-1}\text{s}^{-1}$, Eq. 4-2 has a much higher reaction rate constant of $k = 3.0 \times 10^4 \text{ M}^{-1}\text{s}^{-1}$, indicating a faster generation of sulfate free radicals once Oxone[®] is in contact with Fe(II). Large amounts of $\text{SO}_4^{\cdot-}$ were

responsible for the rapid dye degradation in the first few minutes. The ferric ions generated in Eq. 4-2 would serve as an electron acceptor and further decompose extra Oxone[®] to generate peroxysulfate radicals, which are a weaker oxidant than the sulfate radicals via the Eq. 4-4 expressed as follows:



Ferrous ions regenerated through Eq. 4-4 will further react with Oxone[®]. However, compared with the Fe(II)/Oxone[®] system, previous study showed that the coupling of Fe(III) with Oxone[®] showed a much lower rate in degrading organics (Anipsitakis and Dionysiou, 2004a). This also confirms with the slower second-stage reactions in Figure 4-2 as $Fe(II)/Oxone^{\circledR} \leq 1$. This observation indicates that Fe(II) ions are consumed much more rapidly than they are re-produced. On the other hand, excessive Fe(II) in Fe(II)/Oxone[®] system can act as a sulfate-radical scavenger through Eq. 4-5 which has a far higher rate constant of $k = 3.0 \times 10^8 \text{ M}^{-1} \text{ s}^{-1}$ than that of Eq. 4-2.



Therefore, unlimited increase of Fe(II) in the process is not recommended. In this study, it can be concluded that when the molar ratio $Fe(II)/Oxone^{\circledR} \leq 1$, the rapid first-stage is mainly due to the rapid sulfate radical generation that reacts with dye molecule; while the slower second-stage is likely hindered by the combination of lower sulfate radicals in the solution, the weaker peroxysulfate radicals produced by Fe(III)/Oxone[®] and slow reactivation of Fe(II) catalyst. RhB was degraded mainly through the oxidizing radicals generated via Eqs. 4-2 and 4-4 under this condition. However, in the presence of an excessive amount of Fe(II), especially when the molar ratio $Fe(II)/Oxone^{\circledR}$ is higher than 2 (from Figure 4-3), a sudden drop of the [RhB] and a lowered overall RhB decay was observed. The former is due to the rapid sulfate radicals' generation by the

excessive ferrous ions, while the latter is due to the futile-consumption of $\text{SO}_4^{\bullet-}$ by excess Fe(II) as indicated in Eq. 4-5.

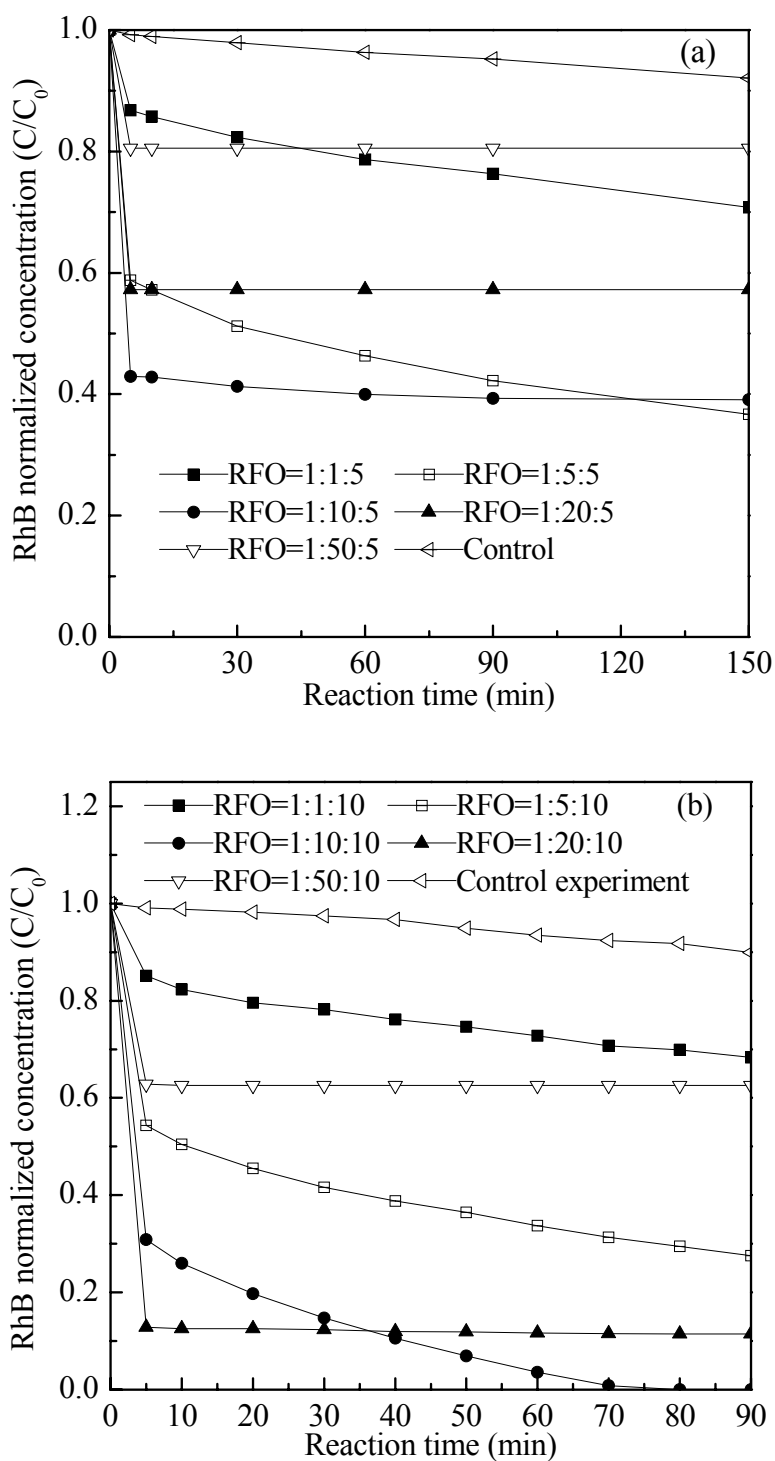


Figure 4-2: Effect of different ratios of RFO on dye degradation. Conditions were (a) 0.02 mM [RhB]₀, 0.10 mM [Oxone[®]]₀ & (b) 0.02 mM [RhB]₀, 0.20 mM [Oxone[®]]₀.

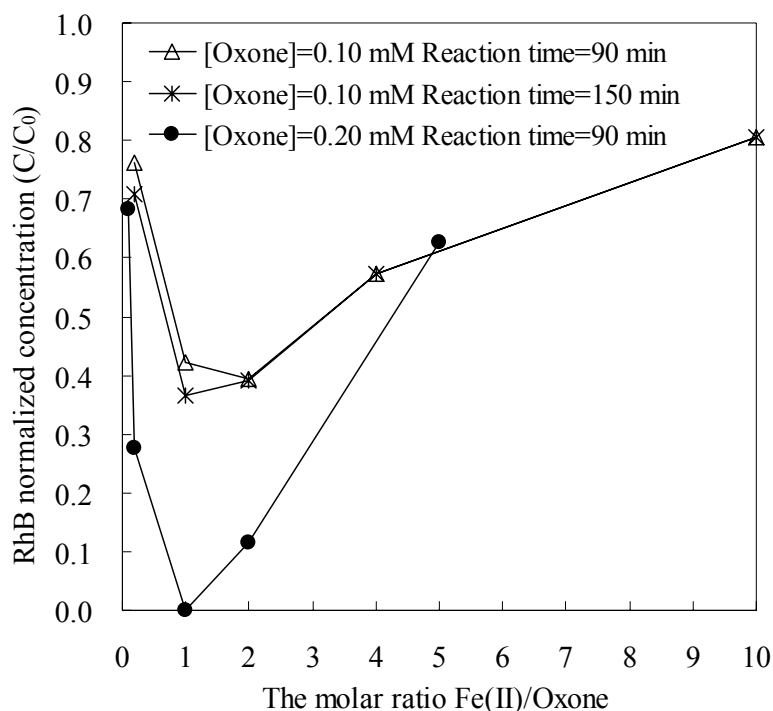


Figure 4-3: Degradation performance as a function of Fe(II)/Oxone[®] molar ratio

4.2.3 Effect of pH level on RhB degradation

The effects of initial solution pH on RhB degradation were explored in an extensive pH range from 2.67 to 10.22 at its optimum Fe(II)/Oxone[®] ratio of 1:1 and the results were illustrated in Figures 4-4 and 4-5, where RhB degrading performance directly depended on the initial solution pH. Optimal dye removal efficiency was observed at an initial pH around 3.5, above or below this pH level, the process performance reduced. Due to the presence of acidic bisulfate in Oxone[®], the solution pH would drop sharply after adding Oxone[®] to the process. The pH variation before and after Oxone[®] addition was monitored and depicted in Figure 4-6, where Oxone[®] addition resulted in a solution pH of 3.51 if no pH adjustment.

The decrease of dye removal efficiency at low pH range is most likely attributed to the formation of $(\text{Fe(II)}(\text{H}_2\text{O}))^{2+}$ at low pH levels (Masomboon et al., 2009), which results

in a decrease of the capacity of Fe(II) catalyst concentration. On the other hand, dye removal performance also rapidly dropped when the solution pH increased to basic conditions. This can be rationalized by two mechanisms. Firstly, the instability of ferrous ions at pH level higher than 4.0 led to the formation of ferrous/ferric hydroxide complexes, which have a lower catalytic activity and thus have a negative impact on the $\text{SO}_4^{\cdot-}$ generation. As shown in Figure 4-4, the rapid first-stage kinetics no longer exists at extremely high pH level of 10.22, indicating a deficiency of catalyst. Secondly, self-dissociation of Oxone[®] at a raised pH level was reported and was observed mainly through non-radical pathways (Donald and John, 1956, Rastogi et al., 2009), which would impair the oxidizing capacity of Oxone[®] towards the probe contaminant. Consequently, an optimal solution pH of 3.5 was recommended for the RhB removal. This is convenient for wastewater treatment because no pH adjustment is required.

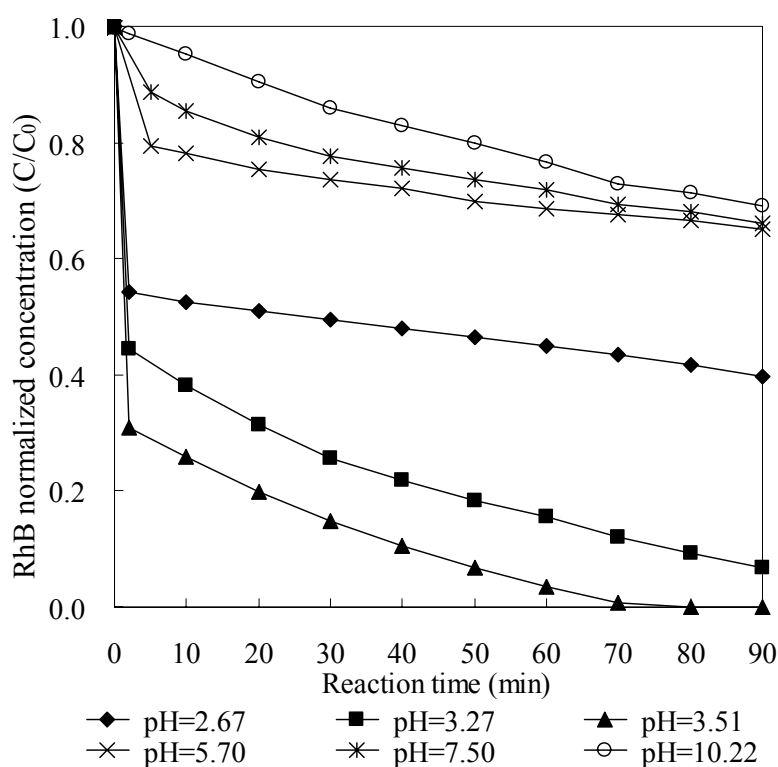


Figure 4-4: Effect of initial solution pH after adding Oxone[®]. Experimental conditions were set at 0.02 mM $[\text{RhB}]_0$ with RFO molar ratio of 1:10:10.

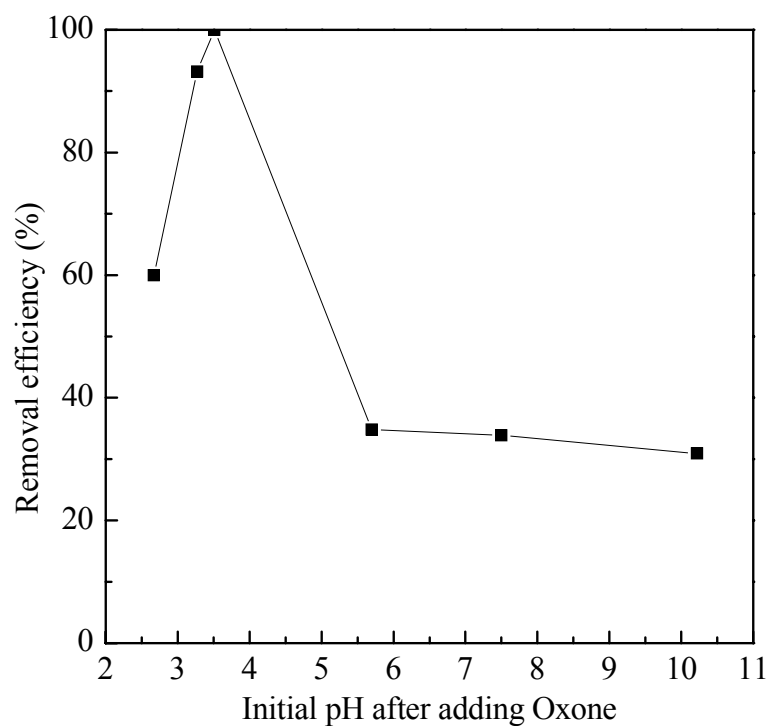


Figure 4-5: Degradation performance as a function of initial solution pH after adding Oxone[®]. Experimental conditions were set at 0.02 mM [RhB]₀ with RFO molar ratio of 1:10:10.

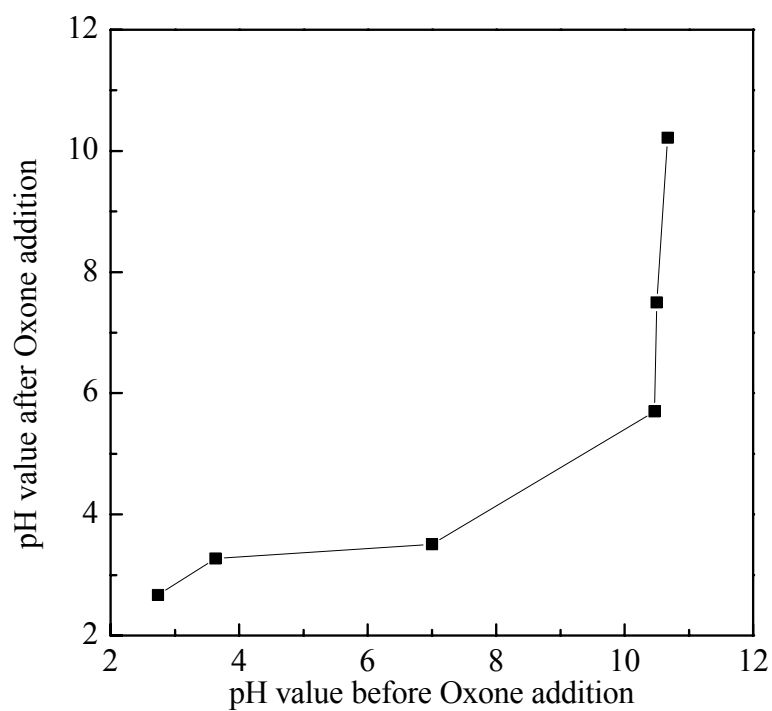


Figure 4-6: The pH variation before and after Oxone[®] addition. Experimental conditions were set at 0.02 mM [RhB]₀ with RFO molar ratio of 1:10:10.

4.2.4 Effect of various inorganic salts

Large amounts of additives and mordants, including inorganic salts, have been utilized in the dyeing process, which result in a complex wastewater and impose a significant influence on its treatment. The performances of degrading RhB by using three different inorganic salts (Na_2SO_4 , NaNO_3 , and NaCl at 0.05 M) were evaluated by comparing with the control (without electrolyte) test, and the results were shown in Figure 4-7. It can be noted that the presence of NaCl , Na_2SO_4 , and NaNO_3 show improved, retarded, and null effects on the dye's degradation with about 91%, 43%, and 71% RhB removal in 5 min, respectively.

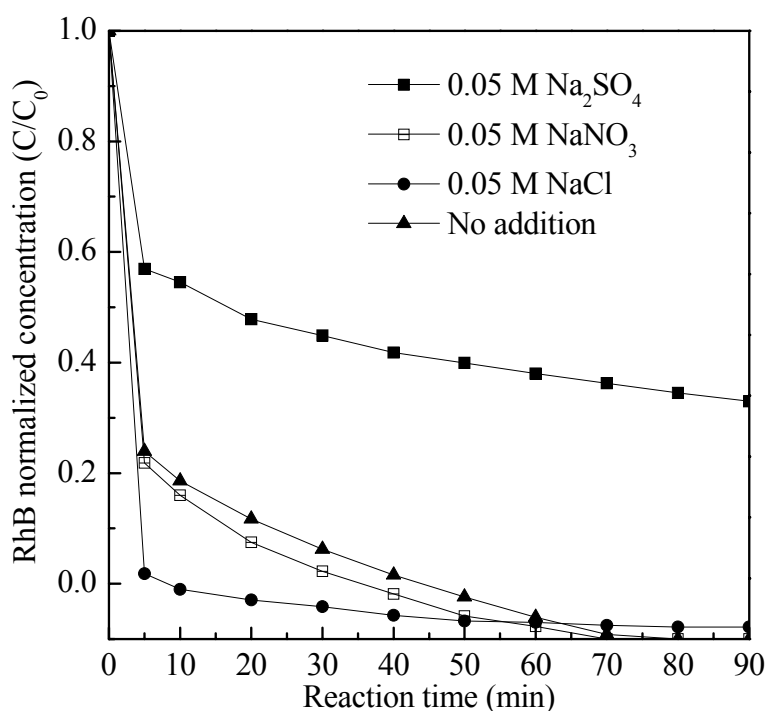
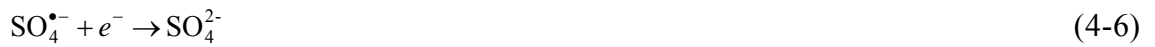


Figure 4-7: Effect of inorganic salts: NaCl , NaNO_3 , Na_2SO_4 . Experimental conditions were set at 0.02 mM $[\text{RhB}]_0$ with RFO molar ratio of 1:10:10 without pH adjustment.

In-depth analysis of Na_2SO_4 and NaCl on the dye removal were therefore conducted to

elucidate the role of SO_4^{2-} and Cl^- in the Fe(II)/Oxone[®] process by varying the $[\text{Na}_2\text{SO}_4]$ and $[\text{NaCl}]$ from 0.0 to 0.1 M. For the SO_4^{2-} , as shown in Figure 4-8, both the first- and second-stage RhB decay rates were decreased with the increment of $[\text{Na}_2\text{SO}_4]$. One possible explanation is that the decomposition of Oxone[®] is likely inhibited by the high-ionic strength (IS) of the solution. As reported by Kolthoff and Miller, the persulfate decomposition rate in a 0.1 M of HClO_4 solution decreased with the increase of IS (Kolthoff and Miller, 1951), while Huang et al. (2002) found that the higher the IS, the slower MTBE degraded by persulfate. However, it is interesting to note that 0.05 M NaNO_3 (giving an IS of 0.05 M) has a higher IS than that of 0.01 M Na_2SO_4 (with an IS of 0.03 M), but the latter demonstrates much higher rate inhibition than the former. Thus, the use of IS alone to justify the retardation effect is not enough. Assuming the reactions involving the consumption of sulfate free radicals (Eq. 4-3) can be simplified into



the corresponding Nernst equation of Eq. (4-6) then can be formulated as (Logic)

$$E_{(\text{SO}_4^{\bullet-}/\text{SO}_4^{2-})} = E_{(\text{SO}_4^{\bullet-}/\text{SO}_4^{2-})}^{\ominus} + \frac{RT}{zF} \ln \frac{[\text{SO}_4^{\bullet-}]}{[\text{SO}_4^{2-}]} \quad (4-7)$$

where, $E_{(\text{SO}_4^{\bullet-}/\text{SO}_4^{2-})}$ is the half-reaction reduction potential, $E_{(\text{SO}_4^{\bullet-}/\text{SO}_4^{2-})}^{\ominus}$ represents the standard half-reaction reduction potential, R is the universal gas constant $8.314472 \text{ JK}^{-1}\text{mol}^{-1}$, T is the absolute temperature, F is the Faraday constant $9.6485 \times 10^4 \text{ Cmol}^{-1}$, z is the number of electrons transferred in the half-reaction. According to Eq. 4-7, it can be seen that the redox potential of $\text{SO}_4^{\bullet-}/\text{SO}_4^{2-}$ can be affected by the concentration of SO_4^{2-} . Higher the $[\text{SO}_4^{2-}]$, lower the $E_{(\text{SO}_4^{\bullet-}/\text{SO}_4^{2-})}$, which directly lower the performance of dye oxidation. Assuming a complete generation of $\text{SO}_4^{\bullet-}$ can be achieved through Eq. 4-2 in the first-stage, it can be calculated that $E_{(\text{SO}_4^{\bullet-}/\text{SO}_4^{2-})}$ will be reduced by 0.1363 V

when $[\text{SO}_4^{2-}]$ increased from 0.010 to 0.10 M under the tested conditions. This was consistent with the reported redox potential of sulfate radicals, which varies from 2.5 to 3.1 V depending on the reaction conditions (Lau et al., 2007).

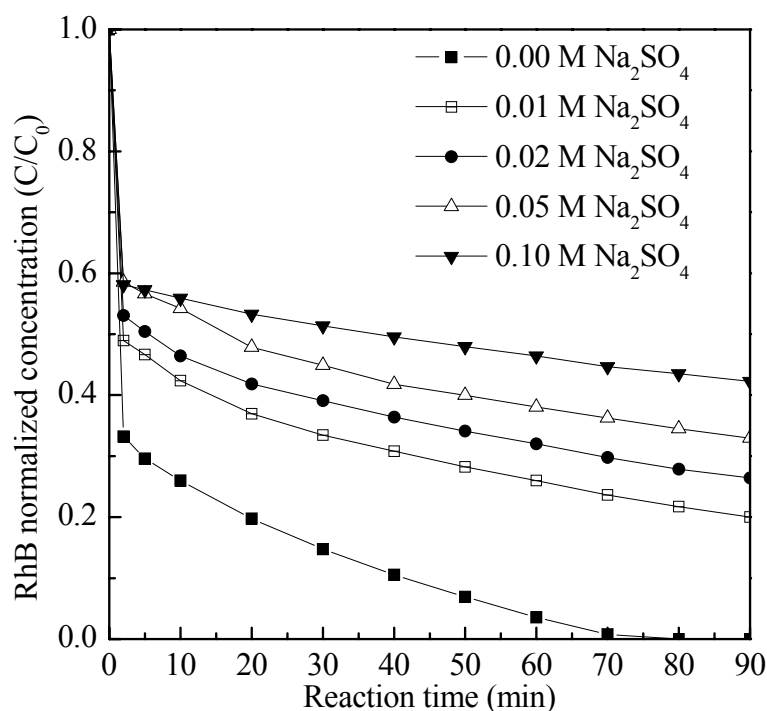


Figure 4-8: Effect of ionic strength: Na_2SO_4 . Experimental conditions were set at 0.02 mM $[\text{RhB}]_0$ with RFO molar ratio of 1:10:10 without pH adjustment. Na_2SO_4 was added in different amount.

Figure 4-9 illustrates the effect of $[\text{NaCl}]$ in the $\text{Fe(II)}/\text{Oxone}^\text{®}$ system. It can be noted that the first-stage degradation rate was accelerated as $[\text{Cl}^-]$ increased. It is interesting to note that Cl^- can still improve the dye degradation even in the absence of Fe(II) , as shown in Figure 4-10, where more than 93% of dye was degraded within 50 minutes at a high $[\text{Cl}^-]$. As expected, the degradation rates of RhB by $\text{Cl}^-/\text{Oxone}^\text{®}/\text{Fe(II)}$ were about 200~3.5 times faster than that of $\text{Cl}^-/\text{Oxone}^\text{®}$ as $[\text{Cl}^-]$ increased from 0.001 to 0.1 M.

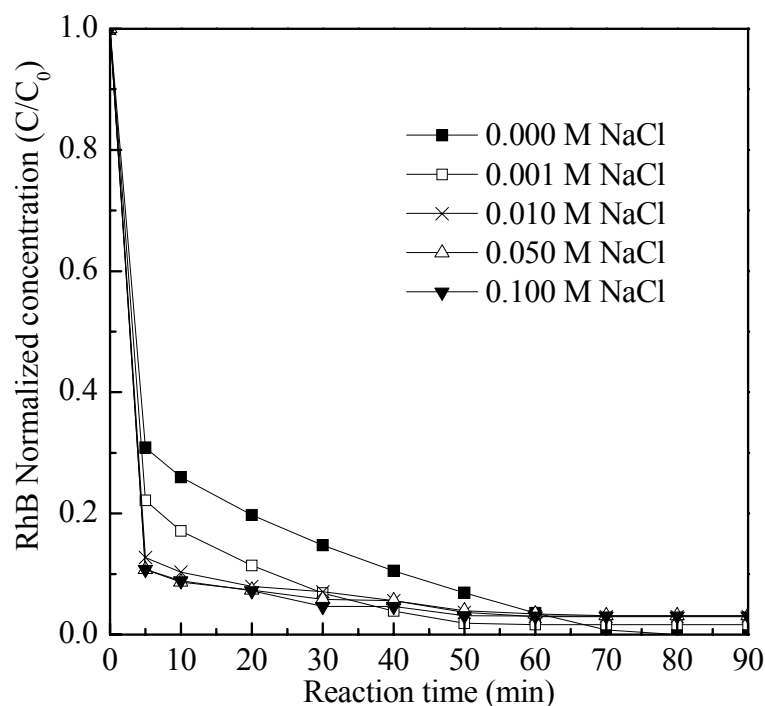


Figure 4-9: Effect of ionic strength: NaCl. Experimental conditions were set at 0.02 mM [RhB]₀ with RFO molar ratio of 1:10:10 without pH adjustment. NaCl was added in different amount.

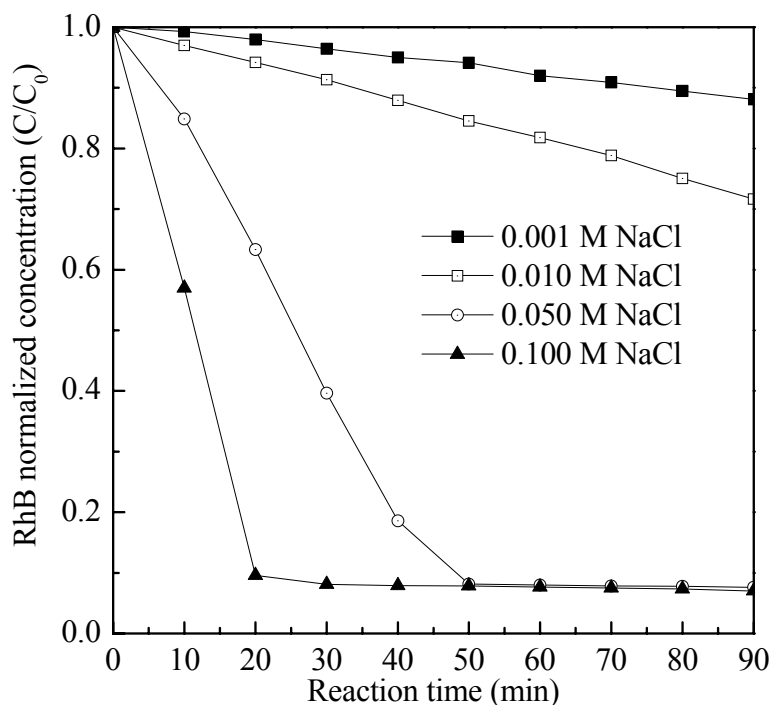


Figure 4-10: Effect of Cl⁻ on the RhB degradation. Experimental conditions were 0.02 mM [RhB]₀, 0.20 mM [Oxone[®]]₀ without catalyst and pH adjustment.

It was known that chloride ions can be oxidized by sulfate radicals to form chlorine radicals via Eq. (4-8) (Anipsitakis et al., 2006), which may result in a series of secondary oxidants as indicated in Eqs. 4-9 to 4-13. In addition, Cl^- can be oxidized thermodynamically by HSO_5^- (1.75 - 1.8 V) to form chlorine ($\text{Cl}_2/2\text{Cl}^-$, 1.36 V) and hypochlorous acid (HOCl/Cl^- , 1.48 V) as also verified by others (Delcomyn et al., 2006, Stuart et al., 2000). These secondary oxidants are likely to contribute and improve the dye's decay by offering parallel decay pathways, which may involve the reactions of chlorine radicals (Eq. (4-16)) and free available chlorine species (Eq. 4-17).

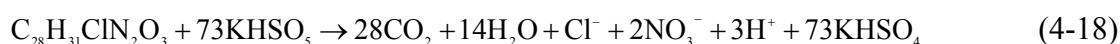


It was reported that para-selective oxychlorination of aromatic compounds is favored by the combination of Oxone[®] with chloride (Narender et al., 2002). Thus, the faster degradation of RhB by the $\text{Fe(II)/Oxone}^\text{®}/\text{Cl}^-$ process may be partly attributed to the favorable chlorination on the aromatic ring of RhB through Eqs. 4-8 to 4-17. However,

for the Oxone[®]/Cl⁻ process, the degradation of RhB is mainly through the non-radical reactions, *i.e.*, Eqs. 4-13 to 4-17, which results in a slower reaction rate. The positive effect by increasing [Cl⁻] in the Fe(II)/Oxone[®] system on RhB degradation may not be suitable for the treatment of other types of wastewater, because some chlorinated by-products formed during the chlorination process may be difficult to be further oxidized or become more toxic. A careful evaluation on each type of wastewater is recommended.

4.2.5 Mineralization of RhB

Mineralization of RhB in the Fe(II)/Oxone[®] process was assessed by measuring the decrease in TOC with an initial RhB concentration of 0.10 mM or 33.6 mgL⁻¹ TOC as calculated stoichiometrically by Eq. 4-18.



The removal of RhB under the molar ratio of RFO at 1: 10: 10 was found to be efficient as discussed previously. Under these circumstances, however, it was found inefficient for TOC removal, where only 30% TOC was removed, as shown in Figure 4-11. This result is reasonable considering the ratio of RFO at 1:10:10 is far less than the required stoichiometric dosage for complete mineralization as indicated in Eq. 4-18. Thus, the tailing of TOC curve is likely attributed to the depletion of Oxone[®]. This can be justified by increasing the RFO ratio to 1:50:50, and that the abatement of TOC was most efficient in the early stage of the reaction and significantly slowed down afterward. This is likely due to the inefficient side reactions of ferrous and Oxone[®] as discussed before. To minimize the involvement of side reactions, it is possible to modify the conventional process into a stepwise dosing approach. For the same RFO ratio at 1:50:50, the oxidant and catalyst were evenly distributed into 5 dosages at one hour

apart. As shown in Figure 4-11 (curve c), the total TOC removal further increased to 75%, which is 20% higher than that of one-off dosing process. In addition, it should be noted that the stepwise addition is 4 times faster to achieve the same level of TOC removal (i.e., 55%) than that of one-off dosing. This is critical for a treatment plant design, since a much smaller reactor can be used for a specific performance.

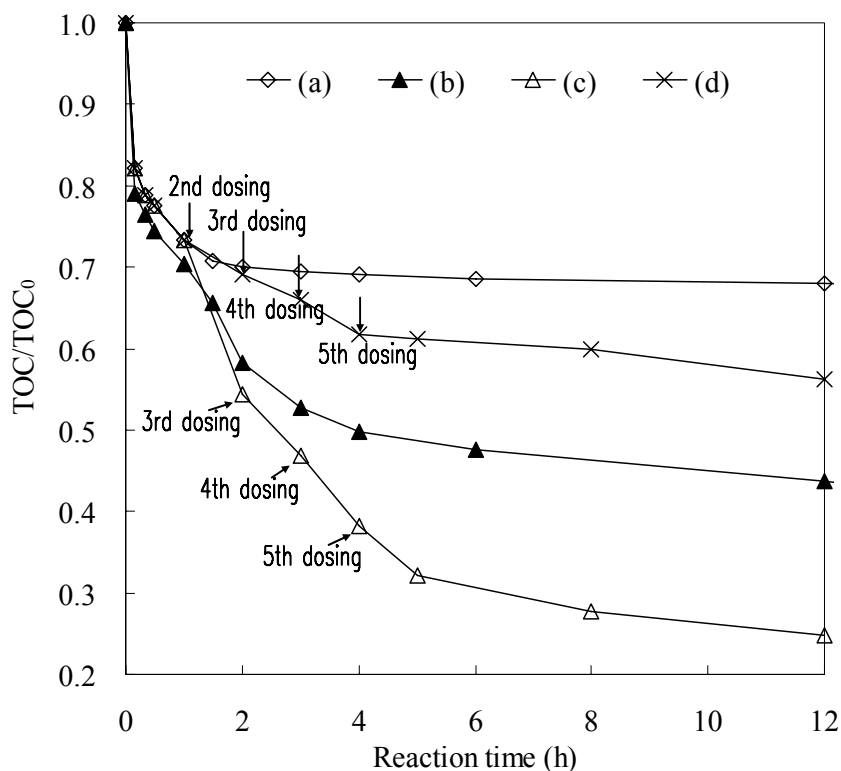


Figure 4-11: TOC removal as a function of reaction time. Experimental conditions: $[\text{RhB}]_0 = 0.10 \text{ mM}$, without pH adjustment. (a) RFO = 1:10:10, (b) RFO = 1:50:50, (c) RFO = 1:50:50, stepwise addition of Fe(II) and Oxone[®], (d) RFO = 1:10:50, stepwise addition of Oxone[®].

The role of Fe(II) catalyst in the stepwise approach was investigated as well. It was carried out by initiating the reaction at a RFO ratio 1:10:10, then the additional Oxone[®] was dosed into the reactor in stepwise until the final RFO reached 1:10:50, as shown by the curve d in Figure 4-11. Compared with the curve c (RFO = 1:50:50), TOC removal

of the curve d reduced to 44%, which was much smaller than that of the curve c (75%). This suggests that the slow regeneration of Fe(II) catalyst can not support the fast oxidation reactions in time. It is necessary to maintain Fe(II) level during the stepwise process to ensure effective and rapid mineralization.

4.3 Summary

In this chapter, an oxidation process using sulfate radicals that activated by transition metal mediated Oxone[®] process has been evaluated in depth by monitoring the degradation of RhB in aqueous solution under different conditions. Ferrous ion was chosen as the transition metal due to its potential catalytic effect and wide availability in printing and dyeing industrial effluent. The effects of parameters including reactant dosing sequence, catalyst/Oxone[®] molar ratio and concentration, solution pH level, and inorganic salts on the process performance have been investigated. Total RhB removal was obtained within 90 min under an optimal Fe(II)/Oxone[®] molar ratio of 1:1 without pH adjustment. The RhB degradation was found to be a two-stage kinetics, consisting of a rapid initial decay and followed by a retarded stage. In addition, experimental results indicated that the presence of certain anions had either positive or negative effect on the Fe(II)-mediated Oxone[®] process. The inhibitory effect on the RhB degradation in the presence of SO_4^{2-} was elucidated by a proposed formula using Nernst equation. Furthermore, mineralization of dye in terms of TOC removal indicates that stepwise addition of Fe(II) and Oxone[®] can significantly improve the process performance by about 20%, and the retention time required for a specific performance can be greatly reduced comparing with the conventional one-off dosing method.

CHAPTER 5

Degradation of 2,4,5-T by Electro-Fe(II)/Oxone[®] Process using Iron Sheet as the Sacrificial Anode

5.1 Introduction

2,4,5-Trichlorophenoxyacetic acid (2,4,5-T) developed in the late 1940s is a chlorophenoxy acetic acid herbicide. It has been used worldwide on a large scale in agriculture to control the growth of broad-leaved weeds on cereal crops, grasslands, lawns (Brillas et al., 2004), and in post-emergence applications (Chang et al., 1998). Although the use of 2,4,5-T was banned in some developed countries due to its toxicity concerns, it is still widely used nowadays in most developing countries for controlling weeds and enhancing crops yield (Chaudhary et al., 2009, de Liphay et al., 2007). 2,4,5-T is considered to be less biodegradable than its analogous herbicide 2,4-D, and has greater resistance to microbial metabolism likely stemming from the additional chlorine constituent on the aromatic ring (Chaudhary et al., 2009). Thus, 2,4,5-T can be detectable in both surface water and groundwater not only during the application of the herbicide, but also after a long period of usage due to its comparatively high resistance to biodegradation in the environment.

Various methods, including adsorption, biological degradation and (AOPs have been investigated and developed to degrade 2,4,5-T. Among these emerging treatment technologies, AOPs are considered effective in water treatment applications (Chan and Chu, 2009). Several AOPs have been explored for the degradation of 2,4,5-T, such as Electro-Fenton process (Brillas et al., 2004), Photoelectro-Fenton process (Boye et al.,

2003), photolytic-electrolytic system (Chaudhary et al., 2009) and UV/TiO₂ (Hemant et al., 2007).

In recent years, existing studies have shown that sulfate radicals generated by the combination of persulfate or peroxymonosulfate with transition metals (Fe²⁺, Ag⁺, Co²⁺) are promising in the degradation of organic contaminants. Moreover, sulfate radicals demonstrate higher standard reduction potential than hydroxyl radicals at neutral pH and are more selective for oxidation than hydroxyl radicals at acidic pH (Anipsitakis and Dionysiou, 2004a). As a result, sulfate radical based-advanced oxidation processes (SR-AOPs) have been a great interest for researchers in water treatment.

In this study, a new approach named as “Electro-Fe(II)/Oxone[®] (EFO)” process by coupling electrochemical process and ferrous mediated activation of Oxone[®] to generate sulfate radicals was investigated. In the EFO, soluble ferrous ions were continuously released to the solution from the surface of an iron electrode via anodic oxidation. Once the Oxone[®] is added into the system, the sulfate radicals are generated through the catalysis of transition metal as follows:



The counter reaction, which simultaneously occurs at the cathode, is the reduction of ferric ions (Isarain-Chavez et al.), shown as follows:



One major benefit of this process is that ferrous ions are electrochemically produced in the process from the sacrificial iron anode, which is reported to be a less

energy-demanding reaction (Figuerola et al., 2009). Moreover, the cathodic reduction reaction enhances the regeneration of Fe^{2+} , whereas in a traditional $\text{Fe(II)/Oxone}^{\text{®}}$ process, the rapid depletion as well as the slow regeneration of Fe(II) usually terminates the production of sulfate radicals as can be observed in the trends of Figure 4-1 in Chapter 4. In contrast, the immediate regeneration of Fe(II) in EFO ensures a smooth and continuous generation of sulfate radicals and makes the best utilization of oxidant. The EFO also has the advantage in minimizing the transportation and utilization problems of commercial ferrous salt.

In this study, the performance of the EFO to degrade 2,4,5-T was investigated through the examination of various operational parameters, including applied current, electrolyte Na_2SO_4 , contaminant concentration, dosage of oxidant, and initial solution pH, by which the optimal experimental conditions were identified. In addition, radicals quenching study was also carried out to identify the predominant active radicals involved in the EFO process.

5.2 Results and Discussion

5.2.1 Comparative study of different processes

The following tests were carried out to evaluate the efficiency of 2,4,5-T degradation using EFO: (1) $\text{Oxone}^{\text{®}}$ alone, (2) Fe(II) -mediated $\text{Oxone}^{\text{®}}$ process by adding ferrous sulfate as the source of Fe(II) catalyst, (3) sole-electrolytic process using iron as anode and graphite as cathode, (4) Electro/ $\text{Oxone}^{\text{®}}$ process using graphite and iron as anode and cathode, respectively, and (5) EFO. The results are compared in Figure 5-1. It can be obviously seen that no appreciable herbicide elimination was observed when $\text{Oxone}^{\text{®}}$ or Electrolytic process was separately applied. A slow and incomplete 2,4,5-T decay

(about 50%) was achieved by the combined Electro/Oxone[®] process within 30 min, which demonstrates that the electrolysis can also be an useful alternative to activate the formation of sulfate radicals (from peroxymonosulfate) in addition to the conventional radiolysis, photolysis, thermal activation, and transition metal catalysis. The activation reactions are shown in Eqs. 5-4 and 5-5.

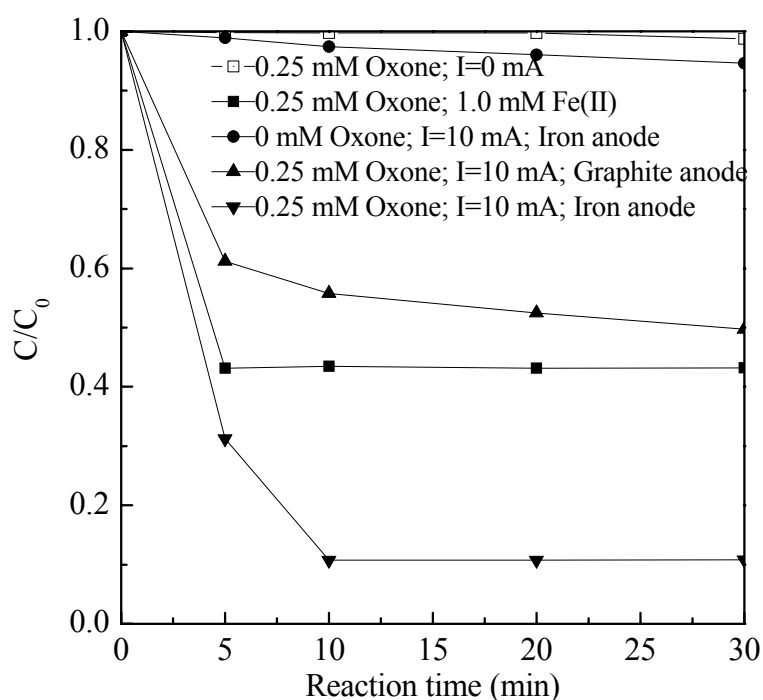


Figure 5-1: 2,4,5-T degradation under various reaction conditions. Experimental conditions: $[2,4,5\text{-T}]_0 = 0.10 \text{ mM}$, $[\text{Na}_2\text{SO}_4]_0 = 0.05 \text{ M}$ as supporting electrolyte, no pH adjustment.

A better herbicide removal efficiency (around 57%) was achieved using the Fe(II)-mediated Oxone[®] process by applying 1.0 mM $[\text{Fe(II)}]$ (the optimal dosage determined separately). In contrast, the EFO demonstrates the fastest and nearly complete herbicide degradation within 10 min. The exceptional performance of the EFO

can be rationalized as follows. Firstly, ferrous ions were electrochemically produced in the reactor from the sacrificial iron anode. Upon the reaction between Fe (II) and Oxone[®], sulfate radicals are generated to degrade the probe, while Fe (II) can be regenerated by the reduction of Fe (III) at cathode, which maintains a higher level of catalyst in the solution. Secondly, the electrolysis itself (i.e., without catalyst) may initiate the activation of peroxymonosulfate, which gives rise to the generation of powerful radical species. Therefore, the synergistic effect by coupling ferrous mediated activation of Oxone[®] with electrochemical activation of peroxymonosulfate facilitates the EFO as an effective process in the generation of highly active radicals.

5.2.2 Effect of applied current

The effect of applied current on the degradation of 2,4,5-T was investigated in the range of 5 to 30 mA at current-controlled conditions without pH adjustment. The results are presented in Figure 5-2, where a significant jump of decay rate (inset) was observed when the applied current increased from 5 to 10 mA. However, the decay rate leveled off (at around 0.24 min⁻¹) as the current further increased over 15 mA. The initial rate increment at lower currents is likely attributed to the elevated ferrous ion concentration nearby the anode as the current increased. A faster ferrous ion generation results in a faster production of sulfate radicals and therefore the faster 2,4,5-T decay. However, as the ferrous ions accumulated to certain level in the solution, the excess ferrous ions may act as sulfate radical scavengers as shown in Eq. 5-6 (Rastogi et al., 2009). Thus, the decay of the probe is retarded due to the competition of sulfate radicals by excessive Fe(II) in the solution when the applied current was too high.



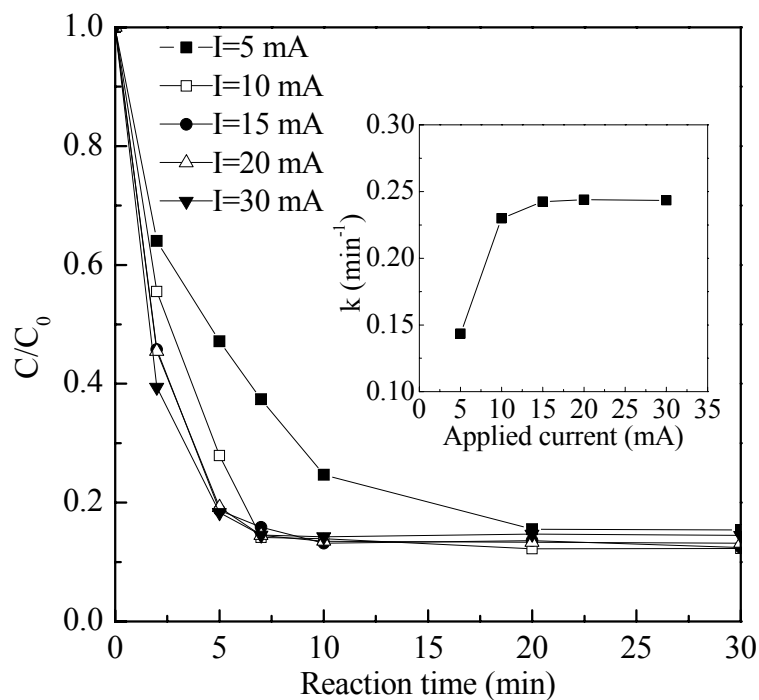


Figure 5-2: Effect of applied current on 2,4,5-T decay by EFO. The inset shows the kinetic constants of herbicide decay at various applied currents. Experimental conditions: [2,4,5-T]₀ = 0.10 mM, [Oxone[®]]₀ = 0.25 mM, [Na₂SO₄] = 0.05 M as supporting electrolyte, I = 10 mA, no pH adjustment.

From the electrical energy consumption point of view, the electrical energy required to degrade 0.1 mM 2,4,5-T by EFO at various applied currents was calculated in terms of kWh·m⁻³ using Eq. 5-7 shown as follows:

$$E = \frac{UIt}{V} \times 10^{-3} \quad (5-7)$$

Where U is the voltage measured during the reaction (volt), I is the applied current (A), t is the electrolysis time (h), and V is the volume of reaction solution (m³) (Khataee et al., 2009). The calculated values are summarized in Table 5-1. As shown, optimal energy consumption was obtained when the applied current was 10 mA. Therefore, to minimize the possible quenching effect at higher current and to achieve efficient energy consumption, applied current of 10 mA was adopted in the rest of this study.

Table 5-1: The electrical energy required to degrade 0.1 mM 2,4,5-T at various applied current by EFO.

Applied current (mA)	Degradation efficiency (%)	Required time (min)	Energy consumption (kWh·m ⁻³)
5	84.5	20	0.0155
10	85.9	7	0.0107
15	84.2	7	0.0344
20	85.5	7	0.0717
30	85.5	7	0.1544

Note: the concentration of Oxone[®] was 0.25 mM.

Additionally, blank experiment was carried out to investigate the Fe ions (all the Fe ions have been transferred to Fe²⁺) generation using 0.05 M Na₂SO₄ as electrolyte at applied current of 10 mA without the addition of contaminant and oxidant. The experimental result is shown in Figure 5-3. It can be noted that the iron ions smoothly increase from 0 mM (0 min) to 1.06 mM (10 min) and finally to 2.08 mM (30 min) in the solution. Compared with Fe²⁺ dosages applied in regular electro-Fenton processes or traditional Fenton process (1 mM (Brillas et al., 2004), 15 mM (Wang et al., 2008) and 25 mM (Sun et al., 2009)), the released iron ion in the solution is relatively low and acceptable.

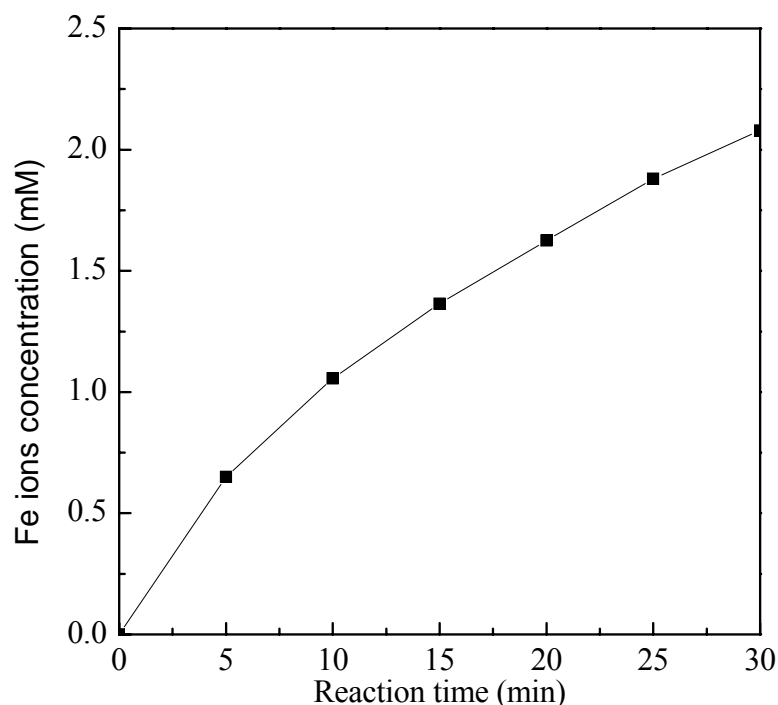


Figure 5-3: Iron ion accumulation in the solution. (Anode: Fe; Cathode: Graphite; 0.05 M Na_2SO_4 as electrolyte; $I = 10 \text{ mA}$).

5.2.3 Effect of electrolyte concentration

Electrolyte concentration directly affects the electrical conductivity of the solution. In this study, the influence of electrolyte concentration on the degradation of 2,4,5-T was examined by varying the concentration of Na_2SO_4 from 0.006 - 0.100 M while keeping other parameters unchanged. The results are demonstrated in Figure 5-4 with inset showing the pseudo first-order rate constants of 2,4,5-T decay versus $[\text{Na}_2\text{SO}_4]$. It is found that the degradation rate increases linearly with $[\text{Na}_2\text{SO}_4]$ increasing from 0.006 to 0.050 M, then levels off at higher $[\text{Na}_2\text{SO}_4]$. The linear increment from low to mid $[\text{Na}_2\text{SO}_4]$ is ascribed to the lower electrolyte concentration in the solution, leading to a lower electrical conductivity and therefore a higher voltage when the current is kept constant. However, if the voltage is too high, the side reactions of O_2 and H_2 evolution occur, reducing the current efficiency and then leading to the decreased decay rate. In

addition, the decay rate may also be retarded with the increment of $[\text{Na}_2\text{SO}_4]$ as can be seen in Chapter 4. Thus, 0.05 M Na_2SO_4 was chosen as the optimal electrolyte concentration and used for the rest of the study.

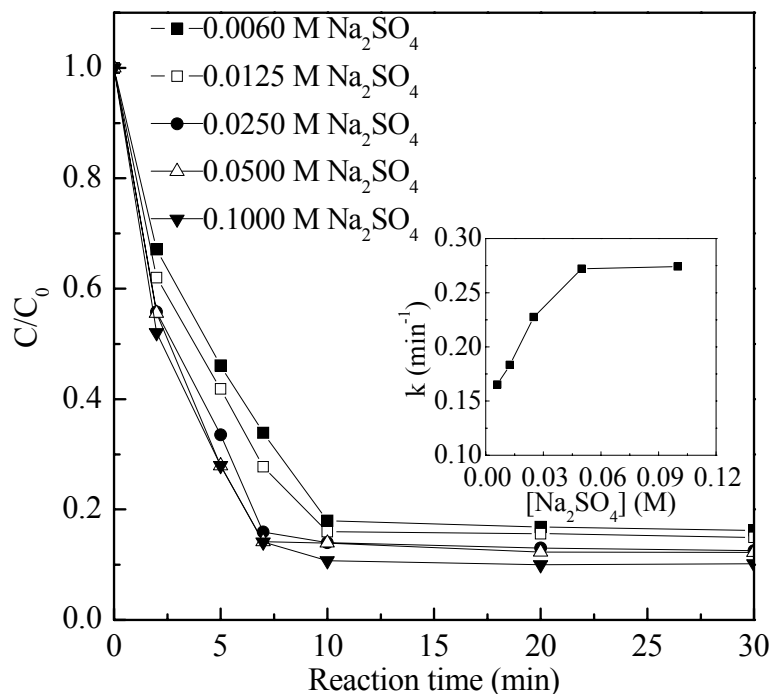


Figure 5-4: Effect of $[\text{Na}_2\text{SO}_4]$ on herbicide decay by EFO. The inset shows the decay rate constants as a function of $[\text{Na}_2\text{SO}_4]$. Experimental conditions: $[2,4,5\text{-T}]_0 = 0.10$ mM, $[\text{Oxone}^{\text{®}}]_0 = 0.25$ mM, $I = 10$ mA, no pH adjustment.

5.2.4 Effect of 2,4,5-T and oxidant dosage

The efficiency of EFO as a function of the initial herbicide concentration was investigated by varying $[2,4,5\text{-T}]$ from 0.025 to 0.200 mM. The results in terms of pseudo first-order kinetics are illustrated in Figure 5-5. As shown in the inset, the decay rate constant linearly decreases as the initial $[2,4,5\text{-T}]$ increases. In addition, the removal percentage of 2,4,5-T decreases from 100 to 69% (at 10 min) when $[2,4,5\text{-T}]$ increases from 0.025 to 0.200 mM.

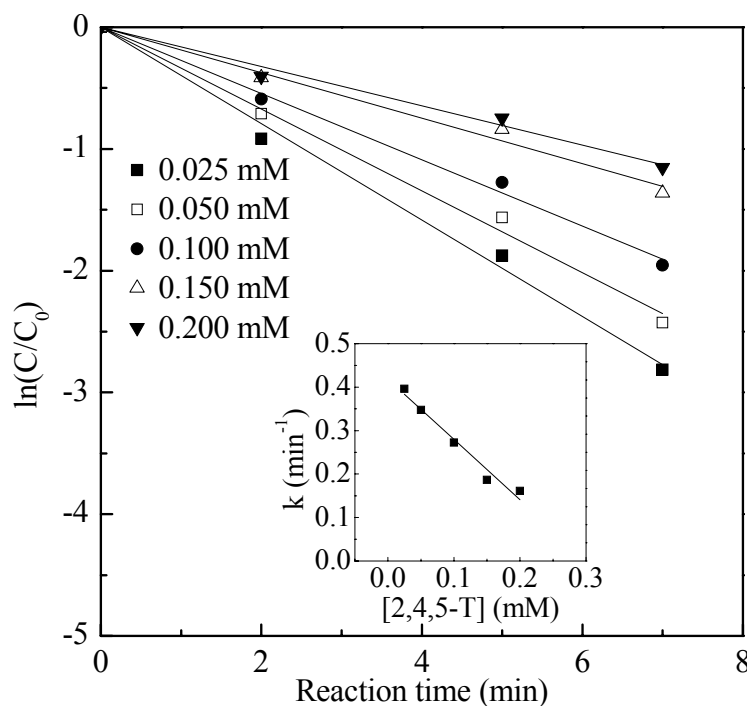


Figure 5-5: Degradation of various initial [2,4,5-T] by EFO. The inset shows the decay rate constants as a function of [2,4,5-T]. Experimental conditions were $[\text{Oxone}^{\text{®}}]_0 = 0.25 \text{ mM}$, $[\text{Na}_2\text{SO}_4] = 0.05 \text{ M}$ as supporting electrolyte, $I = 10 \text{ mA}$, no pH adjustment.

To elucidate the effect of $[\text{Oxone}^{\text{®}}]$ in EFO, the initial $[\text{Oxone}^{\text{®}}]$ was increased from 0.0625 to 0.5000 mM and the final degradation of 2,4,5-T increased from 49 to 97% as shown in Figure 5-6. In general, the higher the oxidant dosage is, the better the herbicide removal efficiency shall be. However, it is interesting to note that the initial decay rates increase with the increment of $[\text{Oxone}^{\text{®}}]$ from 0.0625 to 0.250 mM (i.e. optimized at 0.250 mM), and then the initial rate is retarded as $[\text{Oxone}^{\text{®}}]$ further increased (see inset of Figure 5-6). This observation is inconsistent with previous findings; for example, the decolorization rate of acid red 88 follows zero-order with respect to $[\text{Oxone}^{\text{®}}]$ in a $\text{Co}^{2+}/\text{Oxone}^{\text{®}}$ process (Madhavan et al., 2009). The divergence is possibly caused by the different treatment processes. The slow transformation of Co^{3+} to Co^{2+} could be a rate-limiting factor in $\text{Co}^{2+}/\text{Oxone}^{\text{®}}$ system (Huang et al., 2009),

while it is not the case for EFO due to the fact that ferrous ions can be effectively regenerated through ferric ion reduction at the cathode. In addition, the mechanism of colour (i.e. chromophore) removal is different from that of a molecular decay.

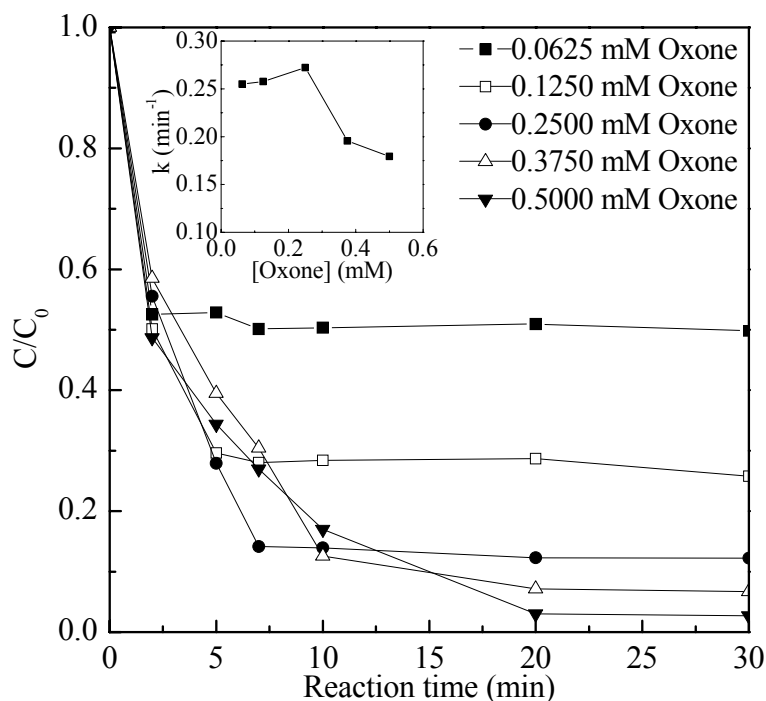


Figure 5-6: Decay of 2,4,5-T with different [Oxone[®]] by EFO. Experimental conditions: [2,4,5-T]₀ = 0.10 mM, [Na₂SO₄] = 0.05 M, I = 10 mA, no pH adjustment.

When the [Oxone[®]] is higher than 0.250 mM (i.e., the optimal dosage in terms of initial decay rate), although the decay rate is retarded, the overall removal of 2,4,5-T at the end of the process is still better than that at the optimal dosage. This suggests that the increase of [Oxone[®]] can still improve the overall removal of 2,4,5-T if an extended reaction time is allowed. However, the performance in the utilization of the valuable sulfate radicals is apparently not optimized. This can be explained by the unfavorable consumption of SO₄^{•-} radicals by the excessive HSO₅⁻, which leads to the scavenging of sulfate radicals, generating of less reactive SO₅^{•-}, and thus slower decay rates, as explained by Eq. 5-8 (Ling et al., 2010, Madhavan et al., 2009),



Because of the overdose of Oxone[®], the HSO_5^- , $\text{SO}_4^{\bullet-}$ and SO_5^{\bullet} radicals remaining in the solution are still in good quantities, and the overall removal of 2,4,5-T is not affected as long as the reaction time is sufficient. In practice, however, an unlimited addition of Oxone[®] in EFO is not suggested and the determination of an optimal dosage is critical for a cost-effective application.

5.2.5 Effect of initial pH

The effect of initial pH levels on the EFO was also explored. Figure 5-7 illustrates the corresponding 2,4,5-T degradation efficiency with the change of solution pH level. Pseudo first-order kinetic was observed with high linear regression coefficient (r^2) above 0.95 at different pH levels. As shown in the inset of Figure 5-7, the herbicide decay rate sharply increases as the solution pH decreases from 4.47 to 1.50, while the rate slows down and levels off for pH levels higher than 4.47. At first glance, it looks similar to the conventional Fenton's process, which is generally regarded to have better performance at acidic condition. However, the Fenton's process is inhibited at extremely acidic environment due to the formation of $(\text{Fe(II)}(\text{H}_2\text{O}))^{2+}$ ($\text{pH} < 2.5$) (Gogate and Pandit, 2004) and Fe(III)-hydroxyl complexes, Fe(OH)^{2+} ($\text{pH} < 3$) (Pignatello et al., 1999). The former reduces the availability of free Fe(II), while the latter inhibits the regeneration of Fe(II) from Fe (III). However, these negative effects are not found in EFO, which performs well at the extreme acidic condition.

To further verify the validity of the above observation at the low pH level, additional tests were conducted at initial pH of 1.5 without Oxone[®] addition and with/without

radical scavenger. As shown in Figure 5-8, the Electro-Fe(II) (i.e., without Oxone[®]) at pH level of 1.5 can remove 40% of 2,4,5-T at 30 min, which is much higher than that at neutral pH (about 5%, see Figure 5-1). This indicates that the low pH level can improve the process performance. In this study, two typical radical quenching agents, methanol and t-butyl alcohol, were employed to investigate the mechanism of Electro-Fe(II) process. As shown in Figure 5-8, the presence of 1 M methanol or 1 M t-butyl alcohol significantly retards the herbicide degradation, indicating that 2,4,5-T decay is dominated by the oxidation of radical species. The degradation of 2,4,5-T in the presence of t-butyl alcohol is slightly higher than that of methanol (with a ratio of 2:1 in terms of removal %), indicating the presence of both hydroxyl and sulfate radicals in Electro-Fe(II) process. This is because methanol contains α -hydrogen that can rapidly quench $\cdot\text{OH}$ and $\text{SO}_4^{\cdot-}$. The t-butyl alcohol however, as a weaker quencher for sulfate radicals, selectively quenches hydroxyl radicals (Anipsitakis and Dionysiou, 2004a) and results in about 2% (see Figure 5-8) higher removal of 2,4,5-T than methanol.

It is therefore very likely that in the Electro-Fe(II) process, Fenton's reagents are generated in the acidic electrolysis medium while utilizing iron as anode and graphite as cathode. Simultaneously, $\text{S}_2\text{O}_8^{2-}$ can be generated from the oxidation of SO_4^{2-} and HSO_4^- ions ($\text{pK}_{\text{a}2}$ of H_2SO_4 is 1.26×10^{-2} so $[\text{SO}_4^{2-}]/[\text{HSO}_4^-] = 0.42$ at pH 1.5) as sulfate medium is used as the electrolyte (Brillas et al., 2009). Therefore, the following reactions (Eqs. 5-9 to 5-13) may be responsible for the radical species' generation in the Electro-Fe(II) process:





In Figure 5-7, the decay rate is gradually leveled off from pH 4.47 to 10.31. This is a result of the formation of ferric hydroxide precipitates, $\text{Fe}(\text{OH})_{3(s)}$, at higher pH level. It not only leads to the decrease of dissolved $\text{Fe}(\text{II})$ and $\text{Fe}(\text{III})$, but also retards the regeneration of ferrous catalyst by partially coating on the electrode surface, which in turn significantly reduces the herbicide degradation efficiency. In addition, Oxone[®] is unstable at basic conditions and its self-dissociation was observed mainly through non-radical pathways, which also contributes to the retardation of the reaction rate.

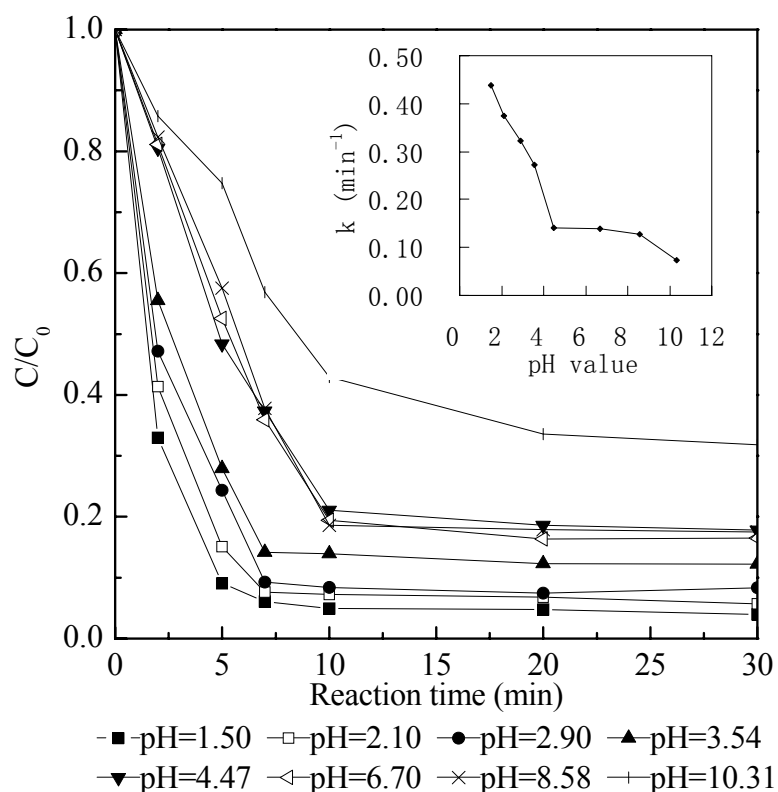


Figure 5-7: Effect of initial solution pH on the decay of 2,4,5-T. The inset shows the decay rate constants as a function of solution pH. Experimental conditions were $[2,4,5\text{-T}]_0 = 0.10 \text{ mM}$, $[\text{Oxone}^{\text{®}}]_0 = 0.25 \text{ mM}$, $[\text{Na}_2\text{SO}_4] = 0.05 \text{ M}$, $I = 10 \text{ mA}$.

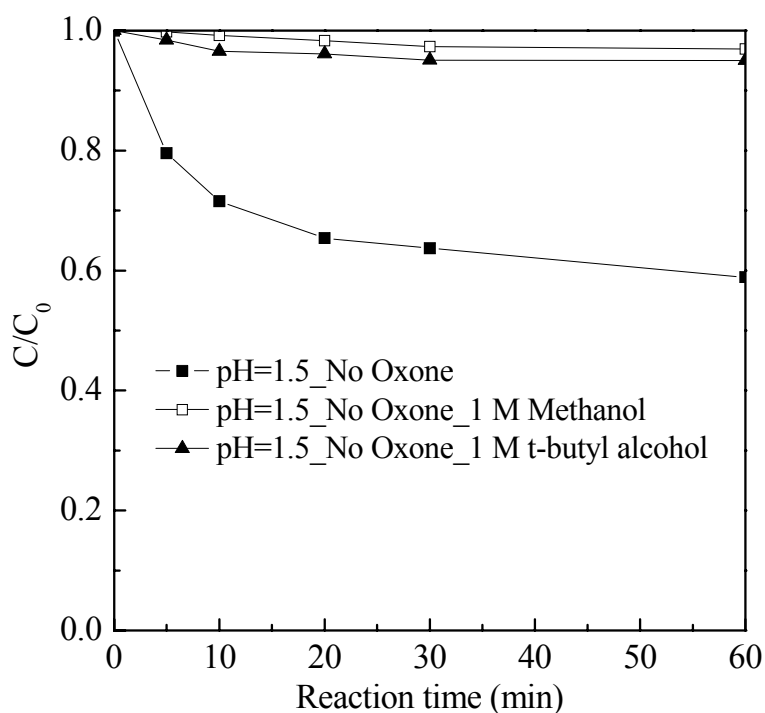


Figure 5-8: Degradation of herbicide by Electro-Fe(II) system in pH = 1.5 solution without the presence of Oxone[®]. Experimental conditions were [2,4,5-T]₀ = 0.10 mM; [Na₂SO₄] = 0.05 M as supporting electrolyte; I = 10 mA.

5.2.6 Radical quenching study

To investigate the 2,4,5-T decay mechanism in EFO, three radical quenching agents were utilized to evaluate the contribution of various radicals or oxidizing species to the process. As indicated in Figure 5-9, the addition of 1 M methanol or 1 M ethanol significantly inhibits the system performance with herbicide decay efficiency decreased from 85.9% to 12.9% and 14.3% in 7 minutes, respectively, whereas the addition of 1 M t-butyl alcohol only results in 53% herbicide decay drop compared with that of 72.6% and 69.1% by the addition of methanol and ethanol, respectively. The differences in the herbicide decay drop by the three radical scavengers imply the involvement of both hydroxyl and sulfate radical in the system as discussed previously. Nevertheless, the 2,4,5-T was not fully quenched suggesting the possibility of insufficient quenching

agent and/or self-dissociation of oxidant through non-radical pathway (Rastogi et al., 2009) in the solution. To verify their contribution, the methanol was further increased to 2 M and the decay of 2,4,5-T was almost stopped, which suggests the former is likely the main cause. Therefore, the decay of herbicide 2,4,5-T in EFO is dominated by radical based mechanisms.

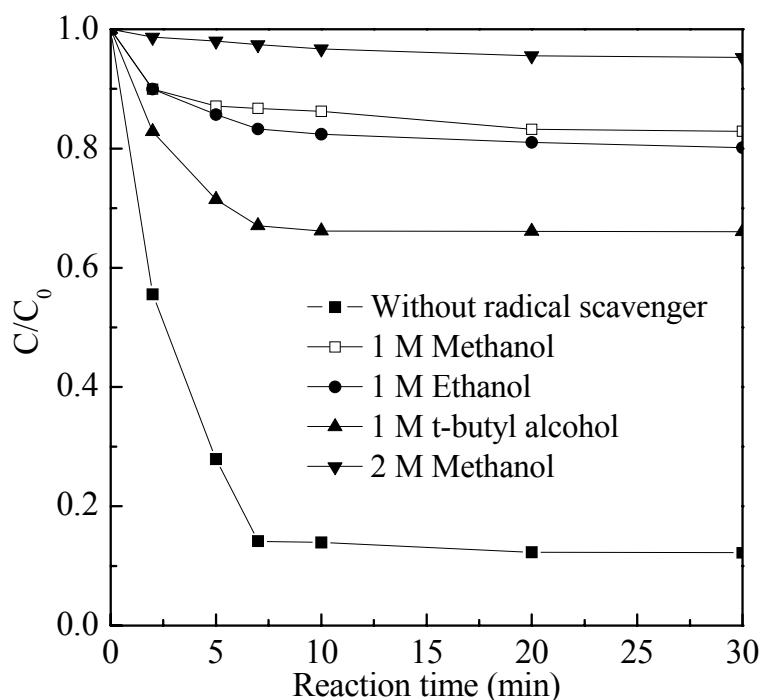


Figure 5-9: Effect of different radical quenching agents on herbicide degradation by EFO. Experimental conditions: $[2,4,5\text{-T}]_0 = 0.10 \text{ mM}$, $[\text{Oxone}^{\text{®}}]_0 = 0.25 \text{ mM}$, $[\text{Na}_2\text{SO}_4] = 0.05 \text{ M}$, $I = 10 \text{ mA}$, no pH adjustment.

5.3 Summary

In this study, the electrochemically enhanced transition metal-activated Oxone[®] process, EFO, was experimentally verified to be very effective in degrading 2,4,5-T with over 90% removal in 10 minutes. Degradation of herbicide 2,4,5-T by EFO was observed to follow pseudo first-order kinetics. The effects of various operational parameters of EFO were also examined to optimize the process. Based on the test results, the optimal

applied current was determined to be 10 mA, in which both the herbicide removal efficiency and energy consumption were optimized. For the effect of [2,4,5-T], experimental results showed that (1) the degradation efficiency for 0.025, 0.05, 0.1, 0.15 and 0.2 mM 2,4,5-T was 100%, 98%, 88%, 78% and 69%, respectively; (2) 2,4,5-T decay rate constant linearly decreases with the increment of initial herbicide concentration. For the effect of Oxone[®] dosage, the test results demonstrate that 0.25 mM Oxone[®] exhibits the optimal 2,4,5-T decay rate and an unlimited increment of [Oxone[®]] is not favorable to the EFO. Moreover, it was found that herbicide decay rate sharply increases as the solution pH decreases. A favorable dual effect was subsequently conducted to elucidate this performance enhancement at acidic conditions. Radicals quenching study revealed the presence of both hydroxyl and sulfate radicals in the process. Generally, a highly effective radicals based-advanced oxidation process was investigated for the degradation of 2,4,5-T in this study. Compared with other AOPs, the proposed EFO has the following advantages: (1) in-situ generation of Fe(II), (2) acceleration of regenerating Fe(II) from Fe(III), (3) minimization of the transportation and utilization problems of commercial ferrous salt, and (4) a less energy-demanding reaction, indicating the proposed EFO is a promising process.

CHAPTER 6

Degradation of 2,4,5-T by Fe(II)/Oxone[®] Process with UV

Irradiation

6.1 Introduction

Chlorophenoxy acid herbicides, one of the most important classes of chlorinated herbicides, are extensively used individually or in combination with other herbicides in agriculture and forestry to control the growth of broadleaf weeds and grasses. They are also known as auxin mimics causing hyperplastic growth. These substances have relatively high solubility in water due to their free acid character and the salt form (Casella and Contursi, 2007). Therefore, these herbicides are easily washed off from the soil into aquatic environment and thus have been frequently detected in groundwater (de Lipthay et al., 2007). Additionally, these compounds may be contaminated by dioxins during the production process, which imposes the potential of high toxicity to the environment (1996). Due to their high water solubility and toxicological risk, several chlorophenoxy acid herbicides (e.g. MCPA, 2,4-D, 2,4-DP and 2,4,5-T) are currently under regulatory control or listed as priority pollutants by some countries (Hassan et al., 2011). Thus, it is imperative to develop alternative treatment technologies which effectively eliminate these compounds from wastewater effluents.

In the past few decades, AOPs have demonstrated as the promising technologies for the degradation of recalcitrant organics. AOPs are based on the generation of highly powerful radicals by combining of oxidants like ozone, hydrogen peroxide, persulfate/Oxone[®] (the source providing peroxymonosulfate, HSO_5^-) with irradiation

(UV or visible), ultrasound, and/or catalysts (such as transition metals or semiconductors). The radicals involved in AOPs are mainly hydroxyl radicals ($\bullet\text{OH}$) and sulfate radicals ($\text{SO}_4^{\bullet-}$). The generation of hydroxyl radicals to eliminate toxic and recalcitrant organic compounds has been comprehensively investigated over the past decades. In recent years, sulfate radicals have attracted intensive attention due to their selectivity for target-orientated oxidation and higher standard reduction potential (2.5-3.1 V) at neutral pH in comparison with hydroxyl radicals (1.8-2.7 V depending on the solution pH) (Anipsitakis and Dionysiou, 2003, Chan and Chu, 2009). A number of studies have demonstrated that transition metal-mediated activation of Oxone[®] is a promising alternative for the generation of sulfate radicals. According to Anipsitakis and Dionysiou (2004a), Co(II) was found as the most efficient metal catalyst for the activation of Oxone[®] among nine investigated transition metals. However, dissolved Co(II) into treated effluent may render adverse effect on human health because cobalt is recognized as a priority of metal pollutant (Shukla et al., 2010). As a result, several attempts have been made in exploring eco-friendly transition metals to effectively activate the decomposition of Oxone[®] so that to form sulfate radicals. Rastogi *et al.* (2009) reported a novel Fe(II)/Oxone[®] (FO) process for PCBs degradation in aqueous and sediment systems. The coupling of Oxone[®] with Fe(II) has also been evaluated for the generation of $\text{SO}_4^{\bullet-}$ in terms of Rhodamine B degradation in aqueous solution in the present study as reported in Chapter 4. However, similar to the Fenton process, the rapid depletion of radicals, the slow regeneration of Fe(II), and production of ferric hydroxide sludge in the traditional FO restrict its use. These limitations could be relaxed by the use of photo-assisted FO process (i.e., Fe(II)/Oxone[®]/UV or FOU). The FOU may potentially improve the reaction through:

- 1) The use of UV (≤ 260 nm) irradiation promotes the production of both $\text{SO}_4^{\bullet-}$ and $\bullet\text{OH}$

radicals through the direct photolysis of Oxone[®] as shown in Eq. 6-1 (Hayon et al., 1972b, Madhavan et al., 2008):



2) In the presence of UV irradiation, the Fe(II)/Fe(III) catalytic circle is propagated by the additional photo-reduction of Fe(III)-complexes, in which Fe^{3+} was reported to exist as Fe^{3+} and/or Fe(III)-complexes (such as $[\text{Fe}(\text{H}_2\text{O})_6]^{3+}$, $[\text{Fe}(\text{OH})]^{2+}$, $[\text{Fe}(\text{OH})_2]^+$ and $[\text{Fe}_2(\text{OH})_2]^{4+}$) depending on the solution pH (Gallard et al., 1999). For example, $\text{Fe}(\text{OH})^{2+}$, as the principal species at acid pH, is photosensitive according to Eq. 6-2:



It should be noted that the above reaction can not only accelerate the regeneration of ferrous ions but also produce additional hydroxyl radicals.

Against the above background, this chapter is to investigate the application of the FOU process for the degradation of a selected probe in detail, and the process was optimized through the examination of reaction kinetics at different reaction conditions. Meanwhile, the role of UV irradiation in FOU process was explored in-depth as compared to the conventional FO process. The chlorophenoxy acid herbicide, 2,4,5-T, was used as the probe compound in this chapter.

Besides, the degradation of 2,4,5-T has been investigated by using various treatment processes, such as the electrochemical method (Oturán et al., 1999), peroxi-coagulation (Boye et al., 2003), electro-Fenton method using a boron-doped diamond anode (Brillas et al., 2004), and TiO_2 mediated photocatalysis (Singh et al., 2007). Though, some simple degradation intermediates resulted from those degradation processes have been demonstrated, a systematically study on the 2,4,5-T decay mechanisms and pathways by

the FOU process is very limited.

The dominant oxidants in the FOU process are hydroxyl and sulfate radicals. They react with organic compounds mainly through the mechanisms of electron transfer, hydrogen-atom abstraction, and hydrogen addition (Neta et al., 1977). Generally, $\text{SO}_4^{\bullet-}$ reacts more selectively with target compounds through electron transfer, while $^{\bullet}\text{OH}$ radical induces reactions more readily via H-abstraction or addition (Anipsitakis and Dionysiou, 2004a). Nevertheless, the majority of the products formed by sulfate radical attack on aromatics are hydroxylation products, which are in accordance with the intermediates from hydroxyl radical attack (Anipsitakis et al., 2006).

As a result, another objective of this chapter is to identify the aromatic intermediates formed during the decay of 2,4,5-T by the proposed FOU (via $\text{SO}_4^{\bullet-}$ and $^{\bullet}\text{OH}$ radical attack) through the examination and comparison of the probe decay by UV alone and Oxone[®]/UV processes. Special attention has been paid to analyze the reaction mechanisms that rule the process. Accordingly, the decay pathways by these processes were proposed and compared. In addition, an attempt was made to investigate the effect of common anions in water on the performance of the FOU process for the decay of 2,4,5-T. Furthermore, the mineralization (referring to TOC reduction) and the release of chlorine ions as a consequence of C-Cl bond cleavage by these three processes have also been studied.

6.2 Results and Discussion

6.2.1 Comparison of direct photolysis and Oxone[®]/UV

Preliminary tests were conducted to investigate the contributions of direct photolysis (UV or near Visible) and UV-assisted activation of Oxone[®] (Oxone[®]/UV or near Visible) to the photodegradation of 2,4,5-T in aqueous solution. As shown in Figure 6-1, the direct photolysis of 2,4,5-T under visible light (419 nm) or near-UV radiation (350 nm) is negligible (< 2%), while slow direct photolysis was observed at 9% and 19% in 30 min for UV 300 and UV 254 nm, respectively. The combination of Oxone[®] and UV irradiation enhanced the efficiency of probe photodegradation compared to that of direct UV photolysis. However, inappreciable promotion (< 7%) of 2,4,5-T degradation was obtained when the wavelength is above 300 nm, suggesting the introduction of UV-A or visible irradiation can not effectively activate the decomposition of Oxone[®]. In contrast, over 80% removal of 2,4,5-T was achieved by Oxone[®]/UV-C process in 30 minutes. This significant improvement under UV 254 nm irradiation is apparently attributed to the photolysis of Oxone[®] as indicated in Eq. 6-1. Stoichiometrically, the photolysis of 1 mole HSO₅⁻ leads to the generation of 1 mole •OH and 1 mole SO₄^{•-} via the homolytic cleavage of its asymmetrical structure. Thus, radical-based oxidation mechanism in Oxone[®]/UV-C process plays a critical role in the degradation of the probe. Additionally, the photodegradation of 2,4,5-T by Oxone[®]/UV-C was found to follow the pseudo first-order kinetics with a rate constant of $5.45 \times 10^{-2} \text{ min}^{-1}$, which is around 6.26 times faster than that of UV alone at 254 nm. The differences in photo-assisted activation of Oxone[®] upon irradiation at various wavelengths can be rationalized from the following reasons. First, it was reported that little or no photochemical decomposition of Oxone[®] is observed if the wavelength is higher than 260 nm (Madhavan et al., 2008). Secondly, the absorption coefficient of a particular species is a key factor determining the absorption behavior under UV irradiation. According to Anipsitakis and Dionysiou (2004b), the molar extinction coefficient of Oxone[®] sharply decreases as wavelength

increases from 190 to 260 nm. As a result, UV 254 nm stands out for the decomposition of Oxone[®] in this study.

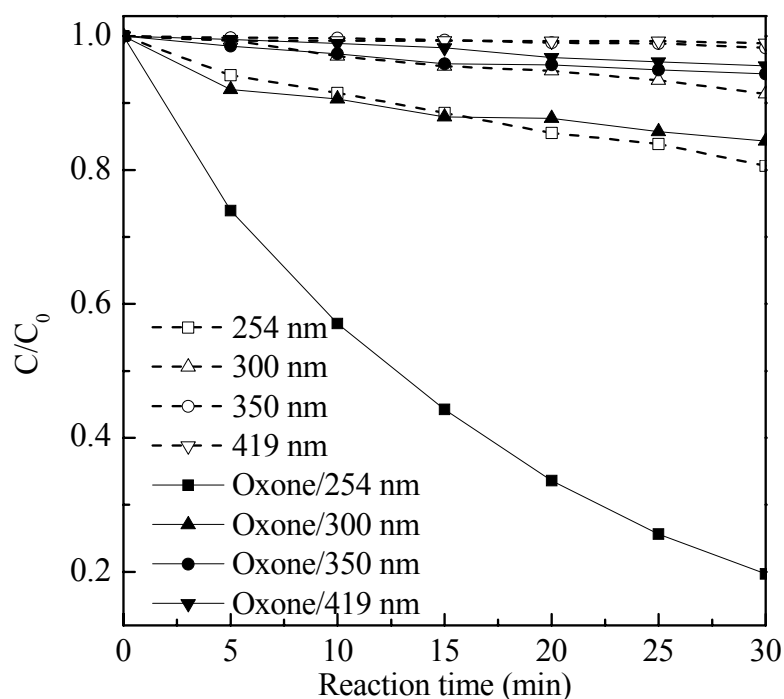


Figure 6-1: Comparison of 2,4,5-T degradation by UV alone and Oxone[®]/UV. Two UV lamps were employed, $[2,4,5-T]_0 = 0.1$ mM, $[Oxone^{\text{®}}]_0 = 0.25$ mM.

6.2.2 Fe(II)-activated Oxone[®] under irradiation at various wavelengths

Photodegradation experiments were carried out to investigate the process performance by Fe(II)-activated decomposition of Oxone[®] under irradiation at various wavelengths and the results were illustrated in Figure 6-2. For comparison purpose, the 2,4,5-T degradation in FO without UV irradiation was also examined. From Figure 6-2, the overall removal efficiency was 53% for the Fe(II)/Oxone[®]/dark process; and this conventional FO process showed a rapid degradation of 2,4,5-T in the first few minutes, following by a retarded second stage, where no appreciable degradation took place. The reaction mechanism of FO process was well elucidated in Chapter 4, where the fast reactive-stage was attributed to the immediate generation of sulfate radicals upon the

mixing of ferrous and Oxone[®]. The lag stage was due to the slow regeneration of Fe(II) from Fe(III), in which the Fe(II)/Fe(III) recycling is considered as the rate-limiting step for the conventional FO process.

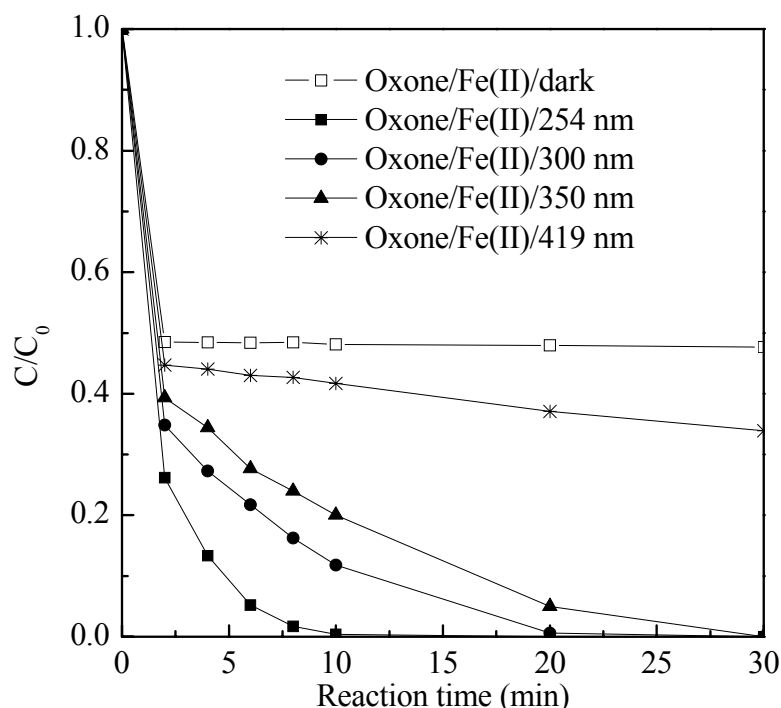


Figure 6-2: 2,4,5-T photo-decay by FOU process under different wavelengths. Two UV lamps were employed, $[2,4,5-T]_0 = 0.1$ mM, $[Oxone^{\text{®}}]_0 = 0.25$ mM, $[Fe(II)]_0 = 0.25$ mM.

However, when UV irradiation is involved, the performance is obviously enhanced due to the synergistic effects of: 1) direct UV photolysis (though minor); 2) $SO_4^{\bullet-}$ and $\bullet OH$ radicals formed by homolytic cleavage of HSO_5^- upon UV irradiation (Eq. 6-1); 3) $SO_4^{\bullet-}$ radicals generated by Fe(II)-mediated decomposition of Oxone[®]; and 4) effective regeneration of Fe(II) and the generation of additional $\bullet OH$ radicals via photo-reduction of Fe(III)-complexes (e.g. Eq. 6-2). In addition, the introduction of photo irradiation leads to complete (i.e., 100%) of 2,4,5-T removal at 254, 300 and 350 nm in 10, 20 and 30 min, respectively. The enhancement was insignificant when visible light (419 nm)

was employed. This is due to a much lower light absorption of Fe(III)-complexes at 419 nm (Brillas et al., 2009, Yan, 2006). As a result, considering the performance of UV-C in activating the photolysis of Oxone[®] and facilitating the regeneration Fe(II)/Fe(III) catalysts, the wavelength of 254 nm was chosen exclusively as the light source for the rest of this study.

6.2.3 Effect of [Fe(II)] and the role of UV irradiation

To examine the effect of Fe(II) concentration and better understand the role of UV irradiation, two sets of experiments were conducted: 1) 2,4,5-T degradation by the FO process under various [Fe(II)] from 0.002 to 5.0 mM; and 2) applying UV-C at 254 nm to the process while keeping other parameters constant. Figures 6-3 and 6-4 show the degradation of 2,4,5-T under various [Fe(II)] and the corresponding change in the remaining [Fe(II)] during the reaction by the FO and FOU, respectively. It should be pointed out that the evolution profile of Fe(II) at 0.002 mM was not given due to the limitation of detection. For the FO process, the addition of ferrous ions may either enhance or inhibit the degradation efficiency depending on the Fe(II) concentrations, as shown in Figure 6-3a. Generally, the 2,4,5-T degradation efficiency firstly increases from 6.6% to 56.8% as [Fe(II)] increases from 0.002 to 1.0 mM (corresponding to a Fe(II)/Oxone[®] ratio of 0.008 - 4.0) and then significantly decreases to 17.3% as [Fe(II)] further increases to 5.0 mM (Fe(II)/Oxone[®] = 20). An optimal [Fe(II)] was therefore observed for the FO process. This phenomenon is similar to the Fenton process with an optimal catalyst dose of iron. Previous studies (Rastogi et al., 2009) and the present study in Chapter 4 also showed that optimal molar ratio of Fe(II)/Oxone[®] at 1:1 or 2:1 (stoichiometric) was observed in Fe(II)-activated Oxone[®] process, suggesting that ferrous ions do not demonstrate true catalytic activity in FO process. Thus, an optimal

[Fe(II)] in this study was found around 1.0 mM, which corresponds to a Fe(II)/Oxone[®] ratio of 4.

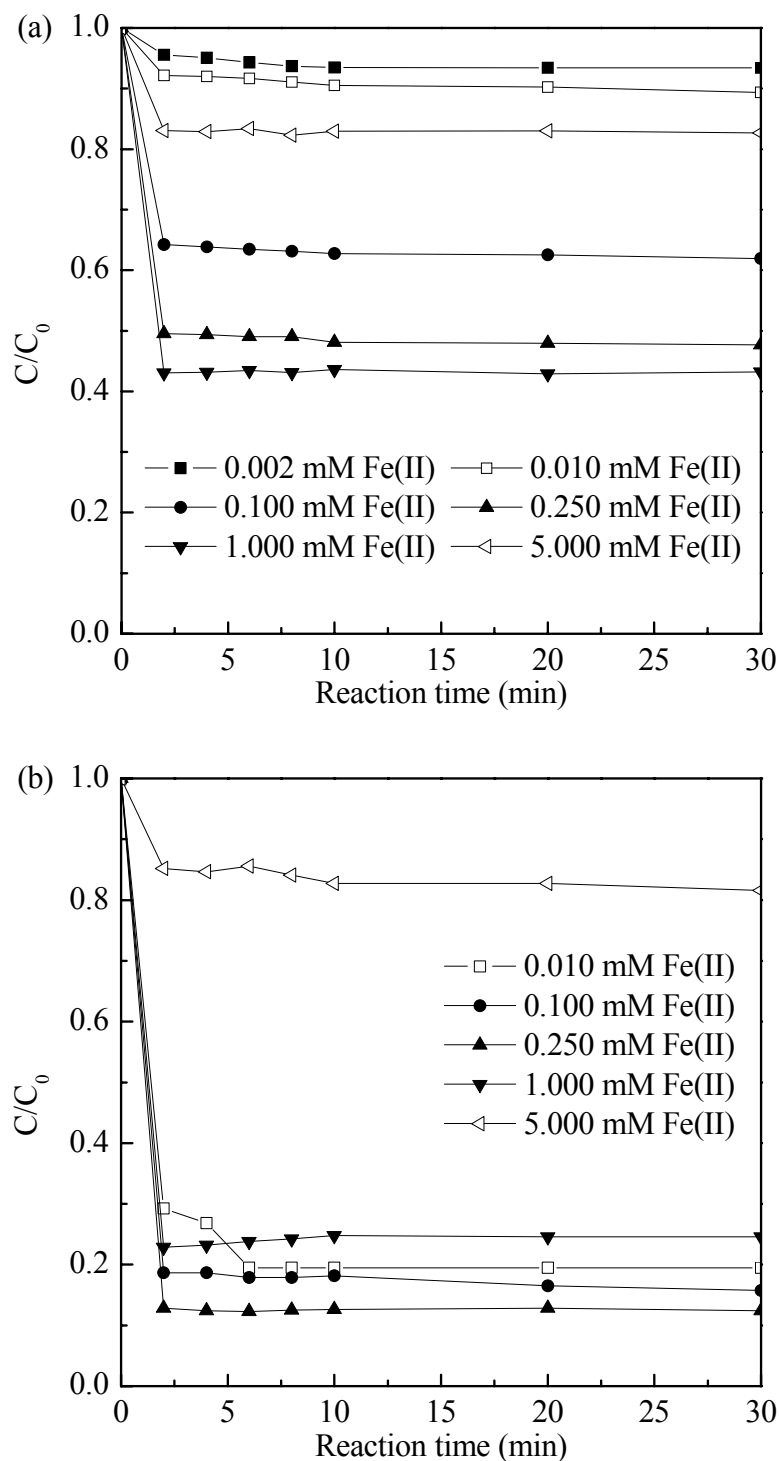


Figure 6-3: (a) Effect of Fe(II) dosage on the degradation of 2,4,5-T by FO process; (b) Change of the remaining [Fe(II)] over reaction time. [2,4,5-T]₀ = 0.1 mM, [Oxone[®]]₀ = 0.25 mM.

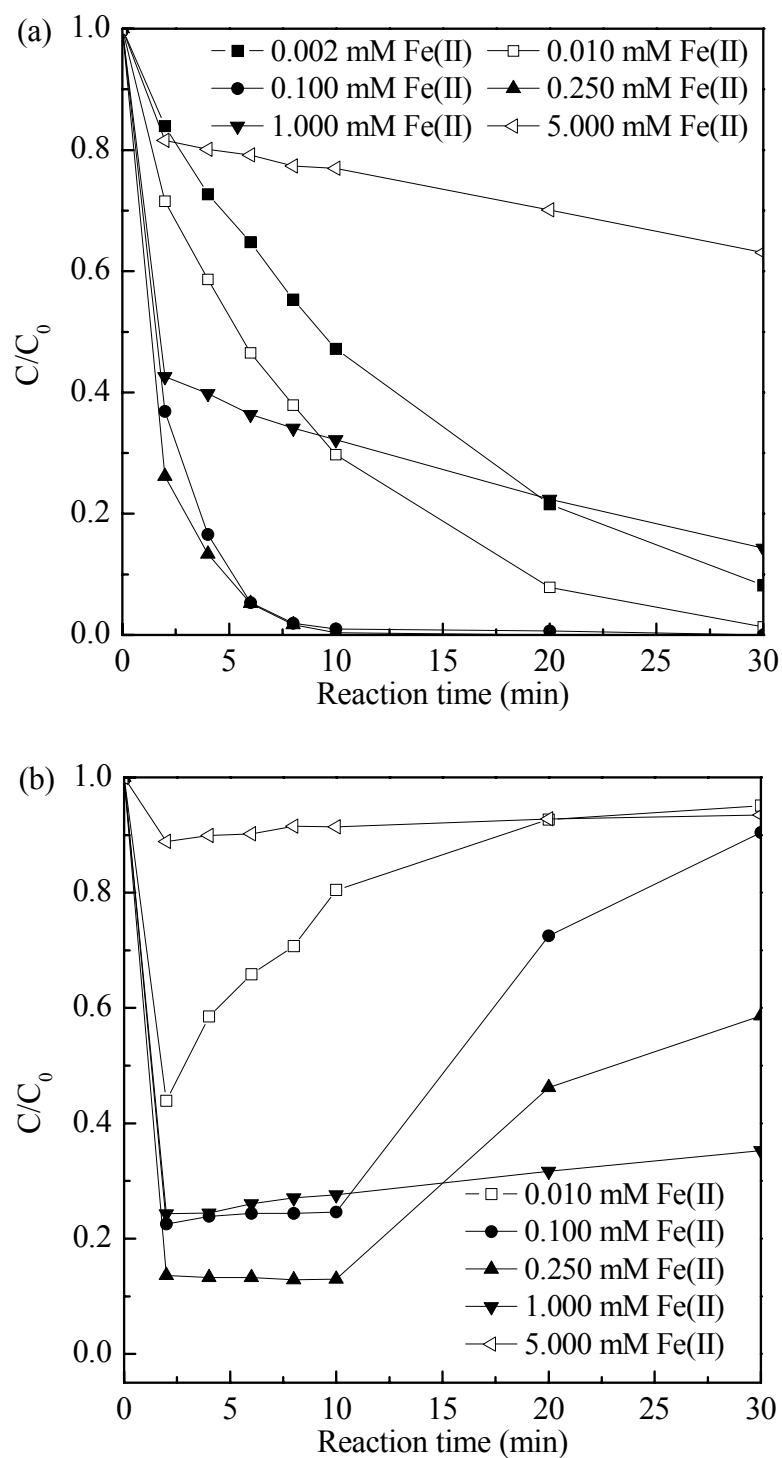


Figure 6-4: (a) Effect of Fe(II) dosage on the photodegradation of 2,4,5-T by FOU process; (b) Change in the remaining [Fe(II)] over reaction time. Two 254 nm UV lamps were employed, $[2,4,5-T]_0 = 0.1$ mM, $[Oxone^{\text{®}}]_0 = 0.25$ mM.

When the [Fe(II)] is low in the solution, the lower probe degradation efficiency is

resulted from the slower Fe(II) regeneration (i.e. the rate-limiting step). To verify this, the [Fe(II)] was monitored as shown in Figure 6-3b, where the rapid reaction of Oxone[®] with ferrous ions leads to a fast consumption (> 80%) of [Fe(II)] in the first few minutes (a similar trend of 2,4,5-T decay was observed simultaneously (Figure 6-3a), and no regeneration of [Fe(II)] was observed throughout the test. On the other hand, the addition of excessive ferrous ions will retard the process due to the SO₄^{•-}-scavenging effect by overdosed Fe(II) as shown in Eq. 6-3:



For the overdosed case using 5.0 mM Fe(II) (Figure 6-3b), over 81% of ferrous ions remained unreacted in the solution, while only 18% of 2,4,5-T was decayed as one of the worst cases. This is unlikely due to the underdose of Oxone[®] (since the cases of lower [Fe(II)] have shown better performance), but more precisely due to the futile consumption of precious radicals by non-target components in the solution such as the ferrous ions in Eq. (6-3). This observation therefore is a strong evidence to justify the quenching of sulfate radicals by high dose of ferrous ions.

In the presence of the UV irradiation, however the trends of 2,4,5-T degradation and [Fe(II)] profiles changed dramatically. As illustrated in Figure 6-4a, the photodegradation of 2,4,5-T was significantly improved under various [Fe(II)] by the FOU process than that of FO process. It is believed that a beneficial Fe(III)/Fe(II) circle has been established due to the introduction of UV irradiation simply by comparing Figures 6-3b and 6-4b. In general, for the investigated [Fe(II)] range of 0.002 - 5.0 mM, two distinct types of 2,4,5-T degradation tendencies were observed as detailed next.

Type one: the probe degradation increases with the increment of ferrous dosage and

follows pseudo first-order kinetics with the ascending rate constant of 0.76×10^{-1} , 1.26×10^{-1} , 4.86×10^{-1} and $5.08 \times 10^{-1} \text{ min}^{-1}$ for 0.002, 0.01, 0.1 and 0.25 mM Fe(II), respectively. The quickest 2,4,5-T photodegradation is observed around 0.1 to 0.25 mM Fe(II), in which 2,4,5-T was completely removed in 10 min for both cases. Their corresponding [Fe(II)] trends (see Figure 6-4b) rapidly dropped in the first 2 min, then leveled off in the following 8 min and significantly increased afterward. The fast reaction upon the interaction of Fe(II) and Oxone[®] is responsible for the sudden [Fe(II)] drop within the first 2 min; the followed steady stage in Fe(II) concentration is likely a steady state between the consumption and regeneration of Fe(II). The [Fe(II)] increment at final stage is likely because the consumption of Fe(II) is terminated after the total exhaustion of Oxone[®], while the regeneration of Fe(II) via the photolysis of Fe(III) remains.

Type two: upon the further increase of [Fe(II)] over 0.25 mM, the photodegradation of the probe was hindered with the increment of ferrous dosage. Under these circumstances, as shown in Figure 6-4a, the probe decay was divided into a two-step kinetics: a rapid initial decay (during the initial 2 min) followed by a slower retardation stage. Concurrently, the [Fe(II)] shows a sudden drop in the first two min and then gradually increases as shown in Figure 6-4b. For the initial rapid decay stage, there is no significant difference between the FO process and FOU, as can be seen by comparing Figures 6-3a and 6-4a. However, the presence of UV irradiation apparently exhibits its advantage in the second stage. In FO, the 2,4,5-T decay was almost stopped in the second stage, but an appreciable decay remained in the second stage in FOU. The reaction mechanisms of the two-step kinetics by FOU and the differences between the FO and FOU can be summarized as follows. Firstly, the rapid decay stage can be

ascribed to the fast radical generation induced by several pathways as discussed in section 3.2 with the instantaneous reaction of Oxone[®] and ferrous ions contributing most to the probe decay. It is rational to assume that [Oxone[®]] is approaching the level of depletion at the end of the first stage. When the Oxone[®] becomes deficient, the photodegradation of 2,4,5-T, due to UV photolysis and the hydroxyl radicals generated via the photo-reduction of $\text{Fe}(\text{OH})^{2+}$, dominates the secondary stage, where the probe, Fe(II) and Fe(III) are the predominant species in the system.

Based on the above discussions, it can be concluded that the involvement of UV in Oxone[®]/Fe(II) system is effective in enhancing the process performance with a faster overall reaction rate due to the simultaneous generation of hydroxyl and sulfate radicals as well as its role in providing a regeneration pathway of Fe(II)/Fe(III). In addition, it was found that the introduction of UV in FOU also demonstrates an advantage of minimizing the required Fe(II) dosage in comparison with the conventional FO process for the similar performance. Accordingly, [Fe(II)] was adopted at 0.1 mM for the remaining study of FOU.

6.2.4 Effect of initial solution pH

Figure 6-5a illustrates the variation in the 2,4,5-T decay efficiency under various pH levels of 1.95-8.6 covering a range from acidic to weak basic condition by the FOU process. The corresponding pseudo first-order kinetic rate constants at five different pH levels were determined and plotted in Figure 6-5b. Generally, the probe decay is favored at acidic range. Over 98.5% of 2,4,5-T removal was observed at pH 1.95 and 2.76 in 20 min and pH 3.68 in 10 min. Optimal 2,4,5-T decay rate was obtained at initial solution pH of 3.68, below or above this pH level would lower the initial rate where the latter, in

fact was significantly retarded. As the solution pH affects the distribution of Fe(II)/Fe(III) speciation and the stability of Oxone[®] is also pH-dependent (Ball and Edwards, 1956), an attempt was made to elucidate the pH-dependency of 2,4,5-T decay by the FOU process from the above two aspects.

At low pH levels, the slower 2,4,5-T decay may be ascribed to the formation of $(\text{Fe(II)(H}_2\text{O)})^{2+}$ (pH < 2.5) (Masomboon et al., 2009), thus reducing the availability of free ferrous ions. From weak acidic to basic conditions, however, Fe(II) was reported to easily convert into Fe(III) at a solution pH > 4.0 (Masomboon et al., 2009), while Fe(III) species start to precipitate as Fe(OH)_3 at pH > 5.0 (Brillas et al., 2009). The precipitate not only decreases the concentration of free iron in the solution, but also blocks the transmission of UV irradiation. In addition, the photoreactive Fe(III) species, i.e. Fe(OH)^{2+} , start to lose their predominant role at pH > ~3.67 according to previous research (Brillas et al., 2009), which also impairs the probe decay rate. Finally, the self-decomposition of Oxone[®] via non-radical pathways also contributes to the decrease of the probe decay rate at higher pH level (Rastogi et al., 2009). It should be pointed out that, as an acidic oxidant, Oxone[®] addition to the process facilitates the reduction of solution pH and thus results in a solution pH of around 3.68 without further pH adjustment in this study. This is beneficial to the application of FOU process due to the fact that the process is optimized without adjusting the pH of most of the water/wastewater. A consequent savings in chemical reagents and a simplified operation are expected.

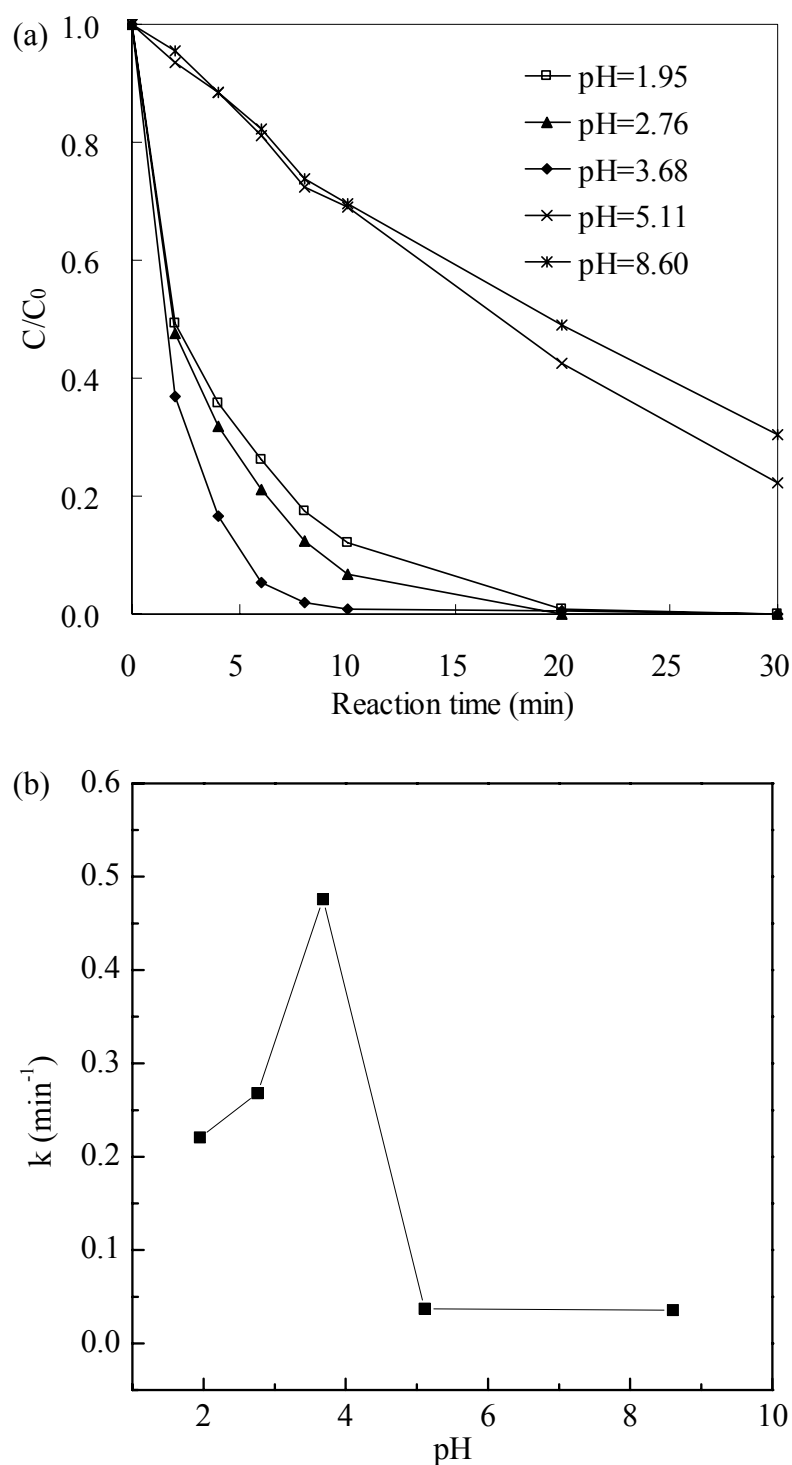


Figure 6-5: (a) Effect of initial solution pH on the photodegradation of 2,4,5-T by FOU process; (b) pseudo first-order rate constant as a function of initial pH. Two 254 nm UV lamps were employed, $[2,4,5-T]_0 = 0.1$ mM, $[Oxone^{\text{®}}]_0 = 0.25$ mM, $[Fe(II)]_0 = 0.10$ mM.

6.2.5 Effect of [Oxone[®]] and the primary intermediate

Oxone[®] dose is a critical parameter for the photodegradation of 2,4,5-T by the FOU process. The efficiency of the FOU process as a function of initial [Oxone[®]] was evaluated by varying its concentration from 0.0625 to 0.75 mM. The experimental results are presented in Figure 6-6a, in which the 2,4,5-T decay efficiency increases from 67.6%, 87.4% to 98.6% as [Oxone[®]] increases from 0.0625 to 0.25 mM for a 10-min reaction. At lower concentrations, the increase in [Oxone[®]] would lead to the generation of more oxidizing radicals, thereby resulting in the enhancement of the probe decay. However, upon further increasing the [Oxone[®]] to 0.75 mM, no appreciable increment of 2,4,5-T decay can be observed, which is similar to the overdose of H₂O₂ in photo-Fenton process (Elmorsi et al., 2010, Trovo et al., 2009). Several reasons have been raised to elucidate this effect, while the radical self-scavenging effect caused by excessive levels of oxidants is the common one (Ling et al., 2010, Madhavan et al., 2009). Another reason may be due to the competitive reaction for the radicals between the parent compound and the intermediates.

Therefore, further tests were performed to investigate the evolution of primary intermediates in terms of 2,4,5-T decay at various initial [Oxone[®]]. 2,4,5-trichlorophenol (2,4,5-TCP) was found to be the primary and dominating intermediate upon the decay of 2,4,5-T, and 2,4,5-TCP's formation and/or destruction profile during the reaction is illustrated in Figure 6-6b. As a result, it can be speculated that the initial attack of both $\bullet\text{OH}$ and $\text{SO}_4^{\bullet-}$ radicals on the probe leads to the formation of 2,4,5-TCP and glycolic acid via the dissociation of the C(1)-O bond of 2,4,5-T, which agrees with previous studies (Boye et al., 2003, Oturan et al., 1999). Additionally, it should be noted that the majority of the products formed by sulfate radical attack on

aromatics are hydroxylation products, which are also intermediates of hydroxyl radical attack (Anipsitakis et al., 2006), as justified by this study. Generally, it can be seen from Figure 6-6b that the [2,4,5-TCP] is rapidly formed in the first stage, which corresponds to the fast disappearance of 2,4,5-T in the first several minutes (see Figure 6-6a). After that, the concentration of 2,4,5-TCP gradually or significantly drops depending on the concentration of Oxone[®]. As the addition of [Oxone[®]] is ≤ 0.25 mM, the higher the Oxone[®] dosage, the higher generation of 2,4,5-TCP in the first stage and the lower accumulation of 2,4,5-TCP in the final solution. Obviously, as the supply of Oxone[®] is insufficient, higher initial [Oxone[®]] leads to higher generation of powerful radicals, thus resulting in enhanced 2,4,5-T removal and accordingly higher primary intermediate 2,4,5-TCP formation in the solution. After the 2,4,5-TCP reached its maximum concentration at 2-6 min, it gradually decayed, where a linearly decay stage was observed. This suggested that the photo-reduction of Fe(III) and direct photolysis may dominate at this stage after the disappearance of oxidant. As [Oxone[®]] is > 0.25 mM, the accumulation of 2,4,5-TCP was lowered in the first 6 min's reaction due to faster destructive reaction (in a serial reaction) until its complete disappearance from the 6th - 30th min as compared to the addition of 0.25 mM Oxone[®]. The lower accumulation and complete destruction of 2,4,5-TCP at higher [Oxone[®]] are likely due to the robust generation of both $\bullet\text{OH}$ and $\text{SO}_4\bullet$ radicals in the process. The evolution behaviors of the primary intermediate 2,4,5-TCP upon the decay of 2,4,5-T at various [Oxone[®]] suggested that the competition of the probe and the intermediates for oxidizing radicals obviously plays an important role in elucidating the effect of Oxone[®] doses. Finally, it should be noted that elevating the oxidant dosage could result in complete or partial decay of both parent and the daughter compounds examined depending on the treatment requirement.

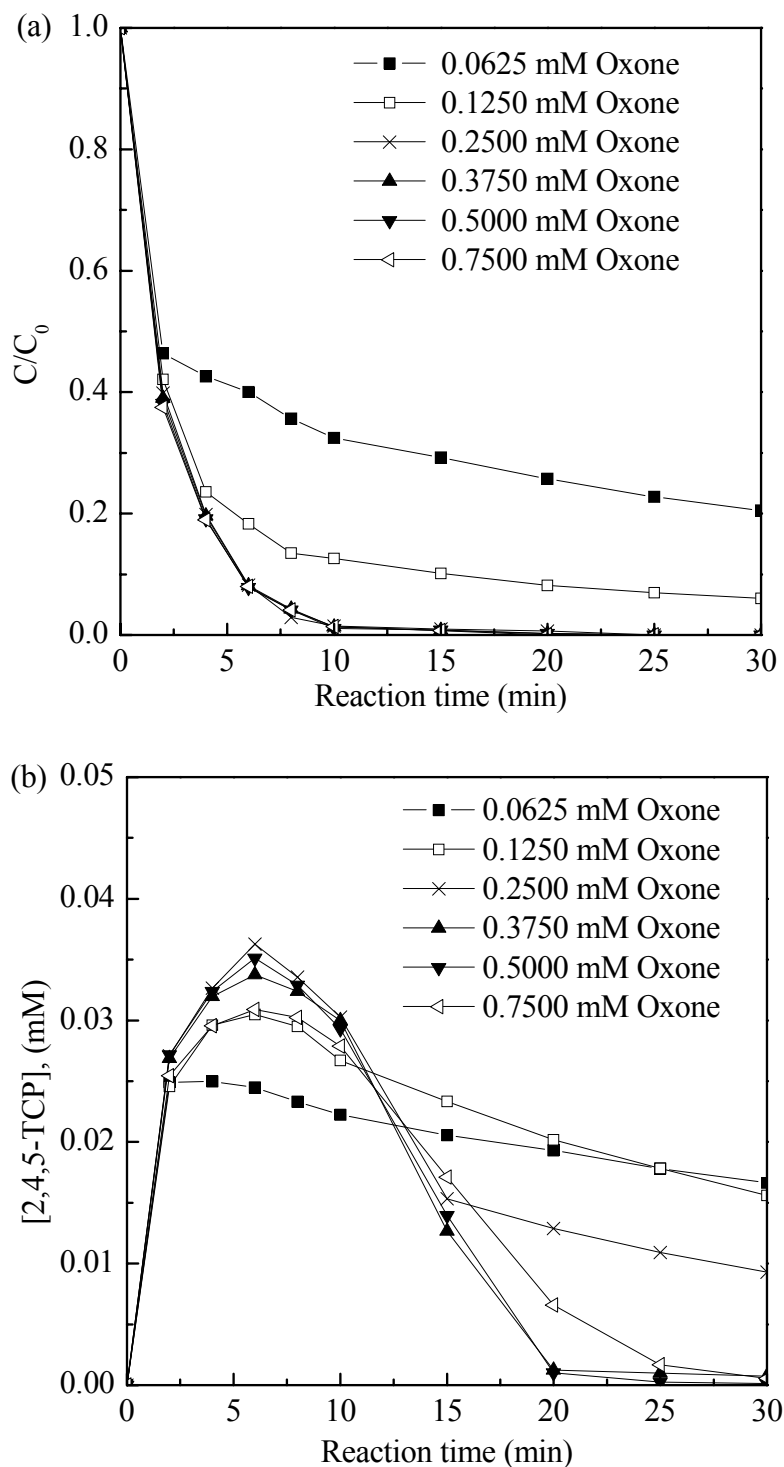


Figure 6-6: (a) Photo-decay of 2,4,5-T at different Oxone[®] concentrations by FOU process. (b) Evolution of 2,4,5-TCP upon photodegradation of 2,4,5-T by FOU process at different [Oxone[®]]. Two 254 nm UV lamps were employed, $[2,4,5-T]_0 = 0.10$ mM, $[Fe^{2+}]_0 = 0.10$ mM.

6.2.6 Variation of 2,4,5-T concentration

To examine the effect of initial probe concentration, tests were carried out by varying [2,4,5-T] from 0.025 to 0.25 mM while keeping other parameters constant as illustrated in Figure 6-7a. The degradation of 2,4,5-T by FOU process was found to follow pseudo first-order kinetics and the obtained decay rate constant as a function of [2,4,5-T] was depicted in the inset of Figure 6-7a. Besides, the corresponding evolution of 2,4,5-TCP at various initial 2,4,5-T concentrations was determined as well (see Figure 6-7b). Apparently, the efficiency of probe degradation decreases with increasing initial 2,4,5-T concentration and the decay rate constants was found to decrease from 1.84 to 0.132 min⁻¹ as increasing [2,4,5-T] from 0.025 to 0.25 mM. When [2,4,5-T] was ≤ 0.05 mM, both the 2,4,5-T and 2,4,5-TCP were rapidly removed as can be seen from Figure 6-7. This is due to the sufficient supply of Oxone[®] at lower [2,4,5-T]. On the contrary, the degradation of 2,4,5-T at higher initial concentration was significantly inhibited, which might be attributed to the competition reaction of generated degradation intermediates (mainly 2,4,5-TCP, see Figure 6-7b) for sulfate and hydroxyl radicals and the depletion of oxidant.

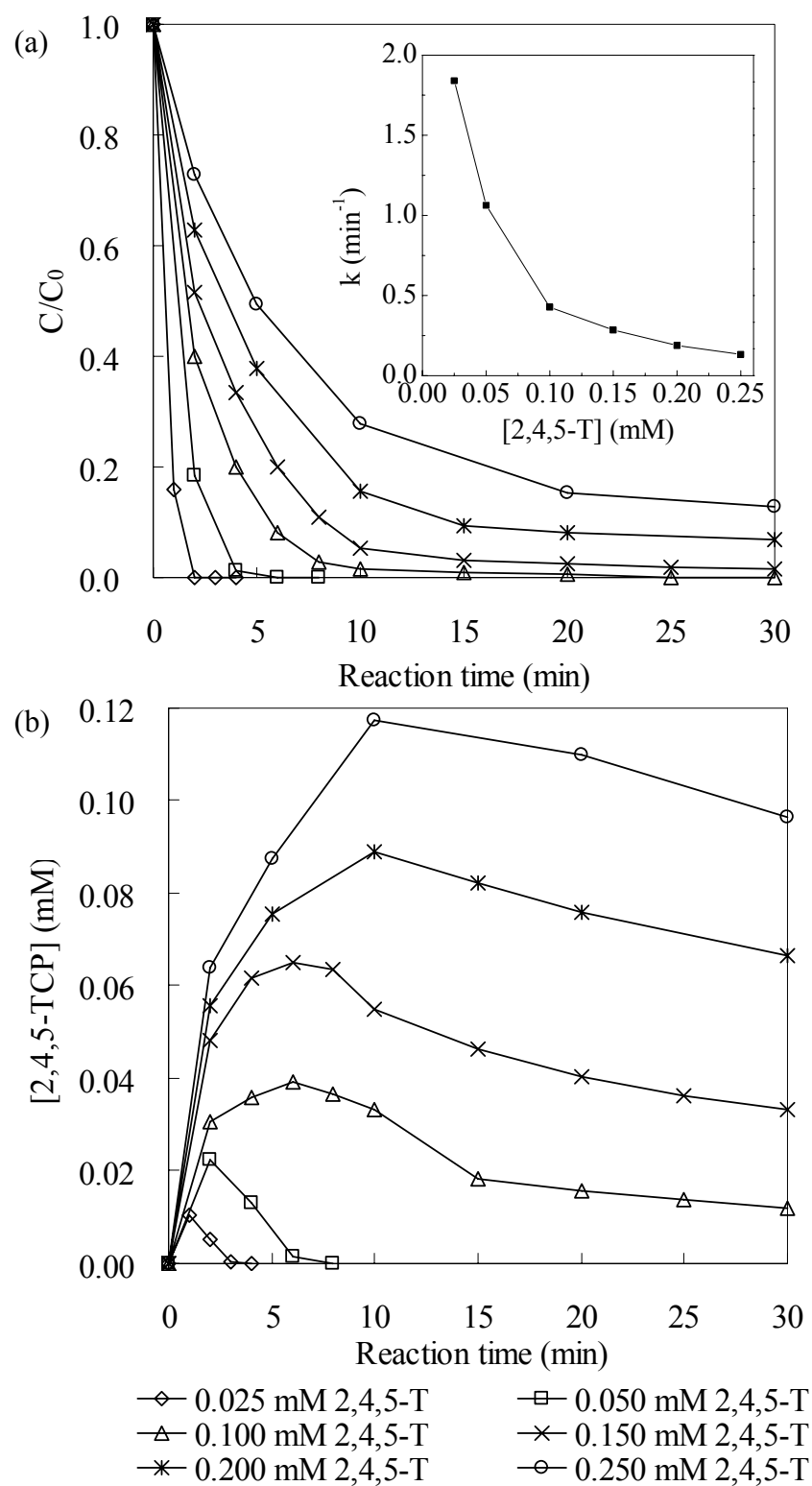


Figure 6-7: (a) Photo-decay of 2,4,5-T at different initial concentrations by FOU process. (b) Evolution of 2,4,5-TCP at different [2,4,5-T] by FOU process. Experimental conditions: [Oxone[®]]₀ = 0.25 mM, [Fe(II)]₀ = 0.10 mM, two 254 nm UV lamps were employed.

6.2.7 The influence of various anions and the variation of solution pH

Various anions such as Cl^- , SO_4^{2-} , and NO_3^- are considered to be common in wastewaters and natural water. Due to their higher reduction potentials, hydroxyl and sulfate radicals can react with these anions in aqueous. The effect of Cl^- , SO_4^{2-} and NO_3^- on the radical-based AOP has been explored in-depth in Chapter 4. Because naturally occurred anions such as carbonate and bicarbonate can also scavenge the radicals, in this study the existence of anions including CO_3^{2-} , HCO_3^- , H_2PO_4^- , CH_3COO^- and $\text{C}_2\text{O}_4^{2-}$ were further investigated for their effect on the decay of 2,4,5-T in FOU process and the results are illustrated in Figure 6-8. In addition, the pH evolution curve due to the presence of 0.01 M anion was also monitored as shown in Figure 6-9. Generally, it can be noted that the presence of these anions has negative effects on the decay of 2,4,5-T by the FOU process compared with the control test without anion addition as indicated in Figure 6-8. For the first 10-min's reaction, the retardation follows the ascending order of $\text{C}_2\text{O}_4^{2-}$, CO_3^{2-} , H_2PO_4^- , CH_3COO^- and HCO_3^- with the 2,4,5-T decay of 81.6%, 59.3%, 41.8%, 34.9% and 20.2%, respectively, comparing to that of 99.1% for the blank. It is interesting to note that the probe decay kinetics can be categorized into three different types upon the addition of anions. The 2,4,5-T decay was found to follow the pseudo first-order kinetics in the presence of $\text{C}_2\text{O}_4^{2-}$ or CO_3^{2-} . The existence of H_2PO_4^- or CH_3COO^- in the system results in a two-step reaction, where a rapid initial decay was followed by a relative slower second stage. The addition of HCO_3^- into the system, however, leads to a zero-order decay of 2,4,5-T by the FOU system.

The negative effects of these anions can be rationalized through the cross-examination with the solution pH variation (see Figure 6-9), because the ion speciation of iron (Fe^{2+} , Fe^{3+}) is strongly pH-dependent.

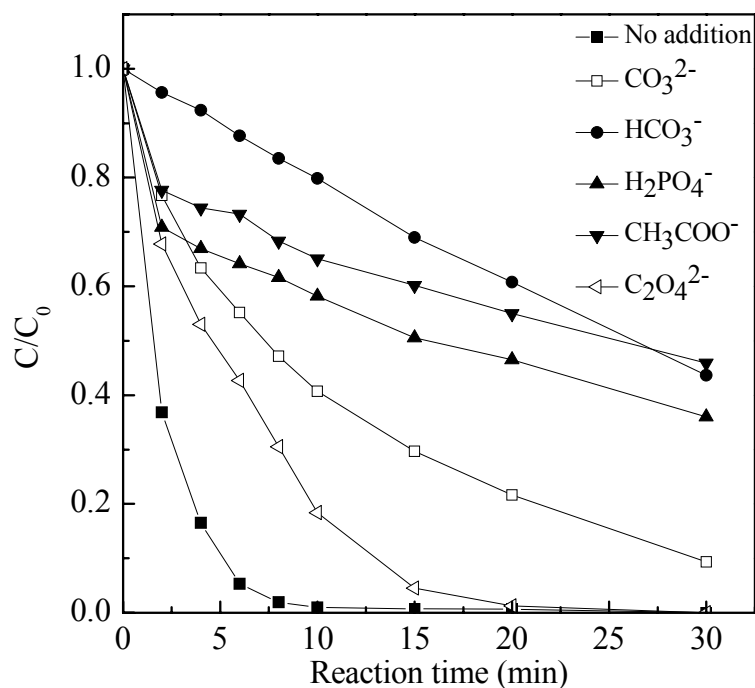


Figure 6-8: The influence of various anions on the photodegradation of 2,4,5-T by the FOU process. Two 254 nm UV lamps were employed, $[2,4,5\text{-T}]_0 = 0.1 \text{ mM}$, $[\text{Fe}^{2+}]_0 = 0.10 \text{ mM}$, $[\text{Oxone}^{\text{®}}]_0 = 0.25 \text{ mM}$, $[\text{anions}] = 0.01\text{M}$.

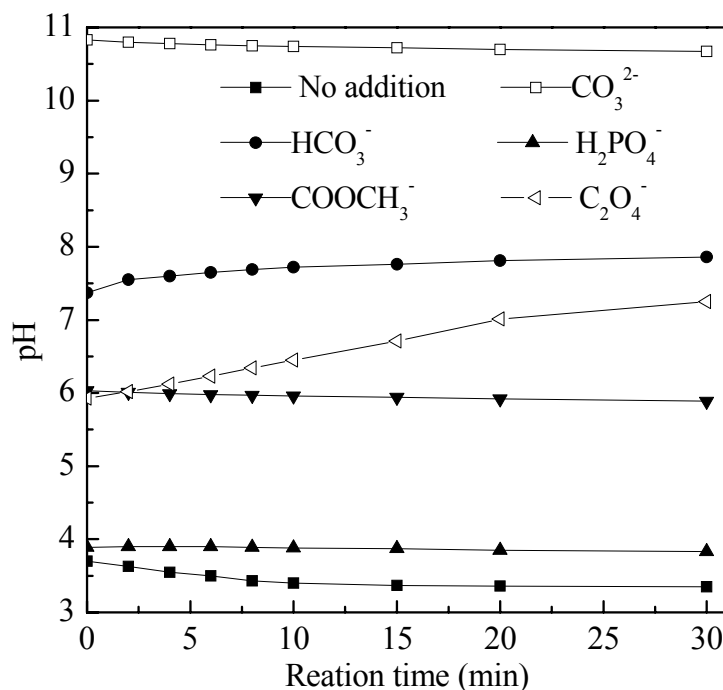
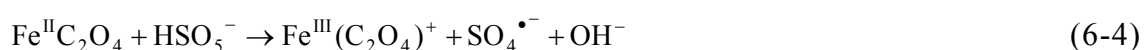


Figure 6-9: Trends of pH variation with the addition of different anions during the treatment of 2,4,5-T by the FOU process. Two 254 nm UV lamps were employed, $[2,4,5\text{-T}]_0 = 0.1 \text{ mM}$, $[\text{Fe}^{2+}]_0 = 0.10 \text{ mM}$, $[\text{Oxone}^{\text{®}}]_0 = 0.25 \text{ mM}$, $[\text{anions}] = 0.01\text{M}$.

For the control test, the initial solution pH was around 3.7 without pH adjustment, which was justified to be the optimal pH for the FOU process in advance. A slight pH drop was observed during the reaction and a final pH of 3.35 was observed at 30-min. The decline in solution pH is likely attributed to the formation of ferric oxyhydroxides, thereby leading to the release of protons into the solution.

The addition of 0.01 M oxalate resulted in an initial solution pH of 5.93, while a steady increase in pH during the reaction was observed and the final pH was 7.25. It was reported that the addition of oxalate into the ferrous solution can generate both $\text{Fe}^{\text{II}}(\text{C}_2\text{O}_4)$ and $\text{Fe}^{\text{II}}(\text{C}_2\text{O}_4)_2^{2-}$ ferrous oxalate complexes, while the former is predominant when $[\text{C}_2\text{O}_4^{2-}]$ is higher than $[\text{Fe}(\text{II})]$ at a pH level of 2.8 (Zuo and Hoigne, 1992). It was also reported that $[\text{Fe}^{\text{II}}(\text{C}_2\text{O}_4)]$ increases with increasing pH and oxalate concentration (Balmer and Sulzberger, 1999). Therefore, $\text{Fe}^{\text{II}}(\text{C}_2\text{O}_4)$ should be dominant in the initial of the reaction as $[\text{C}_2\text{O}_4^{2-}]$ is much higher than $[\text{Fe}(\text{II})]$ in this study. Under these circumstances, the reaction between ferrous oxalate and Oxone[®] can be expressed as Eq. 6-4:



The effects of oxalate concentration on the decay of 2,4-D by photo-Fenton system were well elucidated by Kwan (Kwan, 2005), where the process performance was accelerated at low $[\text{C}_2\text{O}_4^{2-}]$ as both of $\text{Fe}^{\text{II}}(\text{C}_2\text{O}_4)$ and $\text{Fe}^{\text{III}}(\text{C}_2\text{O}_4)^+$ are photosensitive to produce additional hydroxyl radicals. However, an overdose of oxalate was detrimental to the system due to the radical quenching reaction as shown in Eq. 6-5:



Similarly, the 2,4,5-T decay rate retardation in the presence of 0.01 M $\text{C}_2\text{O}_4^{2-}$ may be resulted from analogue quenching or competitive reactions for the $\text{SO}_4^{\bullet-}$. In addition, the

attenuation of light due to the significant light absorption of ferrous oxalate may be another reason of the reduction in the degradation efficiency of the probe compound. For the pH variation, the formation of OH⁻ as indicated in Eqs. 6-4 and 6-5 can justify the increase in solution pH during the reaction.

For the addition of 0.01 M CO₃²⁻, the initial and final pH values of the solution were 10.83 and 10.67, respectively. According to the k_{sp} calculation, the soluble ferrous and ferric ions in the solution are negligible ($< 1.8 \times 10^{-5.4}$ and 6×10^{-25} mM of Fe²⁺ and Fe³⁺, respectively) due to the precipitation of Fe(OH)₂ and Fe(OH)₃ complexes. This suggests that the catalyst role of ferrous ions was inhibited. However, compared to the Oxone[®]/UV process, over 10% of increment in 2,4,5-T decay efficiency was observed by the FOU in the presence of CO₃²⁻ anions. According to Yang et al (Yang et al., 2010), HSO₅⁻ can be activated by CO₃²⁻ at low CO₃²⁻ concentration (0.001 M), while at high concentration, the CO₃²⁻ acts as a radical scavenger. Sulfate radicals are reported to transfer into hydroxyl radicals at the solution pH value higher than 8.5, while •OH becomes predominant at pH >10.5 (Chawla and Fessenden, 1975, Dogliotti and Hayon, 1967). Therefore, the radical quenching reaction can be described in terms of hydroxyl radical consumption reaction (Eq. 6-6):

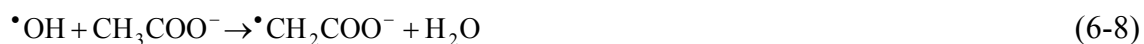


Thus, the 2,4,5-T decay may be ascribed to the combined results of photolysis of Oxone[®], CO₃²⁻ activated decomposition of Oxone[®], radical quenching by excess CO₃²⁻ anions as well as the photolysis of ferric-complexes in this study.

When 0.01 M H₂PO₄⁻ ions were introduced into the FOU system, the solution pH was maintained at around ~3.88 throughout the reaction. The rapid decay of 2,4,5-T in the

first 2 min is a result from the fast generation of radicals upon the mixing of ferrous ions and Oxone[®]. The subsequent slower decay is likely due to the photolysis of Oxone[®] and ferric-complexes (Gallard et al., 1999), and radical quenching reaction by the H₂PO₄⁻ ion, which is an efficient scavenger of hydroxyl radicals (Kochany and Lipczynskakochany, 1992).

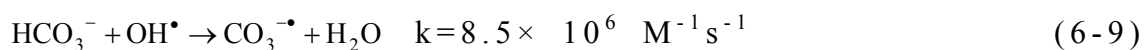
The 2,4,5-T degradation with the addition of 0.01 M CH₃COO⁻ ions by the FOU process showed a similar tendency as compared to that of H₂PO₄⁻ ions. From Figure 6-9, the solution pH was around 6.0 during the reaction, which indicates that the acetate anions are predominant in the solution as its pK_a is 4.76. The attack of the sulfate and hydroxyl radicals on acetic anions leads to the formation of H₃C[•] (Eq. 6-7) and [•]CH₂COO⁻ (Eq. 6-8) radicals, respectively.



From the rate constant of sulfate and hydroxyl radicals towards CH₃COO⁻ ions (4.3 - 28 × 10⁶ and 8.5 × 10⁷ M⁻¹s⁻¹, respectively), it can be concluded that the [•]OH and SO₄^{•-} radicals can be effectively scavenged by acetate anions. Due to the fact that the contribution of the [•]OH radicals become significant only for pH > 9 (Criquet and Leitner, 2009), the quenching reaction of sulfate radicals by CH₃COO⁻ ions should be predominant in this study.

In the presence of HCO₃⁻, the bicarbonate ions significantly slow down the decay rate of 2,4,5-T in the FOU system as demonstrated in Figure 6-8, while the initial solution pH was slightly increased from 7.37 to 7.86 in 30 min. Under this circumstance, the [•]OH

and $\text{SO}_4^{\bullet-}$ radicals should coexist in the system, and the retardation can be rationalized from the consumption of both $\bullet\text{OH}$ and $\text{SO}_4^{\bullet-}$ radical point of view. Firstly, bicarbonate was reported to be an efficient scavenger of hydroxyl radicals (Eq. 6-9) and can quench $\bullet\text{OH}$ more efficiently than H_2PO_4^- (Kochany and Lipczynskakochany, 1992).



Secondly, HCO_3^- can react with $\text{SO}_4^{\bullet-}$ with a rate constant of $2.8\text{-}9.1 \times 10^6 \text{ M}^{-1} \text{ s}^{-1}$ (see Eq. 6-10), which indicates that bicarbonate is also an effective scavenger of sulfate radicals.



From Eqs. 6-9 and 6-10, it can be noted that the introduction of HCO_3^- leads to the consumption of both $\bullet\text{OH}$ and $\text{SO}_4^{\bullet-}$ radicals with the generation of $\text{CO}_3^{\bullet-}$ radical of much lower reactivity. It should be noted that quenching of radical may not be the sole reaction of HCO_3^- ; Yang et al. reported that active species may also be produced from HSO_5^- activated by HCO_3^- (Yang et al., 2010).

Based on the above discussions, the observed retardation in the presence of various anions for the decay of 2,4,5-T by the FOU process is likely a result from the combination of radical scavenging of the anions, UV blocking effect due to the formation of ferrous or ferric complexes, and the change of iron speciation caused by the variation of solution pH.

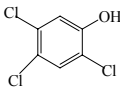
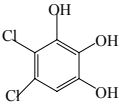
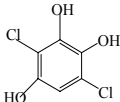
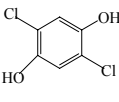
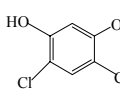
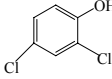
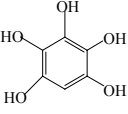
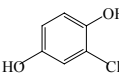
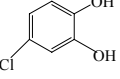
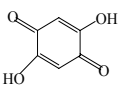
6.2.8 Identification of intermediates and decay pathways

The identification of degradation intermediates is essential in evaluating the efficiency

of the detoxification by the proposed process and proposing the reaction pathways and mechanisms. In order to identify the degradation intermediates of 2,4,5-T by UV alone, Oxone[®]/UV, and FOU processes with better resolution, initial concentration of the probe was increased to 0.5 mM. The disappearance of the parent compound and the formation and/or destruction of aromatic intermediates were monitored by LC-ESI/MS analysis. Totally, 15 intermediates were identified during 2,4,5-T degradation by the above three processes with the retention time (RT), the molecular weight, and structural formula of the identified intermediates summarized in Table 6-1. Ten of them have not been previously reported in the literature (compounds 1-7, 10, 13 and 14).

Table 6-1: Summary of identified aromatic intermediates determined by LC/ESI-MS upon degradation of 2,4,5-T.

Compound	RT	MW	Structural formula	Detected in		
				UV	UV/Oxone [®]	FOU
2,4,5-T	38.81	255		√	√	√
(1)	30.51	271.4			√	√
o-HDA (2)	22.82			√	√	
p-HDA (3)	28.51	237		√	√	√
m-HDA (4)	29.27			√		
(5)	32.09	227.4		√	√	
(6)	33.17	221				√
(7)	16.36	218.5		√		
(8)	34.16	213.4		√	√	√

2,4,5-TCP (9)	45.02	197.5		√	√	√
(10)	23.07	196	 or 		√	√
(11)	27.41	179	 or 	√		√
(12)	39.21	163				√
(13)	15.97	158		√		
(14)	36.01	144.6	 or 			√
(15)	25.92	140				√

Note: RT is retention time; MW presents molecular weight.

6.2.8.1 UV alone process

The photodegradation of 0.5 mM 2,4,5-T by UV alone at two 254 nm lamp irradiation was investigated. The LC-ESI/MS analysis revealed that 9 aromatic intermediates were produced during the reaction as marked in Table 6-1. Figure 6-10 depicts the trends of 2,4,5-T decay, the formation and/or destruction of degradation intermediates, and the mole balance of benzene rings. However, the intermediates **8** and **11** were in trace levels and therefore their formation trends were not shown in Figure 6-10. Generally, the decay of 2,4,5-T by direct photolysis is ineffective, where < 40% transformation of the probe and < 13% of the benzene rings were destroyed (or opened) at the end of the reaction.

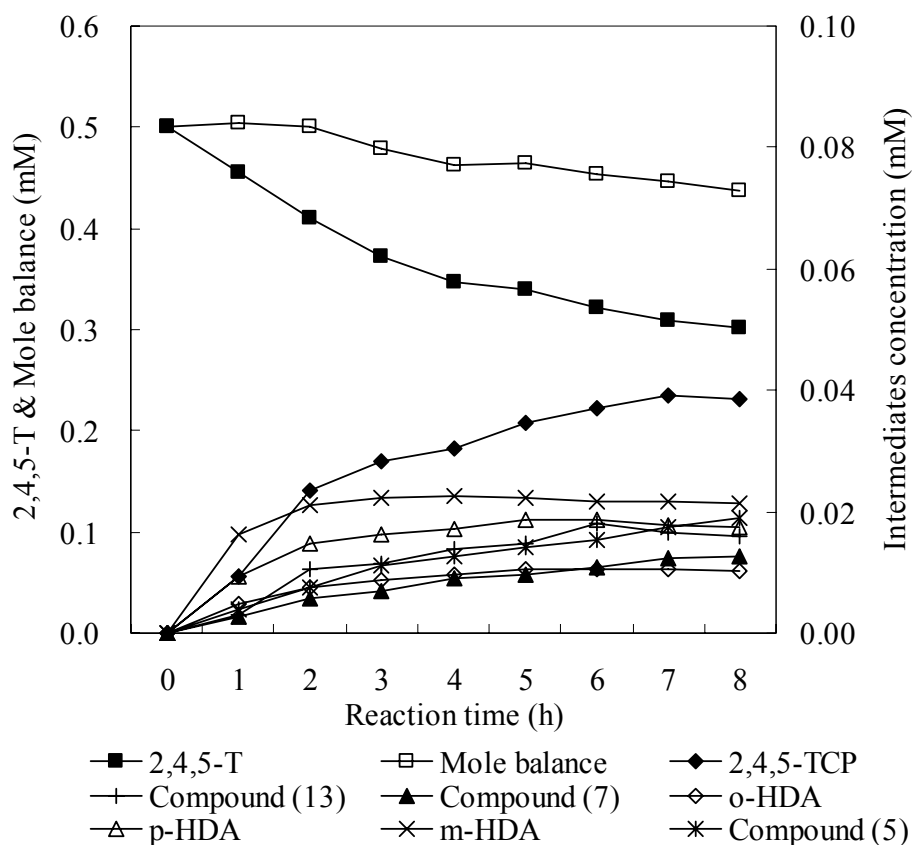
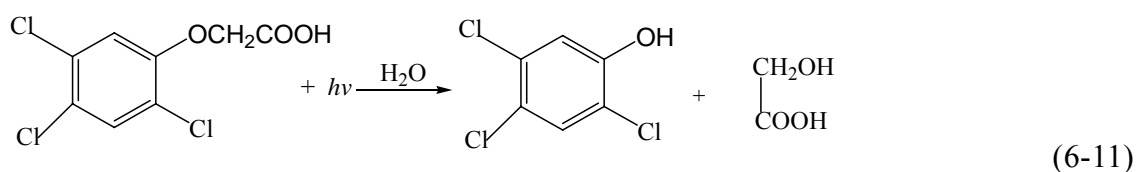


Figure 6-10: The evolution profiles of 2,4,5-T and aromatic intermediates during the photolysis of 0.5 mM 2,4,5-T under the irradiation of two UV 254 nm lamps.

The hydrolytic-photolysis of 2,4,5-T through the cleavage of C(1)-O bond (as indicated in Eq. 6-11) is suggested to be the initial step dominating the 2,4,5-T decay by UV alone process due to the fact that 2,4,5-trichlorophenol (2,4,5-TCP, detected at $m/z = 196$ $[M-H]^-$, 198 $[M+2-H]^-$, 200 $[M+4-H]^-$ and 202 $[M+6-H]^-$) was observed to be the major primary by-product as indicated in Figure 6-10, where it can be noted that 2,4,5-TCP was formed and gradually accumulated up to 0.0392 mM at 7th hr and declined to 0.0386 mM at the end of the run upon the degradation of 0.5 mM 2,4,5-T.



The nucleophilic substitution reaction, the photo-induced C-Cl bond scission from the electronically excited state of 2,4,5-T followed by the Cl substitution with an OH group (dechlorination-hydroxylation) are proposed to be the other two predominant reaction mechanisms, judging from the formation of hydroxyl-dichlorophenoxyacetic acid (HDA) corresponding to the RT of 22.82, 28.51 and 29.27 min as shown in Figure 6-10 and Table 6-1. Different isomers corresponding to the possible sites of C-Cl bond cleavage are expected because 2,4,5-T has three chloride at ortho, meta and para locations. They were detected in this study as 2-hydroxy-4,5-dichlorophenoxyacetic acid (o-HDA), 5-hydroxy-2,4-dichlorophenoxyacetic acid (m-HDA), and 4-hydroxy-2,5-dichlorophenoxyacetic acid (p-HDA), respectively. Generally, the evolution trends of these three isomers of HDA showed a similar formation and/or destruction tendency. They appeared as the primary intermediates from the very beginning of the reaction and reached the maximum concentration at 3-5 h and then slightly decreased with the elapsing of irradiation time. It should be pointed out that the total yield of HDA is much higher than that of 2,4,5-TCP throughout the reaction, suggesting that the decay of 2,4,5-T by UV alone is mainly initiated through the nucleophilic substitution reaction and dechlorination-hydroxylation mechanisms. In addition, the cleavage of C-Cl bond ($339 \text{ kJ}\cdot\text{mol}^{-1}$) by photon is also thermodynamically preferred due to its lower bonding energy compared with C-O ($360 \text{ kJ}\cdot\text{mol}^{-1}$) and C-H ($415 \text{ kJ}\cdot\text{mol}^{-1}$) bonds.

From Figure 6-10, different concentration of HDA isomers was observed, which is likely attributed to the combination effects of *ortho*- and *para*-directory effects resulting from both of -OCH₂CHOOH and chlorine groups and steric hindrance effect. The -OCH₂CHOOH group in the benzene ring is *ortho*- and *para*-directing group with activation, which indicates that its conjugative effect overrides the inductive effect,

thereby leading to the electron-rich positions at the *ortho*- and *para*-sites and the positive charge of C(5) position. Compared to the C(2) and C(4) positions, this effect renders the C(5) position to more easily undergo nucleophilic substitution reaction of chlorine from the 2,4,5-T by water, resulting in the formation of m-HDA with chlorine ion as the leaving group. On the other hand, it is believed that the steric hindrance effect plays a more important role in determining the possible sites of C-Cl bond scission (Tang and Huang, 1995). The *ortho*- position of Cl substituent should be subject to more steric strain as it is closer to the -OCH₂CHOOH group than the *meta*- and *para*-positions, which suggests that the dechlorination-hydroxylation at the *ortho*-position will experience more steric strain. Thus, it is reasonable to assume that the cleavage of C-Cl bond on *para*-position should override the *ortho*-position. Therefore, it is rationalized that the yields of m-HDA and p-HDA should be higher than that of o-HAD and a ratio of 1.0:1.8:2.1 (judging from the max. concentration) is determined from Figure 6-10. Further dechlorination-hydroxylation of m-HDA and p-HDA leads to the production of secondary intermediate of chlorodihydroxyphenoxyacetic acid (compound **7**) as demonstrated in Figure 6-10.

Besides, electrophilic aromatic substitution that introduces the hydroxyl group to the benzene ring of 2,4,5-T and electron transfer followed by the loss of CO₂ are believed to be the possible mechanisms leading to the formation of compound **5** (RT: 32.09). Judging from the low yield of compound **5**, these mechanisms play a minor role upon the decay of 2,4,5-T by UV alone.

Compound **8** detected in trace level was likely ascribed to the hydroxylation of the benzene ring of 2,4,5-TCP, while compound **8** may undergo

dechlorination –hydroxylation giving compound **13** as the tertiary by-product. Another parallel decay pathway of 2,4,5-TCP is through the further dechlorination-hydroxylation mechanism, justified by the formation of trace compound **11** (2,5-dichlorohydroquinone or 4-6-dichlororesorcinol). It is believed that prolonged irradiation will further degrade these intermediates, leading to the ring-opening with the generation of simpler organics.

6.2.8.2 Oxone[®]/UV process

The decay of 2,4,5-T and the evolution of the aromatic intermediates by the Oxone[®]/UV process are depicted in Figure 6-11. Compared to UV alone process, only 7 intermediates (see Table 6-1) were identified during the Oxone[®]/UV process, probably because some of the daughter compounds were rapidly oxidized by the $\text{SO}_4^{\bullet-}$ and $\bullet\text{OH}$ radicals and became undetectable. It should be noted that the intermediates identified as compounds **1** and **8** were not shown in Figure 6-11 due to their trace level. It can be seen that the introduction of Oxone[®] into the UV system significantly promoted the degradation of 2,4,5-T with over 92% being transformed and over 89% of benzene ring being opened within 180 min. Similar to UV alone process, 2,4,5-TCP was also identified as the predominant primary intermediate. However, the yield of 2,4,5-TCP is much higher in Oxone[®]/UV process than that of direct photolysis process as can be seen by comparing Figures 6-10 and 6-11. From Figure 6-11, a bell-shape 2,4,5-TCP formation/decay was observed with a peak concentration of 0.192 mM at 60 min, while the accumulation of other intermediates was generally low. The generation of $\text{SO}_4^{\bullet-}$ and $\bullet\text{OH}$ radicals by the Oxone[®]/UV process clearly contributes to the rapid transformation of 2,4,5-T and its intermediates.

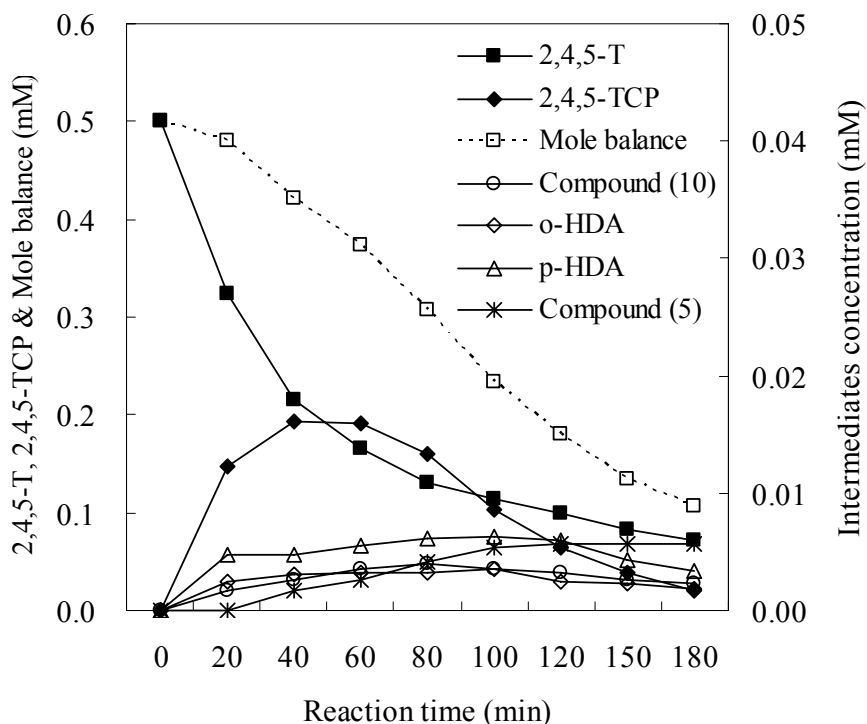


Figure 6-11: The evolution profiles of 2,4,5-T and aromatic intermediates for the photo-decay of 2,4,5-T by the Oxone[®]/UV process. Two 254 nm UV lamps were employed, $[2,4,5\text{-T}]_0 = 0.5 \text{ mM}$, $[\text{Oxone}^{\text{®}}]_0 = 2.5 \text{ mM}$.

The reaction mechanisms for the decay of 2,4,5-T by Oxone[®]/UV process are therefore proposed as follows: the initial cleavage of the lateral chain via the C(1)-O bond of 2,4,5-T (upon the attacks by $\text{SO}_4^{\bullet-}$ and $\bullet\text{OH}$ radicals) generates 2,4,5-TCP by losing the glycolic acid, which is the dominant mechanism judging from the high yield of 2,4,5-TCP. The mass spectrum of the peak at RT of 30.51 with a m/z of 270 ($[\text{M}-\text{H}]$) denoted as compound **1** was detected in a trace level corresponding to the hydrogen abstraction and followed by monohydroxylation of the aromatic ring on 2,4,5-T. The chemical structure of compound **1** is speculated through the examination of electronic properties of the 2,4,5-T molecule. As stated before, the $-\text{OCH}_2\text{CHOOH}$ group in 2,4,5-T with electron-donating character would increase the electron density at the *ortho*- and *para*-positions, while the inductive electron-withdrawing properties of the

chlorine atoms significantly reduced the electron density of the adjacent carbon atom. This synthetic effect will render the C(6)-position at the benzene ring with relatively high π -electron density than that of *meta*-position. Thus, the C(6)-position will be more amenable to the electrophilic attack by $\text{SO}_4^{\bullet-}$ and $\bullet\text{OH}$ radicals as both of them are electrophilic and tend to attack the carbon atoms with higher electron density. Apart from the electronic influence, the electrophilic addition on the *meta*-position is also disfavored by steric hindrance.

Two HDA isomers were detected resulting from the substitution of chlorine by OH group upon the radical attacks, during which two possible mechanisms may occur: (1) the electrophilic $\bullet\text{OH}$ radicals may replace the chlorine atom of 2,4,5-T through attacking the electron-rich positions, and (2) $\text{SO}_4^{\bullet-}$ may react via addition to the ring forming in an unstable state and then give sulfate ion as leaving group upon the transfer of an electron and followed by the breaking of C-Cl bond and hydrolysis. It is suggested that the two isomers detected are p-HDA and o-HDA, as the *para*- and *ortho*-positions hold higher electron density than the C(5) position, while *ortho*-position is subjected to more steric hindrance than the *para*-position as discussed before, rendering the electrophilic attack by hydroxyl and sulfate radicals at the *ortho*-position less favorable compared to the *para*-position, which results in a ratio of 1.81:1 (see Figure 6-11).

Compound **5** was also detected by the Oxone[®]/UV process. The formation mechanism was similar to UV alone process; except that this mechanism is more likely initiated by radical attack in the Oxone[®]/UV process. The subsequent hydrogen abstraction followed by C(6)-hydroxylation of 2,4,5-TCP leads to compound **8** as the secondary intermediate. It may also be formed by the addition of hydroxyl group of compound **1**

via the loss of -OCH₂CHOOH group. Further parallel attack of hydroxyl and sulfate radicals on the compound **8** yields the compounds **10** with dechlorination. Other further oxidative intermediates were not detectable, probably resulting from the intensified radical supply that destroyed the buildup of these derivatives in the process.

6.2.8.3 FOU process

In the FOU process, 10 intermediates were identified. However, most of them rapidly disappeared and did not accumulate in the solution. Therefore, their formation and/or destruction trends can not be established. Figure 6-12 presents the evolution profiles of 2,4,5-T and major intermediates. The FOU process yielded a more rapid and complete removal of 2,4,5-T giving no trace of any aromatics at the end of the reaction. This is mainly attributed to the quick generation of hydroxyl and sulfate radicals by the FOU process through the dual-effect of UV irradiation and ferrous catalysis for Oxone[®] activation. Besides, additional production of •OH radicals and accelerated regeneration of Fe(II) via photo-reduction of Fe(III)-complexes also contributes to the FOU process.

The intermediates detected were similar to the Oxone[®]/UV process except that four additional by-products were identified, while compounds **2** and **5** were not observed in the FOU process. The trace compounds **6** (2,4-dichlorophenxyacetic acid) and **12** (2,4-dichlorophenol) may originate from the dechlorination of 2,4,5-T and 2,4,5-TCP, respectively. Compound **12** may also be generated from the homolysis of C(1)-O bond on the benzene ring of compound **6** upon radical attack, which is the predominant decay pathway of 2,4-dichlorophenxyacetic acid by hydroxyl radical attack as reported by Kwan and Chu (Kwan and Chu, 2004). Subsequent attack of SO₄•⁻ and •OH on the *ortho*- or *para*-positions may replace the chlorine atom of compound **12** yielding

compound **14** (chlorohydroquinone or 4-chlorocatechol) as the tertiary intermediate. Compound **11** is believed to come from the further attack of $\text{SO}_4^{\bullet-}$ and $\bullet\text{OH}$ on the C(4)- or C(5)-positions of 2,4,5-TCP with the addition of hydroxyl group and the release of Cl^- ion, from a previous study (Boye et al., 2003). Compound **11** can undergo further dechlorination-hydroxylation and then be rapidly dehydrogenated to compound **15** (2,5-dihydroxy-*p*-benzoquinone). Further oxidation of compound **15** and other secondary and/or tertiary intermediates will lead to ring opening, resulting in the formation of aliphatics (e.g. carboxylic acids). Judging from the mole balance of benzene ring in Figure 6-12, 100% of ring-opening was achieved in 90 min by the FOU process, suggesting all aromatic compounds have been broken down into aliphatic acids in this study. These low molecular organic acids can be further degraded and finally be mineralized to CO_2 as the end product.

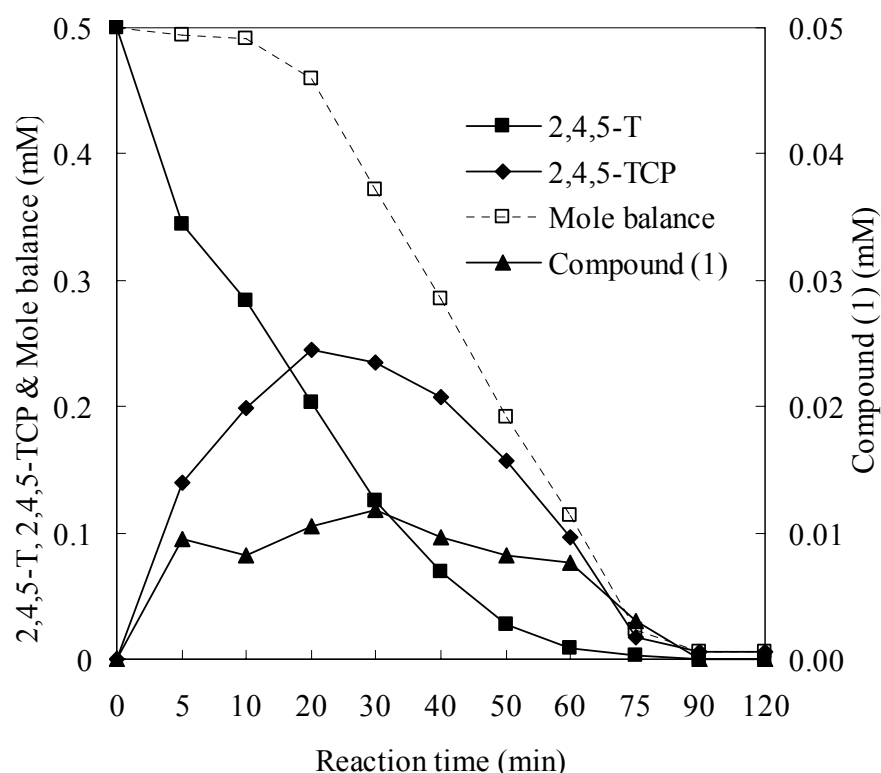
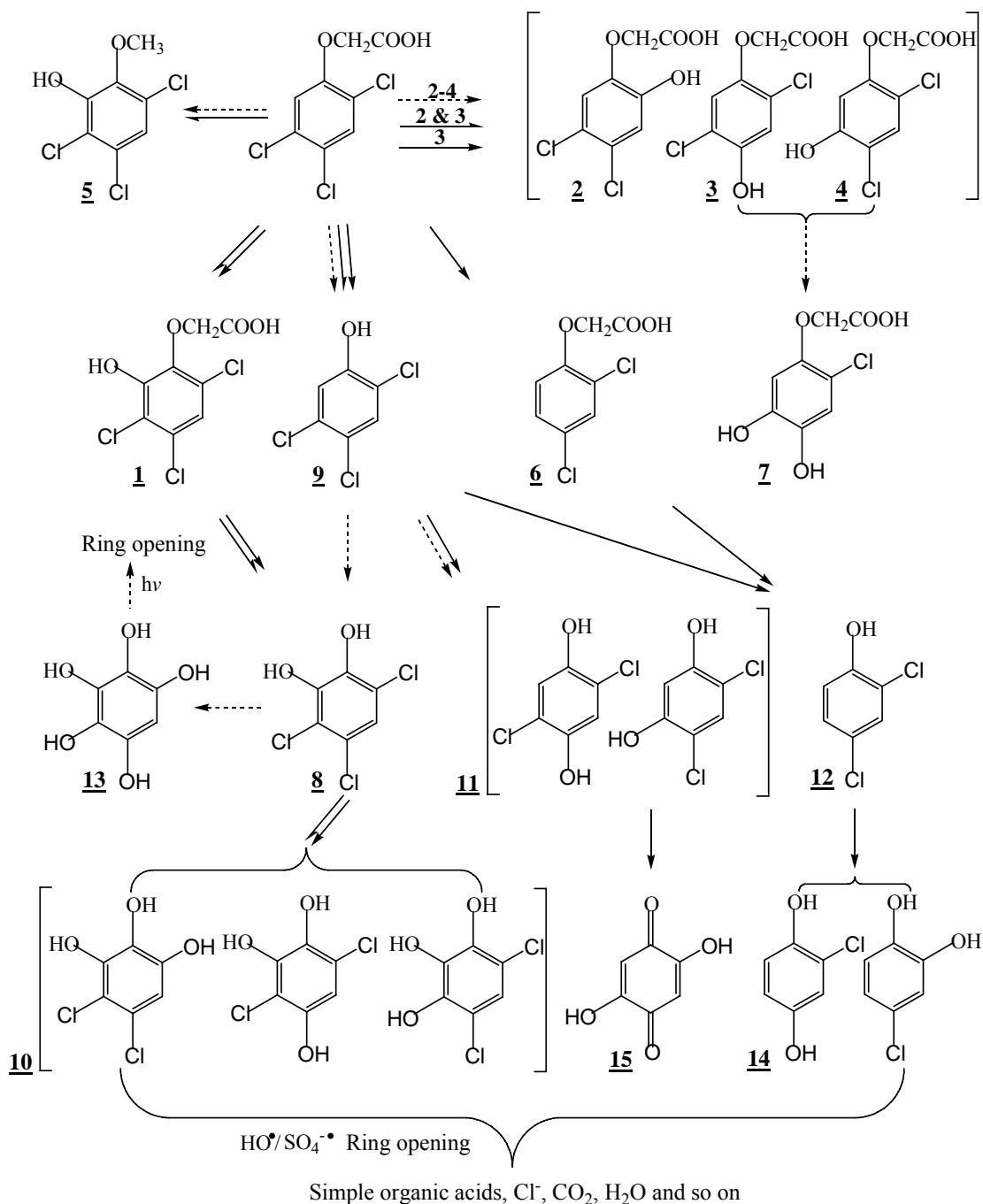


Figure 6-12: The evolution profiles of 2,4,5-T and aromatic intermediates for the photo-decay of 2,4,5-T by the FOU process. Two 254 nm UV lamps were employed, $[2,4,5\text{-T}] = 0.5 \text{ mM}$, $[\text{Fe}^{2+}] = 0.50 \text{ mM}$, $[\text{Oxone}^{\text{®}}] = 2.5 \text{ mM}$.

Based on the aromatic intermediates identified by the LC-MS analysis and above discussions, possible pathways of 2,4,5-T decay by UV alone, Oxone[®]/UV, and FOU processes were accordingly proposed and depicted in Scheme 6-1.



Scheme 6-1: Proposed decay pathways of 2,4,5-T by UV alone (dotted line), Oxone[®]/UV (solid line with single arrow) and FOU (solid line with double arrow) processes.

6.2.9 TOC removal and time-course of Cl^- ions.

Mineralization of 2,4,5-T by UV alone, Oxone[®]/UV and FOU processes were quantified by measuring the TOC contents of the solutions and the results were summarized in Figure 6-13. The mineralization of 2,4,5-T by UV alone was insignificant, where only 1% of TOC is reduced. In contrast, the Oxone[®]/UV and FOU processes remove 41% and 83% TOC in 8 h, respectively, due to faster radical generation as discussed before. It was noted from Figure 6-13 that TOC removal by radicals was fast initially and then slowed down at the later stage, which may be attributed to the following reasons: 1) although the mole balance reduction was around 90% in 180 min and 100% in 90 min for the Oxone[®]/UV and FOU, respectively, the aliphatics (e.g. carboxylic acids) formed by the ring-opening reaction of aromatics are more resistant towards further mineralization as reported by previous study (Oturán et al., 2000); 2) the $\text{SO}_4^{\bullet-}$ and $\bullet\text{OH}$ productions were slowed down due to the depletion of oxidant along the reaction time. Nevertheless, complete mineralization of 2,4,5-T by the FOU process is possible with sufficient supply of oxidant.

Additionally, the mineralization of 2,4,5-T is expected to be accompanied by the release of chloride ion. This was justified by monitoring the $[\text{Cl}^-]$ as shown in Figure 6-13. Similarly, under UV alone irradiation, the chlorine ions linearly increases at a very slow rate as shown in Figure 6-13, where about 9.3 ppm of Cl^- was detected at the end of the reaction (8 h). For both of Oxone[®]/UV and FOU processes, the formation of chlorine ions was rapid in the first two hours, corresponding to the fast transformation of 2,4,5-T and the primary intermediate 2,4,5-TCP (see Figures 6-11 and 6-12). The accumulation leveled off at much slower rates afterward, and finally reached 42.3 and

49.2 ppm in 8 h, corresponding to 79.6% and 92.6% of the initial Cl in 2,4,5-T, respectively. The observation of fast initial formation of chloride ions and leveling off at later stage exactly matches the trend of TOC reduction, suggesting the persistence of carboxylic acids or other aliphatics containing chlorine atom towards further mineralization.

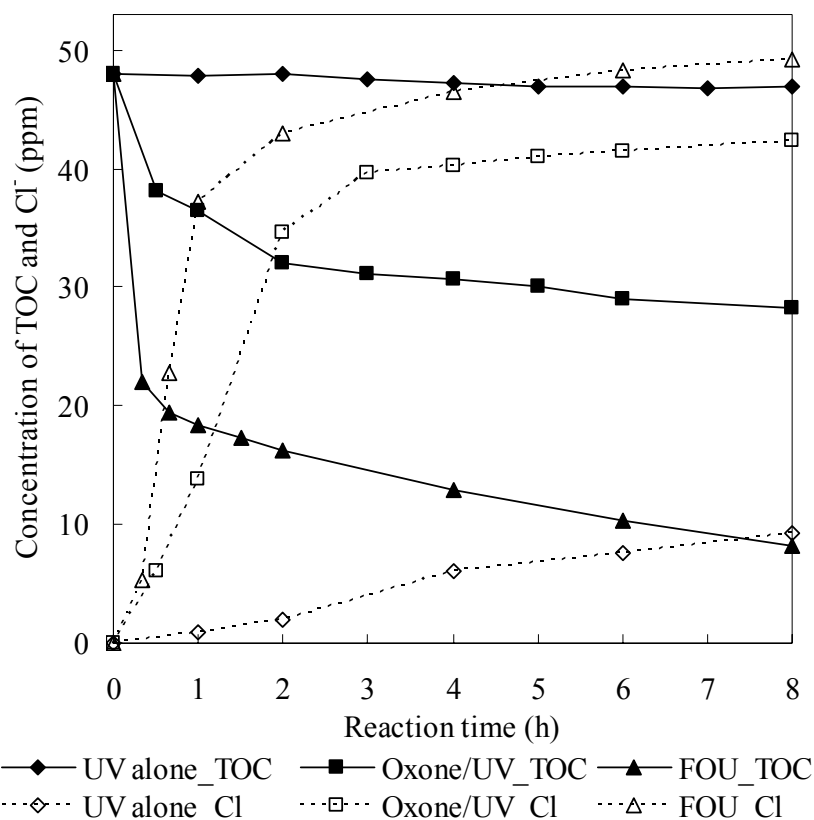


Figure 6-13: Time-course of the concentration of TOC, Cl⁻ for the degradation of 2,4,5-T by UV alone, Oxone[®]/UV and FOU processes.

6.3 Summary

In this chapter, it has been shown that the photo-assisted Fe(II)-catalyzed decomposition of Oxone[®] process is a promising approach for the decay of herbicide in aqueous solution, where complete decay of 2,4,5-T can be achieved within 10 min at optimized experimental conditions. Comparative experiments between the FO and the FOU

process were conducted to elucidate the role of UV light. It was found that the involvement of UV light can significantly accelerate the FO process due to different mechanisms including: direct UV photolysis, radical oxidation by $\text{SO}_4^{\bullet-}$ and $\bullet\text{OH}$ generated via homolytic cleavage of HSO_5^- upon UV irradiation, radical oxidation by $\text{SO}_4^{\bullet-}$ generated by Fe(II)-mediated decomposition of Oxone[®], accelerated regeneration of Fe(II), and additional production of $\bullet\text{OH}$ radicals via photo-reduction of Fe(III)-complexes.

The results show that the degradation of the probe by the FOU process can be controlled by the operating parameters such as the wavelength of UV light, catalyst dosage, initial pH level and the supply of [Oxone[®]]. The use of UV 254 nm demonstrates the best performance, while the optimal pH was determined to be 3.68, which is a benefit of the FOU as it was easily achieved without pH adjustment. The effects of Fe(II) dosages and [Oxone[®]] were well elucidated in this study. In addition, 2,4,5-TCP and glycolic acid have been identified as the primary intermediate upon the decay of 2,4,5-T. The accumulation and disappearance of 2,4,5-TCP in terms of 2,4,5-T under various Oxone[®] concentrations demonstrated that the competitive reaction between the parent and daughter compounds for oxidizing radicals plays an important role in explaining the effect of Oxone[®] doses in addition to the commonly recognized radical self-scavenging effect caused by excessive levels of oxidants.

Furthermore, the effects of various anions on the performance of 2,4,5-T decay by the FOU were also examined. It was found that the addition of 0.01 M anions (such as CO_3^{2-} , HCO_3^- , H_2PO_4^- , CH_3COO^- and $\text{C}_2\text{O}_4^{2-}$) inhibits the decay of 2,4,5-T in different degrees due to the radical scavenger role played by these anions, the UV blocking effect,

and the change of iron speciation caused by the variation of solution pH. A comparative study upon 2,4,5-T transformation by UV alone, Oxone[®]/UV, and FOU processes were conducted. LC-ESI/MS analysis was employed to identify the aromatic intermediates, based on which different decay mechanisms and pathways were proposed and compared. It was found that 2,4,5-T decay was inefficient by UV alone, where only 40% removal of 0.5 mM 2,4,5-T was observed in 8 h, while over 92% and 100% removal were obtained by the Oxone[®]/UV in 180 min and FOU in 80 min, respectively. Total 15 aromatic intermediates were identified by these processes, 10 of which have not been previously reported in the literature. For UV alone process, 2,4,5-TCP and hydroxyl-dichlorophenoxyacetic acid are the main primary intermediates. However, 2,4,5-TCP is the predominant primary intermediate by the Oxone[®]/UV and FOU, while other intermediates are minor due to their low yield or fast decay. Additionally, mineralization in terms of TOC reduction and the release of chloride ions by these three processes have also been comparatively elucidated.

CHAPTER 7

Degradation of 2,4,5-TCP by Electro-Fe(II)/Oxone[®] Process with UV Irradiation

7.1 Introduction

Chlorophenols (CPs) belong to a class of chlorinated organic compounds that are included in the list of priority pollutants by the U. S. Environmental Protection Agency. As mentioned in Chapter 2, they have been widely used as wood preservatives, herbicides, insecticides, disinfectants, fungicides (Sabhi and Kiwi, 2001), and also as raw materials for the production of pesticides and various synthetic compounds (Solanki and Murthy, 2011), leading to their release into the environment. CPs can also enter the environment through the processes of pulp bleaching with chlorine, chlorination of drinking water, and incomplete incineration (Sharma et al., 2010). CPs are commonly detected in soils, surface and ground waters, industrial wastewaters, sediments, and air all over the world (Watts and Cooper, 2008). Most of CPs are resistant to biodegradation and are considered toxic or potentially carcinogenic and mutagenic to mammalian as well as aquatic life (Hou et al., 2010). The occurrence of CPs in water bodies can lead to death of aquatic life in inland water bodies, inhibition of the normal activities of microbial population in wastewater treatment (Zaghouane-Boudiaf and Boutahala, 2011). Therefore, the development of efficient approach for the treatment of wastewater with chlorophenol contaminant is of critical importance from the environmental protection point of view.

2,4,5-TCP is an important representative of CPs and also is one of the most toxic CPs. It

is well established that the toxicity of CPs generally increases with the degree of chlorination (Annachhatre and Gheewala, 1996). Moreover, 2,4,5-TCP is considered to be more resistant to biodegradation than other trichlorophenols (Marsolek et al., 2007). Especially, it is used as the precursor for the manufacture of the widely used herbicide 2,4,5-T and is also formed as the primary intermediate upon the decay of 2,4,5-T by the treatment of AOPs (Boye et al., 2003, Brillas et al., 2004) and also microbial activities (Daubaras et al., 1995). In addition, the test results presented in Chapter 6 already confirmed that 2,4,5-TCP is the major primary intermediate during the transformation of 2,4,5-T by the tested processes (i.e., UV, Oxone[®]/UV, and FOU). Consequently, 2,4,5-TCP was chosen as the target compound in this chapter.

Over the past few decades, AOPs have been proven to be promising technology that can efficiently mineralize organic compounds into CO₂, H₂O, and simple acids under mild experimental conditions. Barbeni et al. (1987) reported that complete mineralization of 2,4,5-TCP into CO₂ and HCl was achieved with half-lives of 30-90 minutes by simulated sunlight irradiation in oxygenated aqueous suspensions of TiO₂. However, these AOPs usually need to be assisted with other treatment techniques to economically achieve the final treatment level as well as to save the operating time. In the meantime, it is shown that some of the weakness of each technique might be eliminated by some characteristics of another (Li et al., 2007) and more important, a favorable synergistic action between different processes that could strongly accelerate organics degradation might be achieved.

Based on the experimental results presented in Chapter 5 and Chapter 6, it can be noted that both of the proposed Electro-Fe(II)/Oxone[®] process and FOU process are very

promising. In the present chapter, an attempt has been made to combine the above two processes together to form a more efficient process, in which the 2,4,5-TCP aqueous solution treated under Electro-Fe(II)/Oxone[®] is simultaneously exposed to UV irradiation (i.e., EFOU). This combined photoassisted electrochemical treatment will be examined through the degradation of 2,4,5-TCP under various operating conditions.

7.2 Results and Discussion

7.2.1 Comparison of Oxone[®] alone, UV alone, FOU, EFO, and EFOU

In an effort to provide supporting evidence on the efficiency of 2,4,5-TCP degradation by the proposed combined EFOU process prior to that of individual process, a comparison of Oxone[®] alone, UV alone, EFO, FOU, and EFOU processes for the degradation of 2,4,5-TCP was conducted and experimental results were presented in Figure 7-1. It can be seen from Figure 7-1 that the ranking of probe decay efficiency by various processes was in the descending order of EFOU > FOU \approx EFO > UV alone > Oxone[®] alone. Generally, negligible (< 3%) degradation was observed by the Oxone[®] alone process for a 20-minute reaction. This result was expected as direct reactions of Oxone[®] with organics in water are generally slow as discussed elsewhere (Bandala et al., 2007, Shukla et al., 2011). Degradation of 2,4,5-TCP by direct photolysis was also ineffective and less than 10% of 2,4,5-TCP was removed at 20 min. The probe degradation in the EFO process is comparable to that in the FOU process as shown in Figure 7-1, where over 82.5% and 84% removal were obtained in EFO and FOU, respectively; while the most effective 2,4,5-TCP degradation (over 92%) was observed by EFOU process. It should be noted that the decay of 2,4,5-TCP by EFOU was rapid in the first 10 min with almost 90% of 2,4,5-TCP being transformed and then the decay

curve leveled off. It is speculated that the retardation stage is likely ascribed to (1) the depletion of Oxone[®] and (2) the competition of parent compound and daughter compounds for the reactive radicals. The former was justified by adding a second dosage of Oxone[®] to the system, as shown in Figure 7-2 that a complete decay of 2,4,5-TCP was achieved right after the second dosing of Oxone[®] at 10 min, suggesting that the exhausting of oxidant is the main reason responsible for the retardation stage in EFOU process.

Compared to the EFO, the involvement of UV irradiation in the EFOU process provides it the advantages of (1) greater hydroxyl radical generation and Fe(II) regeneration due to the photo-reduction of $\text{Fe}(\text{OH})^{2+}$ as discussed in Chapter 6; and (2) faster decomposition of Oxone[®] (via photolysis) into $\bullet\text{OH}$ and $\text{SO}_4^{\bullet-}$, thereby leading to the accelerated degradation of 2,4,5-TCP. Compared to the FOU process, the higher performance of EFOU is likely attributed to the continuous and smooth release of ferrous ions to the solution that can make the best utilization of oxidant. This is because the conventional one-off dosage of ferrous ions in the FOU process results in a rapid reaction between the catalyst and oxidant and a robust generation of sulfate radicals during the first few minutes, which simultaneously leads to the futile consumption of reactive radicals as a consequence of competitive reactions, especially the side reactions of $\text{SO}_4^{\bullet-}$ with Fe^{2+} and HSO_5^- and thus induces the reduced degradation rate.

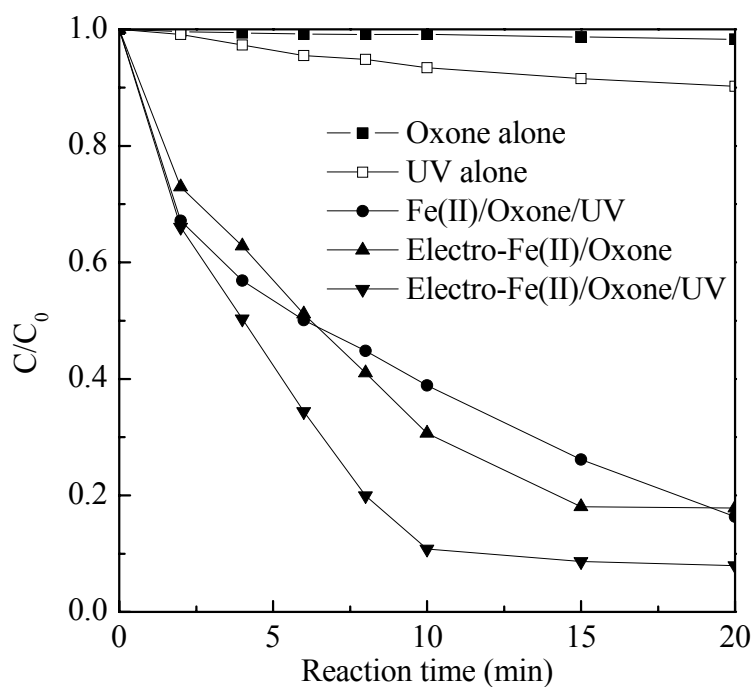


Figure 7-1: Degradation of 0.2 mM 2,4,5-TCP by various processes. [Oxone[®]]₀ = 0.5 mM; for FOU, the addition of Fe(II) is 0.2 mM; for EFO and EFOU, I = 1 mA; pH = 4.35; 50 mM Na₂SO₄ were used as electrolyte; two UV 254 nm lamps were employed.

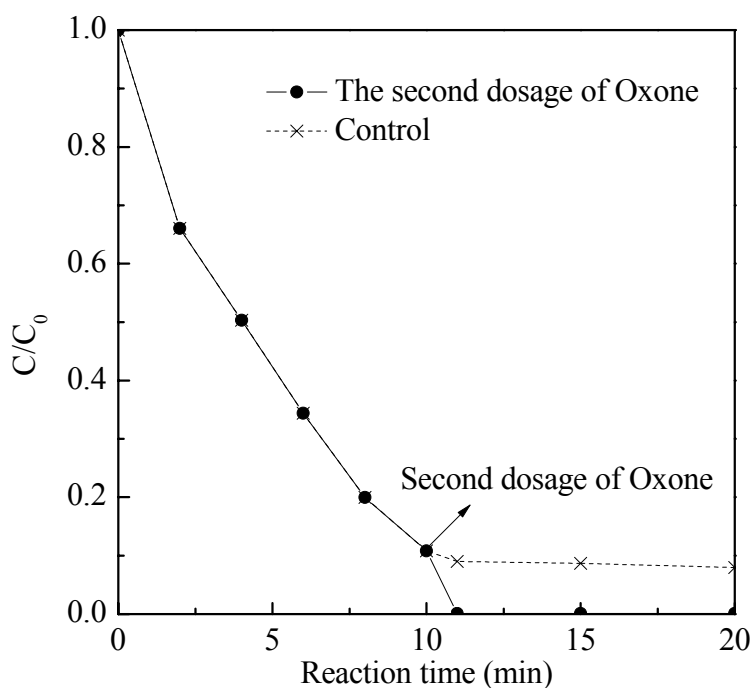


Figure 7-2: Degradation of 0.2 mM 2,4,5-TCP by EFOU process. [Oxone[®]]₀ = 0.50 mM, 50 mM Na₂SO₄ were used as electrolyte, I = 1 mA, pH = 4.35, two UV 254 nm lamps were employed. After 10 min reaction, a second dosage of 0.50 mM Oxone[®] was added into the system.

7.2.2 Effect of applied current

To optimize the operational parameters, the influence of applied current varied from 1 to 5 mA on the degradation of 2,4,5-TCP by EFOU process was firstly examined as shown in Figure 7-3. It is interesting to note that the decay rate of 2,4,5-TCP was slightly inhibited with the increment of applied current. For the first 10 min's reaction, the probe removal efficiency decreased from $\sim 90\%$ to 77% as the applied current increased from 1 to 5 mA.

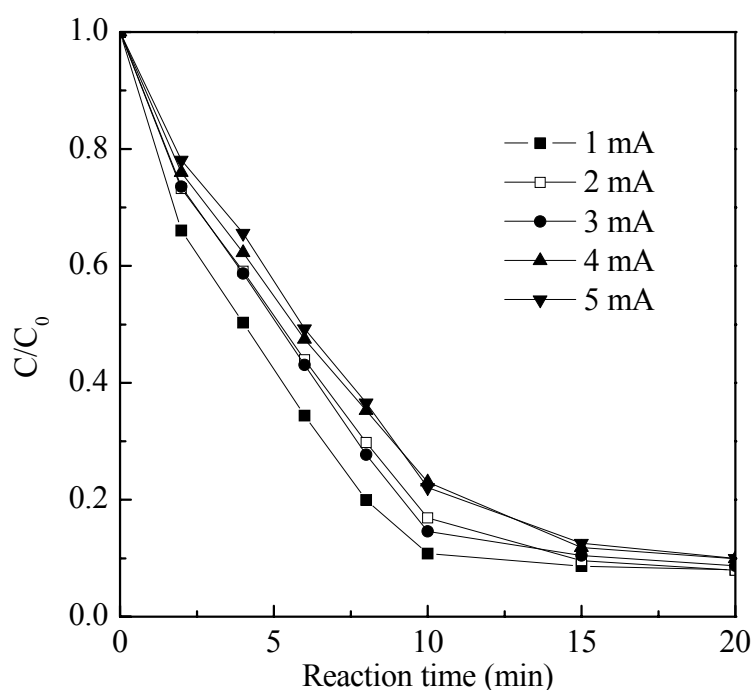


Figure 7-3: Degradation of 0.2 mM 2,4,5-TCP by EFOU process under various applied currents. $[\text{Oxone}^{\text{®}}]_0 = 0.50 \text{ mM}$, $50 \text{ mM Na}_2\text{SO}_4$ were used as electrolyte, $\text{pH} = 4.35$, two UV 254 nm lamps were employed.

In an attempt to interpret the effect of applied current on the probe decay by EFOU process, another test was carried out to monitor the generation of ferrous ions by the electrochemical system under various levels of applied current in the absence of

Oxone[®] and probe-free solutions while keeping other parameters constant. Figure 7-4 illustrates the ferrous ion concentrations in the electrolytic cell as a function of applied current where ferrous ions steadily increase in the solution and higher the applied current faster the accumulation of ferrous ions in the system. It should be noted that the electrogeneration of Fe(II) does not proportionally increase with the current increase. The accumulation of Fe(II) at 20 min was found to increase from 0.30 to 0.56 mM as the applied current increased from 1 to 5 mA. This is probably due to the occurrence of parasitic reactions (e.g., the evolution of H₂ and O₂ as a consequence of water electrolysis) at higher applied current.

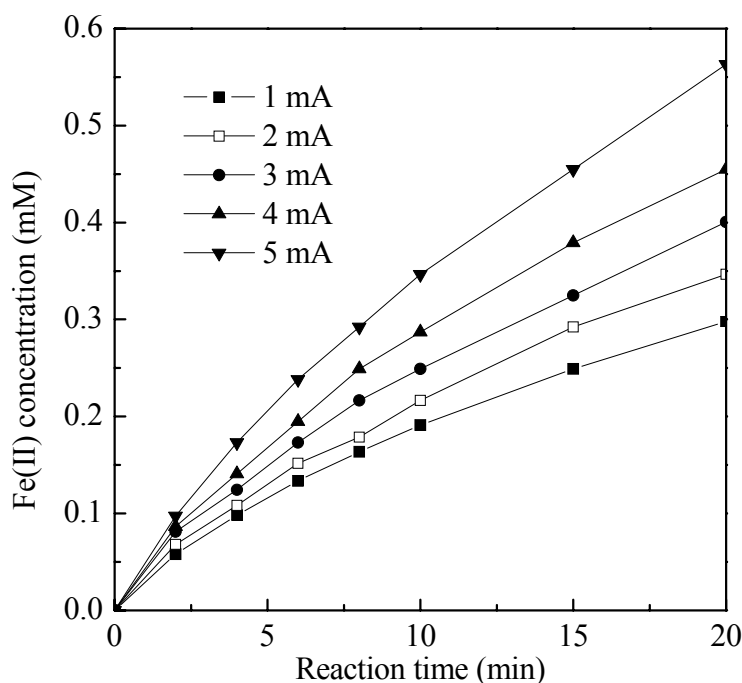


Figure 7-4: The release of Fe(II) into the Electro-Fe(II)/UV system under various applied currents. 50 mM Na₂SO₄ were used as electrolyte, two UV 254 nm lamps were employed.

As far as the Fe(II) concentration is concerned, the plausible explanation regarding the effect of applied current on the degradation of 2,4,5-TCP by the EFOU system is given as following. When the supply of Fe(II) is insufficient, the production of sulfate radical

will be limited, which will consequently weaken the process performance. However, an excess of ferrous ions would also consume the valuable $\bullet\text{OH}$ and $\text{SO}_4\bullet^-$ through unwanted side-reactions (such as Eqs. 2-4 and 2-21) instead of reacting with Oxone[®], suggesting that appropriate ferrous ion supply is an important prerequisite in sulfate and hydroxyl radical-based process. In addition, the evolution of H_2 and O_2 at elevated applied current also contributes to the decreased efficiency, as also reported by others (Sires et al., 2008). As a result, 1 mA was selected as the applied current for the rest of the study from the operational cost and process efficiency points of view.

7.2.3 Effect of initial solution pH

The effect of initial solution pH on the probe decay was examined in the range of 2.5-7.7 and the test results were depicted in Figure 7-5. The reaction is obviously dependent on the initial pH value, and low pH favors the decay of 2,4,5-TCP by the EFOU process. The fastest degradation (93% in 10 min) takes place at the lowest pH of 2.5, which agrees with the trends of pH effect on the decay of 2,4,5-T by EFO process at the low pH level. It is rationalized that electrochemical enhanced process utilizing iron as anode and graphite as cathode at acidic conditions may induce the generation of powerful radical species in accordance with the reactions shown in Eqs. 5-9 to 5-13, which accordingly leads to the excellent performance at the low pH level. Nevertheless, the probe decay efficiency has no significant differences as solution pH increased from 2.5 to 4.35 (the unadjusted pH of the solution) as shown in Figure 7-5. It was therefore suggested that the pH value 2.5-4.35 was applicable for the EFOU process. In considering of chemical savings and process simplification, the solution pH of 4.35 was therefore chosen as the operating pH in the remaining of this study.

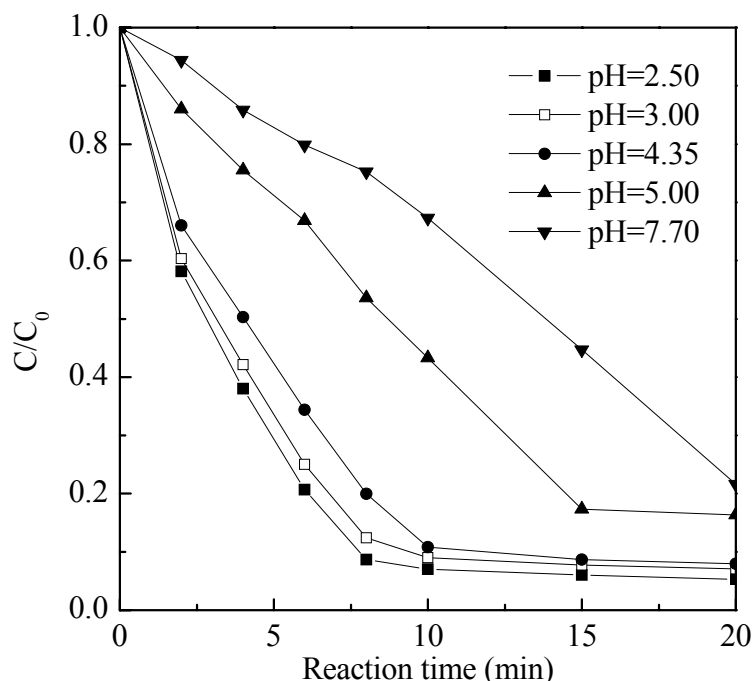


Figure 7-5: Degradation of 0.2 mM 2,4,5-TCP by EFOU process under various initial solution pH levels. [Oxone[®]]₀ = 0.50 mM, 50 mM Na₂SO₄ were used as electrolyte, I = 1 mA, two UV 254 nm lamps were employed.

In contrast, the process performance was significantly inhibited as solution pH level is higher than 5. The removal efficiency of 2,4,5-TCP was found to decrease from 93% to 57% and 55% as the solution pH increased from 2.5 to 5.0 and 7.7, respectively. It is well known that the distribution of iron species strongly depends on the pH of the solution and Fe(III) form different complex species in solution at different pH values. When the solution pH is 3, Fe(III) is dominant by ferric ions and photoactive species, Fe(OH)²⁺ complexes that exist in almost equal proportions. In contrast, solutions with pH higher than 5 lead to the precipitation of ferrous ions as oxyhydroxides, thereby resulting in decreased catalyst activity as well as the probe decay rate. Another issue is the stability of Oxone[®] as mentioned in previous chapters; the non-radical self-decomposition of Oxone[®] at higher pH level also impairs process performance. In application, however, it should be noted that the degradation of 2,4,5-TCP was around

80% at neutral pH of 7.70 at the end of the run (20 min), suggesting that the proposed EFOU process is efficiently workable at a wider range of initial solution pH from acidic to neutral pH levels.

7.2.4 Mode of current-applying

Based on experimental results presented in Figures 7-2 to 7-4, it was validated that the depletion of oxidant results in the retardation stage in EFOU process, while the continuous release of ferrous ions from the sacrificial iron anode at this stage does not lead to notable degradation of 2,4,5-TCP (see the control curve in Figure 7-2). On the contrary, precipitation of an increasing amount of $\text{Fe}(\text{OH})_3$ at a longer electrolytic time will not only induce less photocatalytic activity but also hinder effective light absorption of the solution (Arslan-Alaton and Gurses, 2004). As a result, the EFOU process could be optimized by applying different current modes to obtain an appropriate supply, two different modes where the current supply being switched off respectively at 2 and 10 min were investigated and the results were illustrated in Figure 7-6. Experimental results indicate that switching off the current at 2 min significantly inhibited the degradation efficiency. In contrast, the probe decay was enhanced by switching off the current at 10 min and the degradation efficiency was observed to increase from 92% to 97% at the time of 20 min compared with the original continuous supply mode. Figure 7-4 indicates that the duration of electrolysis directly controls the accumulation of iron ions ($\text{Fe}(\text{II})$, $\text{Fe}(\text{III})$) in the system. Therefore, the performance differences among different current-applying modes could be explained by the change of $[\text{Fe}(\text{II})]$ in the solution by integrating Figure 7-4. It can be calculated that the total amount of iron ions in the system was 0.058, 0.19 and 0.30 mM when the supply of current was switched off at 2, 10 and 20 min, respectively. Compared to the initial

addition of 0.5 mM Oxone[®], 0.058 mM of iron ions was relatively insufficient even though Fe(II) is continuously regenerated by the photo-reduction of Fe(OH)²⁺, thereby resulting in a decrease in the rate of 2,4,5-TCP degradation as the current was cut off at 2 min. As mentioned above, however, as Oxone[®] was exhausted at the later stage, the continuous release of ferrous ions into the system is futile and a proper power control on the electrolysis should be beneficial for the reduction of energy cost.

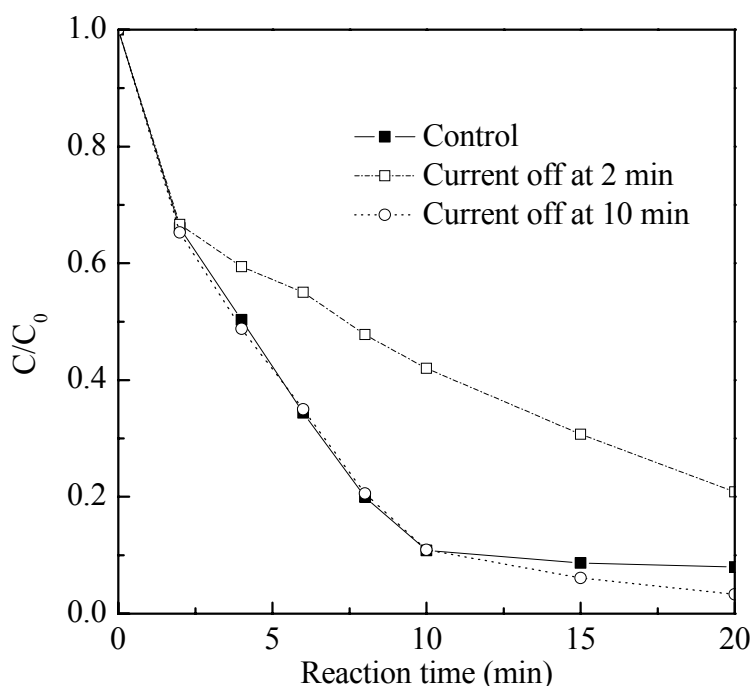


Figure 7-6: Degradation of 0.2 mM 2,4,5-TCP by EFOU process under various current-applying modes. [Oxone[®]]₀ = 0.50 mM, pH = 4.35, 50 mM Na₂SO₄ were used as electrolyte, I = 1 mA, two 254 nm UV lamps were employed.

7.2.5 Tandem addition of Oxone[®]

The strategy of oxidant addition in optimizing the organic degradation was investigated by previous researchers (Yip et al., 2005). Their study suggested that the AOPs could be enhanced by using the strategy of splitting the required dosage of oxidant (H₂O₂) to minimize the scavenging effect that often co-occurs at excessive H₂O₂ doses. In this

section, the tandem addition of Oxone[®] on the effect of process performance was explored. The total load of 0.5 mM Oxone[®] was divided into two equal doses, one at the beginning of the reaction and the other at predetermined time intervals of 6, 8 or 10 min. The control was performed by adding 0.5 mM Oxone[®] at the beginning as a single dose. The obtained results are depicted in Figure 7-7, in which a positive effect was obtained by using the tandem oxidant addition mode compared to the control. Especially, over 98% of 2,4,5-TCP degradation was observed for the case of the tandem addition of second dose at 10 min. These results were in good agreement with the test results reported by Yip et al (2005). This is due to the fact that excessive levels of Oxone[®] in the solution can also provoke the self-scavenging effect of sulfate radicals according to Eq. 7-1:



In addition, it is interesting to note that the later the addition of the second dose, the higher the overall removal at the end. This suggests that the allowing of longer reaction time after the first dosage likely can deplete the remaining radicals in the solution, which minimize the chance of self-scavenging between the radicals (from the first dose) and fresh Oxone[®] (from the second dose), and therefore maximize the total radicals available for the 2,4,5-TCP degradation. However, the delay of second dose should not be overdone; otherwise the reaction time would be prolonged in real applications.

Experimental results indicate that the utilization of tandem addition of Oxone[®] can weaken the negative effect due to the existence of excessive oxidant, which is beneficial to the process but a precise timing control (i.e. process optimization) is necessary.

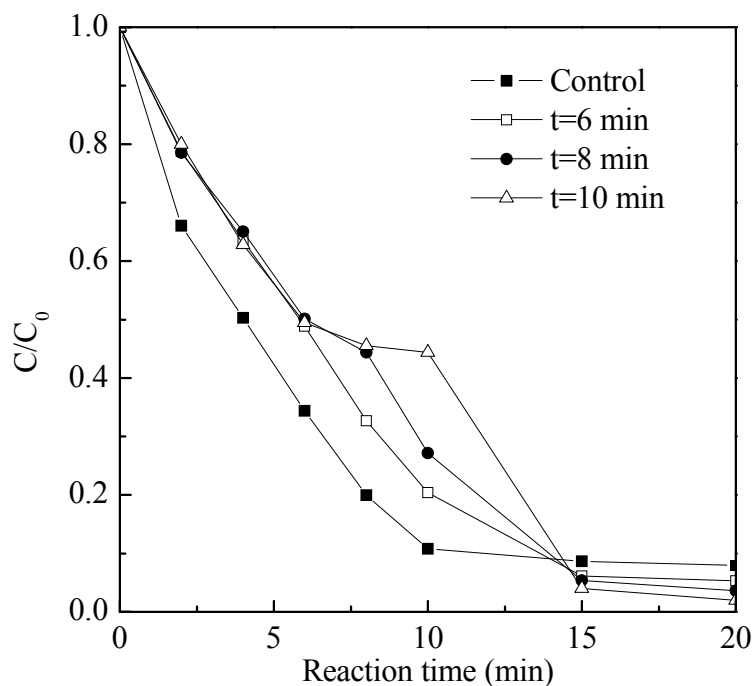


Figure 7-7: Degradation of 0.2 mM 2,4,5-TCP by EFOU process under tandem addition of Oxone[®]. 50 mM Na₂SO₄ were used as electrolyte, I = 1 mA, two 254 nm UV lamps were employed.

7.2.6 Proposed mechanism of 2,4,5-TCP decay

To study the intermediates, 2,4,5-TCP degradation by EFOU process was conducted at a relative higher concentration of 0.5 mM. The electrolytic time was extended to 30 min and Oxone[®] of 1 mM was dosed into the system at the reaction time of 0, 10, and 20 min. Based on the LC-ESI/MS analysis, a proposed mechanism illustrating the formation of measurable aromatic intermediates upon 2,4,5-TCP decay by EFOU process was presented in Scheme 7-1. It should be noted that the portion involving the utilization of dashed arrows were proposed according to literature review (Bertelli and Selli, 2006, Boye et al., 2003, Chaliha and Bhattacharyya, 2008).

2,5-dihydroxy-1,4-benzoquinone (**12**). In another possible route, an electrophilic OH group adds onto the aromatic ring of 2,4,5-TCP, giving rise to the formation compound **4** (detected in trace level). Photodechlorination is believed to be another reaction mechanism during the degradation of 2,4,5-TCP by the EFOU process, judging from the presence of 2,4-DCP (**5**). 2,4-DCP is subsequently photodechlorinated to 2-chlorophenol (**7**) and then undergoes dechlorination-hydroxylation resulting in the formation of catechol (**11**), the presence of which was also reported during the photocatalytic degradation of 2,4,5-TCP by previous researchers (Fabbri et al., 2004). The minor Compound **6** may originate from electrophilic OH addition to the aromatic ring of 2,4-DCP, while the generation of chlorohydroquinone (**8**) and 4-chlorocatechol (**9**) is likely to proceed with the OH group substituting an electron-withdrawing group (i.e., Cl-atom) of 2,4-DCP upon hydroxyl and sulfate radical attacks. 2-chloro-1,4-benzoquinone (**10**) may come from the further degradation of chlorohydroquinone. Further oxidation can break the aromatic rings of these secondary, tertiary intermediates and other hydroxylated products, leading to the formation of malic acids, maleic acids, fumaric acids and simpler organic acids, which is eventually mineralized to CO₂ and H₂O with sufficient sulfate and hydroxyl radical supply.

7.3 Summary

In the present chapter, the application of Electro-Fe(II)/Oxone[®] process assisted with UV irradiation has been investigated in terms of 2,4,5-TCP degradation in aqueous solution. Firstly, the degradation of 2,4,5-TCP under five different treatment processes (i.e., Oxone[®] alone, UV alone, FOU, EFO and EFOU) were comparatively examined. The ranking of probe decay efficiency by various processes was found in the sequence

of EFOU > FOU \approx EFO > UV alone > Oxone[®] alone. Experimental results show that applied current of 1 mA leads to the best performance and the process is slightly inhibited at higher applied current supply due to excessive release of ferrous ions. The effect of solution pH demonstrated that an acidic condition is favorable to the process. Nevertheless, efficient degradation (around 80%) of 2,4,5-TCP was obtained at neutral pH of 7.70 at the end of the reaction (20 min), suggesting that the proposed EFOU process can efficiently work from acidic to neutral pH levels. The investigation on the operational mode of applied current shows that the EFOU process can be optimized by controlling a proper electrolytic duration to maintain an appropriate amount of Fe(II) supply. Additionally, it is found that the process could be enhanced by using the strategy of tandem addition of Oxone[®] to minimize the scavenging effect that often occurs at excessive oxidant doses. Furthermore, the decay pathway of 2,4,5-TCP by EFOU process is proposed based on the identified aromatic intermediates by LC-ESI/MS analysis.

CHAPTER 8

Conclusions and Recommendations

8.1 Conclusions

This thesis has been focused on the investigation of reliable wastewater treatment technologies. Firstly, an environmentally preferred transition metal Fe(II) mediated activation of Oxone[®] process has been explored. To overcome the drawbacks of slow regeneration of Fe(II) catalyst and requirement for strict acidic conditions existing in the FO process, further research and development were conducted. The study showed that the application of either electrochemical technology or UV irradiation to the FO process could significantly enhance process performance (i.e., EFO and FOU). Finally, a more efficient process integrating the merits of both EFO and FOU processes has been proposed. The efficiency of these processes has been validated by examining the degradation of selected synthetic organic compounds.

8.1.1 The degradation of RhB by FO process

Investigation of reactant dosing sequence on the effect of RhB degradation by the FO process showed that Fe(II)-Oxone[®] addition demonstrates a better and faster dye degradation performance than that of Oxone[®]-Fe(II) addition. 100% of RhB removal was obtained within 90 min under an optimal Fe(II)/Oxone[®] molar ratio of 1:1 without pH adjustment. The RhB degradation was found to be a two-stage kinetics, consisting of a rapid initial decay and followed by a retarded stage. The effect of initial solution pH on the degradation of RhB by the FO process was studied over a wide range of pH conditions. Optimal dye removal efficiency was observed at an initial pH around 3.5,

above or below this pH level, the process performance reduced. Especially, the process performance was dramatically inhibited at elevated pH levels due to the formation of ferrous/ferric hydroxide complexes and non-radical self-decomposition of Oxone[®]. In addition, experimental results indicated that the presence of certain anions had an either positive or negative effect on the Fe(II)-mediated Oxone[®] process. The inhibitory effect on the RhB degradation in the presence of SO_4^{2-} was elucidated by a proposed formula using Nernst equation. Furthermore, mineralization of dye in terms of TOC removal indicates that stepwise addition of Fe(II) and Oxone[®] can notably improve the process performance by about 20%, and the retention time required for a specific performance can be greatly reduced comparing with the conventional one-off dosing method.

8.1.2 The degradation of 2,4,5-T by EFO process

Degradation of 2,4,5-T by EFO process is very effective with over 90% removal in 10 minutes. The pseudo first-order kinetics can be used to describe the 2,4,5-T degradation by EFO process. Based on the test results, the optimal applied current was determined to be 10 mA, in which both the herbicide removal efficiency and energy consumption were optimized. For the effect of [2,4,5-T], experimental results showed that (1) the degradation efficiency for 0.025, 0.05, 0.1, 0.15 and 0.2 mM 2,4,5-T was 100%, 98%, 88%, 78% and 69%, respectively; (2) 2,4,5-T decay rate constant linearly decreases with the increment of initial herbicide concentration. For the effect of Oxone[®] dosage, the test results demonstrate that 0.25 mM Oxone[®] exhibits the optimal 2,4,5-T decay rate and an unlimited increment of [Oxone[®]] is not favorable to the EFO. Moreover, it was found that herbicide decay rate sharply increases as the solution pH decreases. A favorable dual effect was subsequently conducted to elucidate this performance enhancement at acidic conditions. Radicals quenching study revealed the presence of

both hydroxyl and sulfate radicals in the process. Compared with the conventional FO process, the proposed EFO has the following advantages: (1) in-situ generation of Fe(II), (2) acceleration of regenerating Fe(II) from Fe(III), (3) minimization of the transportation and utilization problems of commercial ferrous salt, and (4) a less energy-demanding reaction, indicating the proposed EFO is a promising process.

8.1.3 The degradation of 2,4,5-T by FOU process

The potential use of FOU process for the degradation of 2,4,5-T in aqueous solution was conducted under a wide range of conditions. Comparative experiments between the FO and the FOU process were conducted to elucidate the role of UV light. It was found that the involvement of UV light can significantly accelerate the FO process due to different mechanisms including: direct UV photolysis, radical oxidation by $\text{SO}_4^{\bullet-}$ and $^{\bullet}\text{OH}$ generated via homolytic cleavage of HSO_5^- upon UV irradiation, radical oxidation by $\text{SO}_4^{\bullet-}$ generated by Fe(II)-mediated decomposition of Oxone[®], accelerated regeneration of Fe(II), and additional production of $^{\bullet}\text{OH}$ radicals via photo-reduction of Fe(III)-complexes.

The FOU process is optimized by properly selecting the operating parameters such as the wavelength of UV light, catalyst dosage, initial pH level and the supply of [Oxone[®]]. The use of UV 254 nm demonstrates the best performance, while the optimal pH was determined to be 3.68, which is a benefit of the FOU as it was easily achieved without pH adjustment. The effects of Fe(II) dosages and [Oxone[®]] were well elucidated in this study. In addition, 2,4,5-TCP and glycolic acid have been identified as the primary intermediate upon the decay of 2,4,5-T. The accumulation and disappearance of 2,4,5-TCP in terms of 2,4,5-T under various Oxone[®] concentrations demonstrated that

the competitive reaction between the parent and daughter compounds for oxidizing radicals plays an important role in explaining the effect of Oxone[®] doses in addition to the commonly recognized radical self-scavenging effect caused by excessive levels of oxidants. The addition of 0.01 M anions (such as CO_3^{2-} , HCO_3^- , H_2PO_4^- , CH_3COO^- and $\text{C}_2\text{O}_4^{2-}$) into the FOU system was found to inhibit the decay of 2,4,5-T more or less, which are attributed to the following reasons: a) the radical scavenger role of these anions played; b) and/or the UV adsorption block effect; c) and/or the change of iron speciation caused by the variation of solution pH.

Moreover, a comparative study upon 2,4,5-T transformation by UV alone, Oxone[®]/UV, and FOU processes were conducted. LC-ESI/MS analysis was employed to identify the aromatic intermediates, based on which different decay mechanisms and pathways were proposed and compared. Totally, 15 aromatic intermediates were identified by these processes, in which 10 of them have not been previously reported in the literature. Generally, the main reactions upon 2,4,5-T decay include dechlorination-hydroxylation, nucleophilic addition (hydroxylation), dechlorination, H-abstraction, C-O and C-Cl bond cleavage. It was found that 2,4,5-TCP and hydroxyl-dichlorophenoxyacetic acid are the main primary intermediates for the sole-UV. However, 2,4,5-TCP is the predominant primary intermediate by the Oxone[®]/UV and FOU, while other intermediates can be ignored due to their low yield. Additionally, 2,4,5-T decay was inefficient (~ 40% in 8 h) by the sole-UV process, while over 92% and 100% removal of 2,4,5-T were obtained by the Oxone[®]/UV in 3 h and FOU in 80 min, respectively.

Mineralization in terms of TOC reduction and the release of chlorine ions by these three processes have also been comparatively elucidated. Experimental results show that the

proposed FOU process demonstrates the best removal of TOC (> 83% in 8 h). The release of Cl^- was 49.2 ppm in 8 h by the FOU process, corresponding 92.6% of the initial Cl (around 53.15 ppm) in 2,4,5-T.

8.1.4 The degradation of 2,4,5-TCP by EFOU process

A combined version (EFOU) of EFO and FOU processes has been proposed. The degradation of 2,4,5-TCP by these processes was comparatively examined. Over 82.5% removal of 2,4,5-TCP in EFO treatment and 84% in FOU treatment were obtained for a 20-min reaction, respectively. As expected, the most effective 2,4,5-TCP degradation (over 92%) was obtained by EFOU process. It was found that an acidic condition is favorable to the process and over 92% removal of 0.2 mM 2,4,5-TCP in the pH range of 2.5 – 4.35 was rapidly obtained by the proposed EFOU process. Nevertheless, efficient degradation (around 80%) of 2,4,5-TCP at initial solution pH of 7.70 in 20 min suggests that the proposed EFOU process can efficiently work from acidic to neutral pH levels. Experimental results show that applied current of 1 mA leads to the best performance, while the process is slightly inhibited at higher applied current supply as a result of excessive release of ferrous ions. The EFOU process can be further optimized by controlling a proper electrolytic duration to ensure an appropriate supply of Fe(II) ions. It is also found that the process could be enhanced using the strategy of tandem addition of Oxone[®] to minimize the scavenging effect that often occurs at excessive oxidant doses. Furthermore, aromatic intermediates such as 2,4-chlorophenol, 2,5-dichlorohydroquinone, 4,6-dichlororesorcinol, and so on are identified by using LC-ESI/MS analysis, based on which a possible decay pathway of 2,4,5-TCP by EFOU process is proposed.

8.2 Recommendations for Future Works

Based on the results presented in this thesis, the investigated sulfate- and hydroxyl radical-based AOPs (FO, EFO, FOU, and EFOU processes) were shown to effectively degrade and remove specific pollutants. However, each process presented in this thesis could lead to various future investigative paths. Some recommendations on the improvements of these processes and on the further research directions of the issues are detailed as following.

In this study, all the reactions were conducted in a lab-scale batch reactor with the aim of destroying sole target compound in aqueous solution. For practical applications, future research work may be extended to develop corresponding continuous pilot scale reactors for these processes. Especially, it was validated that the process performance could be enhanced by using stepwise addition of Oxone[®] or tandem addition of Oxone[®]. It is therefore inferred that the development of continuous dosing of oxidant can significantly promote the process efficiency.

The experiments related to the electrochemical processes in this thesis were conducted in solutions containing single supporting electrolyte. However, real wastewater typically contains various anions such as phosphate and carbonate. Such anions may be initially present in the wastewater or formed as end products from the compounds undergoing degradation (Pignatello et al., 2007). Therefore, it is recommended to examine the process performance in presence of these anions. Besides, in this thesis, the iron sheet anode was employed to provide continuous release of ferrous ion catalyst, while the graphite cathode was used mainly as an inert electrical conductor. Another suggestion would be an examination of the role of different cathode materials (e.g., Pt).

In addition, due to analytical constraints, the detection of $\bullet\text{OH}$ and $\text{SO}_4^{\bullet-}$ was not conducted in this study. However, this route of investigation may give rise to a better understanding of the mechanisms of target compound decay upon sulfate and hydroxyl radical attacks by each process.

REFERENCES

- (1996) Guidelines for drinking-water quality, World Health Organization, Geneva.
- Adams, C.D. and Randtke, S.J. (1992) Ozonation by-products of atrazine in synthetic and natural-waters. *Environmental Science & Technology* 26(11), 2218-2227.
- Ai, Z.H., Lu, L.R., Li, J.P., Zhang, L.Z., Qiu, J.R. and Wu, M.H. (2007) Fe@Fe₂O₃ core-shell nanowires as iron reagent. 1. Efficient degradation of Rhodamine B by a novel sono-Fenton process. *Journal of Physical Chemistry C* 111(11), 4087-4093.
- AlHamed, F.H., Rauf, M.A. and Ashraf, S.S. (2009) Degradation studies of Rhodamine B in the presence of UV/H₂O₂. *Desalination* 239(1-3), 159-166.
- Anandkumar, J. and Mandal, B. (2011) Adsorption of chromium(VI) and Rhodamine B by surface modified tannery waste: Kinetic, mechanistic and thermodynamic studies. *Journal of Hazardous Materials* 186(2-3), 1088-1096.
- Anipsitakis, G.P. and Dionysiou, D.D. (2003) Degradation of organic contaminants in water with sulfate radicals generated by the conjunction of peroxymonosulfate with cobalt. *Environmental Science & Technology* 37(20), 4790-4797.
- Anipsitakis, G.P. and Dionysiou, D.D. (2004a) Radical generation by the interaction of transition metals with common oxidants. *Environmental Science & Technology* 38(13), 3705-3712.
- Anipsitakis, G.P. and Dionysiou, D.D. (2004b) Transition metal/UV-based advanced oxidation technologies for water decontamination. *Applied Catalysis B-Environmental* 54(3), 155-163.
- Anipsitakis, G.P., Dionysiou, D.D. and Gonzalez, M.A. (2006) Cobalt-mediated activation of peroxymonosulfate and sulfate radical attack on phenolic compounds. Implications of chloride ions. *Environmental Science & Technology* 40(3),

1000-1007.

- Annachhatre, A.P. and Gheewala, S.H. (1996) Biodegradation of chlorinated phenolic compounds. *Biotechnology Advances* 14(1), 35-56.
- Anotai, J., Lu, M.C. and Chewpreecha, P. (2006) Kinetics of aniline degradation by Fenton and electro-Fenton processes. *Water Research* 40(9), 1841-1847.
- Arslan-Alaton, I. and Gurses, F. (2004) Photo-Fenton-like and photo-fenton-like oxidation of Procaine Penicillin G formulation effluent. *Journal of Photochemistry and Photobiology a-Chemistry* 165(1-3), 165-175.
- Ashraf, S.S., Rauf, M.A. and Alhadrami, S. (2006) Degradation of Methyl Red using Fenton's reagent and the effect of various salts. *Dyes and Pigments* 69(1-2), 74-78.
- Asilturk, M., Sayilkan, F., Erdemoglu, S., Akarsu, M., Sayilkan, H., Erdemoglu, M. and Arpac, E. (2006) Characterization of the hydrothermally synthesized nano-TiO₂ crystallite and the photocatalytic degradation of Rhodamine B. *Journal of Hazardous Materials* 129(1-3), 164-170.
- Bai, C.P., Xiong, X.F., Gong, W.Q., Feng, D.X., Xian, M., Ge, Z.X. and Xu, N.A. (2011) Removal of rhodamine B by ozone-based advanced oxidation process. *Desalination* 278(1-3), 84-90.
- Ball, D.L. and Edwards, J.O. (1956) The Kinetics and Mechanism of the Decomposition of Caro's Acid. I. *Journal of the American Chemical Society* 78(6), 1125-1129.
- Balmer, M.E. and Sulzberger, B. (1999) Atrazine degradation in irradiated iron oxalate systems: Effects of pH and oxalate. *Environmental Science & Technology* 33(14), 2418-2424.
- Bandala, E.R., Brito, L. and Pelaez, M. (2009) Degradation of domoic acid toxin by UV-promoted Fenton-like processes in seawater. *Desalination* 245(1-3), 135-145.
- Bandala, E.R., Pelaez, M.A., Dionysiou, D.D., Gelover, S., Garcia, J. and Macias, D.

- (2007) Degradation of 2,4-dichlorophenoxyacetic acid (2,4-D) using cobalt-peroxymonosulfate in Fenton-like process. *Journal of Photochemistry and Photobiology a-Chemistry* 186(2-3), 357-363.
- Barbeni, M., Morello, M., Pramauro, E., Pelizzetti, E., Vincenti, M., Borgarello, E. and Serpone, N. (1987) Sunlight photodegradation of 2,4,5-trichlorophenoxy-acetic acid and 2,4,5-trichlorophenol on TiO_2 -Identification of intermediates and degradation pathway. *Chemosphere* 16(6), 1165-1179.
- Bertelli, M. and Selli, E. (2006) Reaction paths and efficiency of photocatalysis on TiO_2 and of H_2O_2 photolysis in the degradation of 2-chlorophenol. *Journal of Hazardous Materials* 138(1), 46-52.
- Bielski, B.H.J., Cabelli, D.E., Arudi, R.L. and Ross, A.B. (1985) Reactivity of HO_2/O_2^- radicals in aqueous solution. *Journal of Physical and Chemical Reference Data* 14(4), 1041-1100.
- Blackburn, R.S. (2004) Natural polysaccharides and their interactions with dye molecules: Applications in effluent treatment. *Environmental Science & Technology* 38(18), 4905-4909.
- Boye, B., Dieng, M.M. and Brillas, E. (2003) Electrochemical degradation of 2,4,5-trichlorophenoxyacetic acid in aqueous medium by peroxi-coagulation. Effect of pH and UV light. *Electrochimica Acta* 48(7), 781-790.
- Brillas, E., Boye, B., Sires, I., Garrido, J.A., Rodriguez, R.M., Arias, C., Cabot, P.L. and Comninellis, C. (2004) Electrochemical destruction of chlorophenoxy herbicides by anodic oxidation and electro-Fenton using a boron-doped diamond electrode. *Electrochimica Acta* 49(25), 4487-4496.
- Brillas, E., Sires, I. and Oturan, M.A. (2009) Electro-Fenton Process and Related Electrochemical Technologies Based on Fenton's Reaction Chemistry. *Chemical*

Reviews 109(12), 6570-6631.

Bukowska, M. (2004) 2,4,5-T and 2,4,5-TCP induce oxidative damage in human erythrocytes: the role of glutathione. *Cell Biology International* 28(7), 557-563.

Buxton, G.V., Greenstock, C.L., Helman, W.P. and Ross, A.B. (1988) Critical review of rate constants for reactions of hydrated electrons, hydrogen atoms and hydroxyl radicals ($\cdot\text{OH}/\cdot\text{O}^-$) in aqueous solution. *Journal of Physical and Chemical Reference Data* 17(2), 513-886.

Cao, G.M., Sheng, M., Niu, W.F., Fei, Y.L. and Li, D. (2009) Regeneration and reuse of iron catalyst for Fenton-like reactions. *Journal of Hazardous Materials* 172(2-3), 1446-1449.

Cao, J.S., Zhang, W.X., Brown, D.G. and Sethi, D. (2008) Oxidation of lindane with Fe(II)-activated sodium persulfate. *Environmental Engineering Science* 25(2), 221-228.

Casella, I.G. and Contursi, M. (2007) Electrocatalytic reduction of chlorophenoxy acids at palladium-modified glassy carbon electrodes. *Electrochimica Acta* 52(24), 7028-7034.

Chacon, J.M., Leal, M.T., Sanchez, M. and Bandala, E.R. (2006) Solar photocatalytic degradation of azo-dyes by photo-Fenton process. *Dyes and Pigments* 69(3), 144-150.

Chaliha, S. and Bhattacharyya, K.G. (2008) Catalytic wet oxidation of 2-chlorophenol, 2,4-dichlorophenol and 2,4,6-trichlorophenol in water with Mn(II)-MCM41. *Chemical Engineering Journal* 139(3), 575-588.

Chan, K.H. and Chu, W. (2009) Degradation of atrazine by cobalt-mediated activation of peroxymonosulfate: Different cobalt counteranions in homogenous process and cobalt oxide catalysts in photolytic heterogeneous process. *Water Research* 43(9),

2513-2521.

- Chan, K.H. and Chu, W. (2003) Modeling the reaction kinetics of Fenton's process on the removal of atrazine. *Chemosphere* 51(4), 305-311.
- Chang, B.V., Liu, J.Y. and Yuan, S.Y. (1998) Dechlorination of 2,4-dichlorophenoxyacetic acid and 2,4,5-trichlorophenoxyacetic acid in soil. *Science of the Total Environment* 215(1-2), 1-8.
- Chaudhary, A.J., Hassan, M.U. and Grimes, S.M. (2009) Simultaneous recovery of metals and degradation of organic species: Copper and 2,4,5-trichlorophenoxyacetic acid (2,4,5-T). *Journal of Hazardous Materials* 165(1-3), 825-831.
- Chawla, O.P. and Fessenden, R.W. (1975) Electron spin resonance and pulse radiolysis studies of some reactions of peroxysulfate ($\text{SO}_4^{\cdot-}$). *The Journal of Physical Chemistry* 79(24), 2693-2700.
- Chen, W.S. and Liang, J.S. (2008) Decomposition of nitrotoluenes from trinitrotoluene manufacturing process by Electro-Fenton oxidation. *Chemosphere* 72(4), 601-607.
- Chen, X.Y., Qiao, X.L., Wang, D.G., Lin, J. and Chen, J.W. (2007) Kinetics of oxidative decolorization and mineralization of Acid Orange 7 by dark and photoassisted Co^{2+} -catalyzed peroxymonosulfate system. *Chemosphere* 67(4), 802-808.
- Cheng, H.F. and Hu, Y.A. (2011) Economic Transformation, Technological Innovation, and Policy and Institutional Reforms Hold Keys to Relieving China's Water Shortages. *Environmental Science & Technology* 45(2), 360-361.
- Cheng, H.F., Hu, Y.A. and Hao, J.F. (2009) Meeting China's Water Shortage Crisis: Current Practices and Challenges. *Environmental Science & Technology* 43(2), 240-244.
- Couto, S.R. (2009) Dye removal by immobilized fungi. *Biotechnology Advances* 27, 227-235.

- Criquet, J. and Leitner, N.K.V. (2009) Degradation of acetic acid with sulfate radical generated by persulfate ions photolysis. *Chemosphere* 77(2), 194-200.
- Daubaras, D.L., Danganan, C.E., Hubner, A., Ye, R.W., Hendrickson, W. and Chakrabarty, A.M. (1996) Biodegradation of 2,4,5-trichlorophenoxyacetic acid by *Burkholderia cepacia* strain AC1100: Evolutionary insight. *Gene* 179(1), 1-8.
- Daubaras, D.L., Hershberger, C.D., Kitano, K. and Chakrabarty, A.M. (1995) Sequence-analysis of a gene-cluster involved in metabolism of 2,4,5-trichlorophenoxyacetic acid by *Burkholderia-cepacia* Ac 1100. *Applied and Environmental Microbiology* 61(4), 1279-1289.
- de Liphay, J.R., Sorensen, S.R. and Aamand, J. (2007) Effect of herbicide concentration and organic and inorganic nutrient amendment on the mineralization of mecoprop, 2,4-D and 2,4,5-T in soil and aquifer samples. *Environmental Pollution* 148(1), 83-93.
- Delcomyn, C.A., Bushway, K.E. and Henley, M.V. (2006) Inactivation of biological agents using neutral Oxone-chloride solutions. *Environmental Science & Technology* 40(8), 2759-2764.
- Deng, Y. and Englehardt, J.D. (2006) Treatment of landfill leachate by the Fenton process. *Water Research* 40(20), 3683-3694.
- Dogan, D. and Turkdemir, H. (2005) Electrochemical oxidation of textile dye indigo. *Journal of Chemical Technology and Biotechnology* 80(8), 916-923.
- Dogliotti, L. and Hayon, E. (1967) Flash photolysis of per[oxydi]sulfate ions in aqueous solutions. The sulfate and ozonide radical anions. *The Journal of Physical Chemistry* 71(8), 2511-2516.
- Donald, L.B. and John, O.E. (1956) The kinetics and mechanism of the decomposition of Caro's acid. *Journal of the American Chemical Society* 78 1125-1129.

- Donia, A.M., Atia, A.A., Al-amrani, W.A. and El-Nahas, A.M. (2009) Effect of structural properties of acid dyes on their adsorption behaviour from aqueous solutions by amine modified silica. *Journal of Hazardous Materials* 161(2-3), 1544-1550.
- Dulman, V., Ungureanu, M., Nemtoi, G. and Popa, V.I. (2004) The electrochemical behaviour of ammonium lignosulphonate solutions degraded with $S_2O_8^{2-}/Ag^+$ and Fenton oxidative systems. *Cellulose Chemistry and Technology* 38(5-6), 353-362.
- Eleren, S.C. and Alkan, U. (2009) Reducing effect of aerobic selector on the toxicity of synthetic organic compounds in activated sludge process. *Bioresource Technology* 100(23), 5714-5720.
- Elmorsi, T.M., Riyad, Y.M., Mohamed, Z.H. and Abd El Bary, H.M.H. (2010) Decolorization of Mordant red 73 azo dye in water using H_2O_2/UV and photo-Fenton treatment. *Journal of Hazardous Materials* 174(1-3), 352-358.
- Fabbri, D., Prevot, A.B. and Pramauro, E. (2004) Kinetic effects of SDS on the photocatalytic degradation of 2,4,5-trichlorophenol. *Applied Catalysis B-Environmental* 49(4), 233-238.
- Falkenmark, M. and Widstrand, C. (1992) Population and water resources: A delicate balance. *Popul. Bull.* 47(3), 1-36.
- Farre, M.J., Domenech, X. and Peral, J. (2006) Assessment of photo-Fenton and biological treatment coupling for Diuron and Linuron removal from water. *Water Research* 40(13), 2533-2540.
- Feng, J.Y., Hu, X.J. and Yue, P.L. (2006) Effect of initial solution pH on the degradation of Orange II using clay-based Fe nanocomposites as heterogeneous photo-Fenton catalyst. *Water Research* 40(4), 641-646.
- Fenton, H.J.H. (1894) Oxidation of tartaric acid in presence of iron. *Journal of the*

Chemical Society 65, 899-910.

- Figueroa, S., Vazquez, L. and Alvarez-Gallegos, A. (2009) Decolorizing textile wastewater with Fenton's reagent electrogenerated with a solar photovoltaic cell. *Water Research* 43(2), 283-294.
- Forgacs, E., Cserhati, T. and Oros, G. (2004) Removal of synthetic dyes from wastewaters: a review. *Environment International* 30(7), 953-971.
- Freeman, J.L. and Rayburn, A.L. (2006) Aquatic herbicides and herbicide contaminants: In vitro cytotoxicity and cell-cycle analysis. *Environmental Toxicology* 21(3), 256-263.
- Fu, F.L., Wang, Q. and Tang, B. (2010) Effective degradation of CI Acid Red 73 by advanced Fenton process. *Journal of Hazardous Materials* 174(1-3), 17-22.
- Gad, H.M.H. and El-Sayed, A.A. (2009) Activated carbon from agricultural by-products for the removal of Rhodamine-B from aqueous solution. *Journal of Hazardous Materials* 168(2-3), 1070-1081.
- Gallard, H., De Laat, J. and Legube, B. (1999) Spectrophotometric study of the formation of iron(III)-hydroperoxy complexes in homogeneous aqueous solutions. *Water Research* 33(13), 2929-2936.
- Garcia-Montano, J., Ruiz, N., Munoz, I., Domenech, X., Garcia-Hortal, J.A., Torrades, F. and Peral, J. (2006) Environmental assessment of different photo-Fenton approaches for commercial reactive dye removal. *Journal of Hazardous Materials* 138(2), 218-225.
- Gogate, P.R. and Pandit, A.B. (2003) A review of imperative technologies for wastewater treatment II: hybrid methods. *Advances in Environmental Research* 8, 553-597.
- Gogate, P.R. and Pandit, A.B. (2004) A review of imperative technologies for

- wastewater treatment I: oxidation technologies at ambient conditions. *Advances in Environmental Research* 8(3-4), 501-551.
- Gomezjimenez, L., Garciarodriguez, A., Lopezgonzalez, J.D. and Navarreteguijosa, A. (1987) Study of the kinetics of the adsorption by activated carbons of 2,4,5-Trichlorophenoxyacetic acid from aqueous solution. *Journal of Chemical Technology and Biotechnology* 37(4), 271-280.
- Gozmen, B., Oturan, M.A., Oturan, N. and Erbatur, O. (2003) Indirect electrochemical treatment of bisphenol a in water via electrochemically generated Fenton's reagent. *Environmental Science & Technology* 37(16), 3716-3723.
- Graillet, C. and Girard, J. (1994) Embryotoxic potency of 2,4,5-trichlorophenoxyacetic acid on sea urchin eggs: association with calcium homoeostasis. *Toxicology in Vitro* 8, 1097-1106.
- Guan, Y.H., Ma, J., Li, X.C., Fang, J.Y. and Chen, L.W. (2011) Influence of pH on the Formation of Sulfate and Hydroxyl Radicals in the UV/Peroxymonosulfate System. *Environmental Science & Technology* 45(21), 9308-9314.
- Hassan, J., Shamsipur, M., Es'haghi, A. and Fazili, S. (2011) Determination of Chlorophenoxy Acid Herbicides in Water Samples by Suspended Liquid-Phase Microextraction–Liquid Chromatography. *Chromatographia*, 999-1003.
- Hay, A. (1978) United-States producers fear ban on 2,4,5-trichlorophenol. *Nature* 275(5680), 471-471.
- Hayon, E., Treinin, A. and Wilf, J. (1972a) Electronic-spectra, photochemistry, and autoxidation mechanism of sulfate-bisulfite-pyrosulfite systems- SO_2^- , SO_3^- , SO_4^- , and SO_5^- radicals. *Journal of the American Chemical Society* 94(1), 47-&.
- Hayon, E., Treinin, A. and Wilf, J. (1972b) Electronic spectra, photochemistry, and autoxidation mechanism of the sulfite-bisulfite-pyrosulfite systems. SO_2^- , SO_3^- , SO_4^- ,

- and SO_5^- radicals. *Journal of the American Chemical Society* 94(1), 47-&.
- He, M.H. and Wei, C.H. (2010) Performance of membrane bioreactor (MBR) system with sludge Fenton oxidation process for minimization of excess sludge production. *Journal of Hazardous Materials* 176(1-3), 597-601.
- Hemant, K.S., Mohd Saquib and Haque, M.M. (2007) Titanium dioxide mediated photocatalysed degradation of phenoxyacetic acid and 2,4,5-trichlorophenoxyacetic acid, in aqueous suspensions. *Journal of Molecular Catalysis a-Chemical* 264, 66-72.
- Hou, M.F., Liao, L., Zhang, W.D., Tang, X.Y., Wan, H.F. and Yin, G.C. (2011) Degradation of rhodamine B by Fe(0)-based Fenton process with H_2O_2 . *Chemosphere* 83(9), 1279-1283.
- Hou, Y., Li, X.Y., Zhao, Q.D., Quan, X. and Chen, G.H. (2010) Electrochemically Assisted Photocatalytic Degradation of 4-Chlorophenol by ZnFe_2O_4 -Modified TiO_2 Nanotube Array Electrode under Visible Light Irradiation. *Environmental Science & Technology* 44(13), 5098-5103.
- Huang, K.C., Richard, A.C. and George, E.H. (2002) Kinetics of heat-assisted persulfate oxidation of methy tert-butyl ether(MTBE). *Chemosphere* 49, 413-420.
- Huang, Y.H., Huang, Y.F., Huang, C.I. and Chen, C.Y. (2009) Efficient decolorization of azo dye Reactive Black B involving aromatic fragment degradation in buffered Co^{2+} /PMS oxidative processes with a ppb level dosage of Co^{2+} -catalyst. *Journal of Hazardous Materials* 170(2-3), 1110-1118.
- Hwang, S., Huling, S.G. and Ko, S. (2010) Fenton-like degradation of MTBE: Effects of iron counter anion and radical scavengers. *Chemosphere* 78(5), 563-568.
- Isarain-Chavez, E., Arias, C., Cabot, P.L., Centellas, F., Rodriguez, R.M., Garrido, J.A. and Brillas, E. Mineralization of the drug beta-blocker atenolol by electro-Fenton

- and photoelectro-Fenton using an air-diffusion cathode for H₂O₂ electrogeneration combined with a carbon-felt cathode for Fe²⁺ regeneration. *Applied Catalysis B-Environmental* 96(3-4), 361-369.
- Jain, R., Mathur, M., Sikarwar, S. and Mittal, A. (2007) Removal of the hazardous dye rhodamine B through photocatalytic and adsorption treatments. *Journal of Environmental Management* 85(4), 956-964.
- Jeong, J. and Yoon, J. (2005) pH effect on OH radical production in photo/ferrioxalate system. *Water Research* 39(13), 2893-2900.
- Jiang, Y.L., Chen, Y.S., Younos, T., Huang, H.Q. and He, J.P. (2010) Urban Water Resources Quota Management: The Core Strategy for Water Demand Management in China. *Ambio* 39(7), 467-475.
- Johnson, R.L., Tratnyek, P.G. and Johnson, R.O. (2008) Persulfate Persistence under Thermal Activation Conditions. *Environmental Science & Technology* 42(24), 9350-9356.
- Joshi, D.K. and Gold, M.H. (1993) Degradation of 2,4,5-trichlorophenol by the lignin-degrading basidiomycete *Phanerochaete chrysosporium*. *Applied and Environmental Microbiology* 59(6), 1779-1785.
- Kadirvelu, K., Karthika, C., Vennilamani, N. and Pattabhi, S. (2005) Activated carbon from industrial solid waste as an adsorbent for the removal of Rhodamine-B from aqueous solution: Kinetic and equilibrium studies. *Chemosphere* 60(8), 1009-1017.
- Kaichouh, G., Oturan, N., Oturan, M.A., El Kacemi, K. and El Hourch, A. (2004) Degradation of the herbicide imazapyr by Fenton reactions. *Environmental Chemistry Letters* 2(1), 31-33.
- Kassinis, D., Varnava, N., Michael, C. and Piera, P. (2009) Homogeneous oxidation of aqueous solutions of atrazine and fenitrothion through dark and photo-Fenton

- reactions. *Chemosphere* 74(6), 866-872.
- Kennedy, R.J. and Stock, A.M. (1960) The oxidation of organic substances by potassium peroxymonosulfate. *Journal of Organic Chemistry* 25, 1901-1906.
- Khataee, A.R., Vatanpour, V. and Ghadim, A.R.A. (2009) Decolorization of CI Acid Blue 9 solution by UV/Nano-TiO₂, Fenton, Fenton-like, electro-Fenton and electrocoagulation processes: A comparative study. *Journal of Hazardous Materials* 161(2-3), 1225-1233.
- Killian, P.F., Bruell, C.J., Liang, C.J. and Marley, M.C. (2007) Iron (II) activated persulfate oxidation of MGP contaminated soil. *Soil & Sediment Contamination* 16(6), 523-537.
- Kochany, J. and Lipczynskakochany, E. (1992) Application of the EPR spin-trapping technique for the investigation of the reactions of carbonate, bicarbonate, and phosphate anions with hydroxyl radicals generated by the photolysis of H₂O₂. *Chemosphere* 25(12), 1769-1782.
- Kolthoff, I.M. and Miller, I.K. (1951) The kinetics and mechanism of the decomposition of the persulfate ion in aqueous medium. *Journal of the American Chemical Society* 73, 3055-3059.
- Kusic, H., Peternel, I., Ukic, S., Koprivanac, N., Bolanca, T., Papic, S. and Bozic, A.L. (2011) Modeling of iron activated persulfate oxidation treating reactive azo dye in water matrix. *Chemical Engineering Journal* 172(1), 109-121.
- Kwan, C.Y. (2005) The degradation of 2,4-Dichlorophenoxyacetic acid herbicide by advanced oxidation system. Ph.D., The Hong Kong Polytechnic University, Hong Kong.
- Kwan, C.Y. and Chu, W. (2004) A study of the reaction mechanisms of the degradation of 2,4-dichlorophenoxyacetic acid by oxalate-mediated photooxidation. *Water*

Research 38(19), 4213-4221.

- Kwan, C.Y., Chu, W. and Lam, W.S. (2007) The role of oxalate in the kinetics of 2,4-D oxidation over ferrous ion-supported catalysts. *Journal of Molecular Catalysis a-Chemical* 274(1-2), 50-57.
- Lau, T.K., Chu, W. and Graham, N.J.D. (2007) The aqueous degradation of butylated hydroxyanisole by UV/S₂O₈²⁻: Study of reaction mechanisms via dimerization and mineralization. *Environmental Science & Technology* 41(2), 613-619.
- Li, G.Z., Park, S., Kang, D.W., Krajmalnik-Brown, R. and Rittmann, B.E. (2011) 2,4,5-Trichlorophenol Degradation Using a Novel TiO₂-Coated Biofilm Carrier: Roles of Adsorption, Photocatalysis, and Biodegradation. *Environmental Science & Technology* 45(19), 8359-8367.
- Li, J.P., Ai, Z.H. and Zhang, L.Z. (2009a) Design of a neutral electro-Fenton system with Fe@Fe₂O₃/ACF composite cathode for wastewater treatment. *Journal of Hazardous Materials* 164(1), 18-25.
- Li, N., Wang, P., Zuo, C., Cao, H.L. and Liu, Q.S. (2010) Microwave-Enhanced Fenton Process for DMSO-Containing Wastewater. *Environmental Engineering Science* 27(3), 271-280.
- Li, S.X., Wei, D., Mak, N.K., Cai, Z., Xu, X.R., Li, H.B. and Jiang, Y. (2009b) Degradation of diphenylamine by persulfate: Performance optimization, kinetics and mechanism. *Journal of Hazardous Materials* 164(1), 26-31.
- Li, X.Z., Zhao, B.X. and Wang, P. (2007) Degradation of 2,4-dichlorophenol in aqueous solution by a hybrid oxidation process. *Journal of Hazardous Materials* 147(1-2), 281-287.
- Liang, C., Lee, I.L., Hsu, I.Y., Liang, C.P. and Lin, Y.L. (2008) Persulfate oxidation of trichloroethylene with and without iron activation in porous media. *Chemosphere*

70(3), 426-435.

- Liang, C.J. and Su, H.W. (2009) Identification of Sulfate and Hydroxyl Radicals in Thermally Activated Persulfate. *Industrial & Engineering Chemistry Research* 48(11), 5558-5562.
- Lin, S.H. and Yeh, K.L. (1993) Looking to treat wastewater? Try ozone. *Chemical Engineering* 100(5), 112-116.
- Ling, S.K., Wang, S.B. and Peng, Y.L. (2010) Oxidative degradation of dyes in water using $\text{Co}^{2+}/\text{H}_2\text{O}_2$ and Co^{2+} /peroxymonosulfate. *Journal of Hazardous Materials* 178(1-3), 385-389.
- Liu, G.M., Wu, T.X., Zhao, J.C., Hidaka, H. and Serpone, N. (1999) Photoassisted degradation of dye pollutants. 8. Irreversible degradation of alizarin red under visible light radiation in air-equilibrated aqueous TiO_2 dispersions. *Environmental Science & Technology* 33(12), 2081-2087.
- Liu, H., Wang, C., Li, X.Z., Xuan, X.L., Jiang, C.C. and Cui, H.N. (2007) A novel electro-Fenton process for water treatment: Reaction-controlled pH adjustment and performance assessment. *Environmental Science & Technology* 41(8), 2937-2942.
- Lopez, A., Pagano, M., Volpe, A. and Di Pinto, A.C. (2004) Fenton's pre-treatment of mature landfill leachate. *Chemosphere* 54(7), 1005-1010.
- Madhavan, J., Maruthamuthu, P., Murugesan, S. and Anandan, S. (2008) Kinetic studies on visible light-assisted degradation of acid red 88 in presence of metal-ion coupled Oxone reagent. *Applied Catalysis B-Environmental* 83(1-2), 8-14.
- Madhavan, J., Maruthamuthu, P., Murugesan, S. and Ashokkumar, M. (2009) Kinetics of degradation of acid red 88 in the presence of Co^{2+} -ion/peroxomonosulphate reagent. *Applied Catalysis a-General* 368(1-2), 35-39.
- Mantzavinos, D., Kassinos, D. and Parsons, S.A. (2009) Applications of advanced

- oxidation processes in wastewater treatment. *Water Research* 43(16), 3901-3901.
- Marsolek, M.D., Kirisits, M.J. and Rittmann, B.E. (2007) Biodegradation of 2,4,5-trichlorophenol by aerobic microbial communities: biorecalcitrance, inhibition, and adaptation. *Biodegradation* 18(3), 351-358.
- Masomboon, N., Ratanatamskul, C. and Lu, M.C. (2009) Chemical Oxidation of 2,6-Dimethylaniline in the Fenton Process. *Environmental Science & Technology* 43(22), 8629-8634.
- Matus, V., Vasquez, M., Vicente, M. and Gonzalez, B. (1996) Microbial mineralization of 2,4,5-trichlorophenol in soil. *Environmental Science & Technology* 30(5), 1472-1476.
- Merka, O., Yarovy, V., Bahnemann, D.W. and Wark, M. (2011) pH-Control of the Photocatalytic Degradation Mechanism of Rhodamine B over $\text{Pb}_3\text{Nb}_4\text{O}_{13}$. *Journal of Physical Chemistry C* 115(16), 8014-8023.
- Migliorini, F.L., Braga, N.A., Alves, S.A., Lanza, M.R.V., Baldan, M.R. and Ferreira, N.G. (2011) Anodic oxidation of wastewater containing the Reactive Orange 16 Dye using heavily boron-doped diamond electrodes. *Journal of Hazardous Materials* 192(3), 1683-1689.
- Mirsalis, J., C.K, T., K.L, S., E.K, L., C.M, H., J.P, B. and J.W, S. (1989) Measurement of unscheduled DNA synthesis and S-phase synthesis in rodent hepatocytes following in vivo treatment: Testing of 24 compounds. *Environmental and Molecular Mutagenesis* 14 (3), 155-164.
- Mittal, A.K. and Venkobachar, C. (1996) Uptake of cationic dyes by sulfonated coal: Sorption mechanism. *Industrial & Engineering Chemistry Research* 35(4), 1472-1474.
- Moeser, G.D., Roach, K.A., Green, W.H., Laibinis, P.E. and Hatton, T.A. (2002)

- Water-based magnetic fluids as extractants for synthetic organic compounds. *Industrial & Engineering Chemistry Research* 41(19), 4739-4749.
- Narender, N., Srinivasu, P., Kularni, S.J. and Raghavan, K.V. (2002) Highly efficient, para-selective oxychlorination of aromatic compounds using potassium chloride and Oxone. *Synthetic Communications* 32(279-286).
- Neta, P., Madhavan, V., Zemel, H. and Fessenden, R.W. (1977) Rate constants and mechanism of reaction of sulfate radical anion with aromatic compounds. *Journal of the American Chemical Society* 99(1), 163-164.
- Neyens, E. and Baeyens, J. (2003) A review of classic Fenton's peroxidation as an advanced oxidation technique. *Journal of Hazardous Materials* 98(1-3), 33-50.
- Oh, S.Y., Kim, H.W., Park, J.M., Park, H.S. and Yoon, C. (2009) Oxidation of polyvinyl alcohol by persulfate activated with heat, Fe^{2+} , and zero-valent iron. *Journal of Hazardous Materials* 168(1), 346-351.
- Oturan, M.A., Aaron, J.J., Oturan, N. and Pinson, J. (1999) Degradation of chlorophenoxyacid herbicides in aqueous media, using a novel electrochemical method. *Pesticide Science* 55(5), 558-562.
- Oturan, M.A., Peirotten, J., Chartrin, P. and Acher, A.J. (2000) Complete destruction of p-nitrophenol in aqueous medium by electro-Fenton method. *Environmental Science & Technology* 34(16), 3474-3479.
- Ozcan, A., Sahin, Y., Koparal, A.S. and Oturan, M.A. (2009) A comparative study on the efficiency of electro-Fenton process in the removal of prothion from water. *Applied Catalysis B-Environmental* 89(3-4), 620-626.
- Panda, G.C., Das, S.K. and Guha, A.K. (2009) Jute stick powder as a potential biomass for the removal of congo red and rhodamine B from their aqueous solution. *Journal of Hazardous Materials* 164(1), 374-379.

- Pandurengan, T. and Maruthamuthu, P. (1981) Kinetics and mechanism of oxidation of dimethyl sulfoxide by peroxomonosulphate. *Bulletin of the Chemical Society of Japan* 54(Bulletin of the Chemical Society of Japan), 3551-3555.
- Papic, S., Koprivanac, N., Bozic, A.L., Vujevic, D., Dragievic, S.K., Kusic, H. and Peternel, I. (2006) Advanced oxidation processes in azo dye wastewater treatment. *Water Environment Research* 78(6), 572-579.
- Pazdzior, K., Klepacz-Smolka, A., Ledakowicz, S., Sojka-Ledakowicz, J., Mrozinska, Z. and Zylla, R. (2009) Integration of nanofiltration and biological degradation of textile wastewater containing azo dye. *Chemosphere* 75(2), 250-255.
- Perez-Estrada, L.A., Malato, S., Gernjak, W., Aguera, A., Thurman, E.M., Ferrer, I. and Fernandez-Alba, A.R. (2005) Photo-fenton degradation of diclofenac: Identification of main intermediates and degradation pathway. *Environmental Science & Technology* 39(21), 8300-8306.
- Perez-Moya, M., Graells, M., Buenestado, P. and Mansilla, H.D. (2008) A comparative study on the empirical modeling of photo-Fenton treatment process performance. *Applied Catalysis B-Environmental* 84(1-2), 313-323.
- Piao, S.L., Ciais, P., Huang, Y., Shen, Z.H., Peng, S.S., Li, J.S., Zhou, L.P., Liu, H.Y., Ma, Y.C., Ding, Y.H., Friedlingstein, P., Liu, C.Z., Tan, K., Yu, Y.Q., Zhang, T.Y. and Fang, J.Y. (2010) The impacts of climate change on water resources and agriculture in China. *Nature* 467(7311), 43-51.
- Pignatello, J.J., Liu, D. and Huston, P. (1999) Evidence for an additional oxidant in the photoassisted Fenton reaction. *Environmental Science & Technology* 33(11), 1832-1839.
- Pignatello, J.J., Oliveros, E. and MacKay, A. (2007) Advanced oxidation processes for organic contaminant destruction based on the Fenton reaction and related chemistry

- (vol 36, pg 1, 2006). Critical Reviews in Environmental Science and Technology 37(3), 273-275.
- Pimentel, M., Oturan, N., Dezotti, M. and Oturan, M.A. (2008) Phenol degradation by advanced electrochemical oxidation process electro-Fenton using a carbon felt cathode. Applied Catalysis B-Environmental 83(1-2), 140-149.
- Pouloupoulos, S.G., Korologos, C.A., Boulamanti, A. and Philippopoulos, C.J. (2007) Treatment of 2-chlorophenol aqueous solutions by wet oxidation. Water Research 41(6), 1263-1268.
- Primo, O., Rivero, M.J. and Ortiz, I. (2008) Photo-Fenton process as an efficient alternative to the treatment of landfill leachates. Journal of Hazardous Materials 153(1-2), 834-842.
- Rao, Y.F. and Chu, W. (2009) Reaction Mechanism of Linuron Degradation in TiO₂ Suspension under Visible Light Irradiation with the Assistance of H₂O₂. Environmental Science & Technology 43(16), 6183-6189.
- Rastogi, A., Ai-Abed, S.R. and Dionysiou, D.D. (2009) Sulfate radical-based ferrous-peroxymonosulfate oxidative system for PCBs degradation in aqueous and sediment systems. Applied Catalysis B-Environmental 85(3-4), 171-179.
- Richard, J.K. and Albert, M.S. (1960) The oxidation of organic substances by potassium peroxymonosulfate. Journal of Organic Chemistry 25 1901-1906
- Rigg, T., Taylor, W. and Weiss, J. (1954) The rate constant of the reaction between hydrogen peroxide and ferrous ions. J. Chem. Phys. 22(4), 575-577.
- Rochat, J., Demenge, P. and Rerat, J.C. (1978) Toxicologic study of a fluorescent tracer: rhodamine B. Toxicological European Research 1, 23-26.
- Sabhi, S. and Kiwi, J. (2001) Degradation of 2,4-dichlorophenol by immobilized iron catalysts. Water Research 35(8), 1994-2002.

- Sanroman, M.A., Pazos, M., Ricart, M.T. and Cameselle, C. (2005) Decolourisation of textile indigo dye by DC electric current. *Engineering Geology* 77(3-4), 253-261.
- Schmidt, C.W. (2002) Economy and environment: China seeks a balance. *Environmental Health Perspective* 110(9), 517-522.
- Sharma, H.A., Barber, J.T., Ensley, H.E. and Polito, M.A. (1997) A comparison of the toxicity and metabolism of phenol and chlorinated phenols by *Lemna gibba*, with special reference to 2,4,5-trichlorophenol. *Environmental Toxicology and Chemistry* 16(2), 346-350.
- Sharma, S., Mukhopadhyay, M. and Murthy, Z.V.P. (2010) Degradation of 4-Chlorophenol in Wastewater by Organic Oxidants. *Industrial & Engineering Chemistry Research* 49(7), 3094-3098.
- Shukla, P., Sun, H.Q., Wang, S.B., Ang, H.M. and Tade, M.O. (2011) Co-SBA-15 for heterogeneous oxidation of phenol with sulfate radical for wastewater treatment. *Catalysis Today* 175(1), 380-385.
- Shukla, P., Wang, S.B., Singh, K., Ang, H.M. and Tade, M.O. (2010) Cobalt exchanged zeolites for heterogeneous catalytic oxidation of phenol in the presence of peroxymonosulphate. *Applied Catalysis B-Environmental* 99(1-2), 163-169.
- Singh, H.K., Saquib, M., Haque, M.M., Muneer, M. and Bahnemann, D.W. (2007) Titanium dioxide mediated photocatalysed degradation of phenoxyacetic acid and 2,4,5-trichlorophenoxyacetic acid, in aqueous suspensions. *Journal of Molecular Catalysis a-Chemical* 264(1-2), 66-72.
- Sires, I., Garrido, J.A., Rodriguez, R.M., Brillas, E., Oturan, N. and Oturan, M.A. (2007) Catalytic behavior of the $\text{Fe}^{3+}/\text{Fe}^{2+}$ system in the electro-Fenton degradation of the antimicrobial chlorophene. *Applied Catalysis B-Environmental* 72(3-4), 382-394.
- Sires, I., Guivarch, E., Oturan, N. and Oturan, M.A. (2008) Efficient removal of

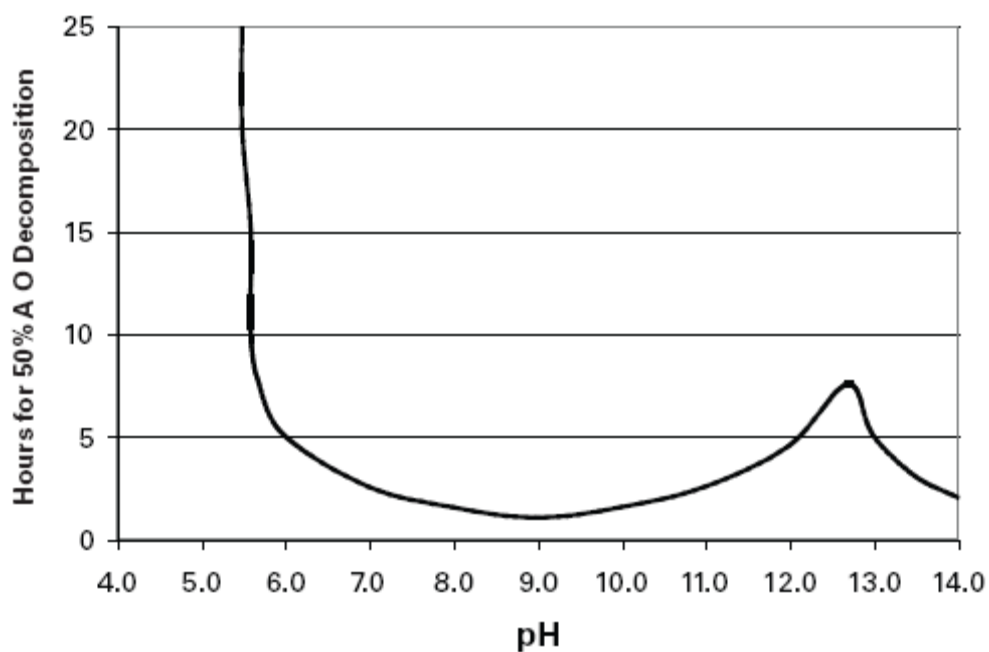
- triphenylmethane dyes from aqueous medium by in situ electrogenerated Fenton's reagent at carbon-felt cathode. *Chemosphere* 72(4), 592-600.
- Sitting, M. (1981) *Handbook of toxic and hazardous chemicals*, Noyes Publications, Park Ridge, N.J.
- Solanki, J.N. and Murthy, Z.V.P. (2011) Reduction of 4-Chlorophenol by Mg and Mg-Ag Bimetallic Nanocatalysts. *Industrial & Engineering Chemistry Research* 50(24), 14211-14216.
- Stuart, J.N., Goerges, A.L. and Zaleski, J.M. (2000) Characterization of the Ni(III) intermediate in the reaction of (1,4,8,11-tetraazacyclotetradecane)nickel(II) perchlorate with KHSO_5 : implications to the mechanism of oxidative DNA modification. *Inorganic Chemistry* 39, 5976-5984.
- Sun, J.H., Li, X.Y., Feng, J.L. and Tian, X.K. (2009) Oxone/ Co^{2+} oxidation as an advanced oxidation process: Comparison with traditional Fenton oxidation for treatment of landfill leachate. *Water Research* 43(17), 4363-4369.
- Suryaman, D. and Hasegawa, K. (2010) Biological and photocatalytic treatment integrated with separation and reuse of titanium dioxide on the removal of chlorophenols in tap water. *Journal of Hazardous Materials* 183(1-3), 490-496.
- Tamura, H., Goto, K., Yotsuyan.T and Nagayama, M. (1974) Spectrophotometric determination of iron(II) with 1,10-phenanthroline in presence of large amounts of iron(III). *Talanta* 21(4), 314-318.
- Tang, W.Z. and Huang, C.P. (1995) The effect of chlorine position of chlorinated phenols on their dechlorination kinetics by Fenton's reagent. *Waste Management* 15(8), 615-622.
- Trovo, A.G., Nogueira, R.F.P., Aguera, A., Fernandez-Alba, A.R., Sirtori, C. and Malato, S. (2009) Degradation of sulfamethoxazole in water by solar photo-Fenton.

- Chemical and toxicological evaluation. *Water Research* 43(16), 3922-3931.
- Vass, A. (2002) Over half the world will face water shortages by 2032. *British Medical Journal* 324(7349), 1293-1293.
- Ventura, A., Jacquet, G., Bermond, A. and Camel, V. (2002) Electrochemical generation of the Fenton's reagent: application to atrazine degradation. *Water Research* 36(14), 3517-3522.
- Waldemer, R.H., Tratnyek, P.G., Johnson, R.L. and Nurmi, J.T. (2007) Oxidation of chlorinated ethenes by heat-activated persulfate: Kinetics and products. *Environmental Science & Technology* 41(3), 1010-1015.
- Wang, C.T., Hu, J.L., Chou, W.L. and Kuo, Y.M. (2008) Removal of color from real dyeing wastewater by Electro-Fenton technology using a three-dimensional graphite cathode. *Journal of Hazardous Materials* 152(2), 601-606.
- Watts, M.J. and Cooper, A.T. (2008) Photocatalysis of 4-chlorophenol mediated by TiO_2 fixed to concrete surfaces. *Solar Energy* 82(3), 206-211.
- Yan, K.C. (2006) The degradation of 2, 4-Dichlorophenoxyacetic acid herbicide by advanced oxidation system, The Hong Kong Polytechnic University, Hong Kong.
- Yang, S.Y., Wang, P., Yang, X., Shan, L., Zhang, W.Y., Shao, X.T. and Niu, R. (2010) Degradation efficiencies of azo dye Acid Orange 7 by the interaction of heat, UV and anions with common oxidants: Persulfate, peroxymonosulfate and hydrogen peroxide. *Journal of Hazardous Materials* 179(1-3), 552-558.
- Yang, Y., Wang, P., Shi, S.J. and Liu, Y. (2009) Microwave enhanced Fenton-like process for the treatment of high concentration pharmaceutical wastewater. *Journal of Hazardous Materials* 168(1), 238-245.
- Yip, A.C.K., Lam, F.L.Y. and Hu, X.J. (2005) Chemical-vapor-deposited copper on acid-activated bentonite clay as an applicable heterogeneous catalyst for the

- photo-Fenton-like oxidation of textile organic pollutants. *Industrial & Engineering Chemistry Research* 44(21), 7983-7990.
- Yuan, S.H., Tian, M., Cui, Y.P., Lin, L. and Lu, X.H. (2006) Treatment of nitrophenols by cathode reduction and electro-Fenton methods. *Journal of Hazardous Materials* 137(1), 573-580.
- Zaghouane-Boudiaf, H. and Boutahala, M. (2011) Adsorption of 2,4,5-trichlorophenol by organo-montmorillonites from aqueous solutions: Kinetics and equilibrium studies. *Chemical Engineering Journal* 170(1), 120-126.
- Zazo, J.A., Casas, J.A., Mohedano, A.F., Gilarranz, M.A. and Rodriguez, J.J. (2005) Chemical pathway and kinetics of phenol oxidation by Fenton's reagent. *Environmental Science & Technology* 39(23), 9295-9302.
- Zazo, J.A., Casas, J.A., Molina, C.B., Quintanilla, A. and Rodriguez, J.J. (2007) Evolution of ecotoxicity upon Fenton's oxidation of phenol in water. *Environmental Science & Technology* 41(20), 7164-7170.
- Zimbron, J.A. and Reardon, K.F. (2009) Fenton's oxidation of pentachlorophenol. *Water Research* 43(7), 1831-1840.
- Zuo, Y.G. and Hoigne, J. (1992) Formation of hydrogen peroxide and depletion of oxalic acid in atmospheric water by photolysis of iron(III)-oxalato complexes. *Environmental Science & Technology* 26(5), 1014-1022.

APPENDIX I: Chemistry of Oxone®

parameter	Value/Information
Chemical structure	$ \begin{array}{c} \text{O} \\ \parallel \\ \text{HO}-\text{O}-\text{S}-\text{O}^-\text{K}^+ \\ \parallel \\ \text{O} \\ \parallel \\ \text{O} \\ \parallel \\ \text{HO}-\text{O}-\text{S}-\text{O}^-\text{K}^+ \end{array} \quad \begin{array}{c} \text{O} \\ \parallel \\ \text{HO}-\text{S}-\text{O}^-\text{K}^+ \\ \parallel \\ \text{O} \\ \parallel \\ \text{O} \\ \parallel \\ \text{K}^+\text{O}^--\text{S}-\text{O}^-\text{K}^+ \end{array} $
name	Oxone®
Other name	Potassium hydrogen triple salt, Caroat
Molecular formula	$2\text{KHSO}_5 \cdot \text{KHSO}_4 \cdot \text{K}_2\text{SO}_4$
Formula weight	614.76
Appearance	Off-white powder
Solubility in water	25.6 WT% at 20°C
pK _a	pK _{a1} < 0 and pK _{a2} = 9.4 at 25°C in water



Effect of pH on Oxone® solution stability (3 wt% solution at 32°C)